

Atmospheric Oxidation of Selected Aromatic Hydrocarbons



Thesis submitted to the Faculty of Chemistry
Bergische Universität Gesamthochschule Wuppertal
for the Degree of Doctor of Science
(Dr. rerum naturalium)

by
Romeo Iulian Olariu

October, 2001

The work described in this thesis was carried out in the Department of Physical Chemistry, the Bergische Universität Gesamthochschule Wuppertal under the scientific supervision of Prof. Dr. K. H. Becker, during the period of March, 1998 - October, 2001.

Referee: Prof. Dr. K. H. Becker

Co-referee: Prof. Dr. E. H. Fink

soției mele, Irina
și
fiicei noastre, Ana

I would like to express my sincere thanks to Prof. Dr. Karl Heinz Becker for the opportunity of doing this Ph.D. in his research group and for the supervision of this work.

I would like to thank Prof. Dr. Ewald Fink for agreeing to co-referee the thesis and for his useful comments.

My sincere gratitude also to Dr. Ian Barnes who not only helped me to understand at least a part of the immense and fascinating domain of the atmospheric chemistry but also followed with special care my scientific work.

I express my thanks to Prof. Dr. Raluca Delia Mocanu for trusting me and making many valuable suggestions.

The help given by Dr. Björn Klotz, especially at the beginning of my Ph.D. work, is much appreciated.

Thanks are also due to my colleague Cecilia Arsene for suggestions and critical observations.

Many colleagues helped by supplying advanced information, suggestions and comments on laboratory work. Of these I would like to mention particularly Dr. Klaus Brockmann, Markus Spittler, Dr. Jörg Kleffmann, Dr. Klaus Wirtz (Valencia) and the technical staff of this group.

Abstract

This work presents investigations on the gas-phase chemistry of phenol and the cresol isomers performed in a 1080 l quartz glass reactor in Wuppertal and in a large-volume outdoor photoreactor EUPHORE in Valencia, Spain. The studies aimed at clarifying the oxidation mechanisms of the reactions of these compounds with OH and NO₃ radicals.

Product investigations on the oxidation of phenol and the cresol isomers initiated by OH radicals were performed in the 1080 l quartz glass reactor with analyses by in situ FT-IR absorption spectroscopy. The primary focus of the investigations was on the determination of product yields. This work represents the first determination and quantification of 1,2-dihydroxybenzenes in the OH oxidation of phenolic compounds. Possible reaction pathways leading to the observed products have been elucidated. The products observed and their respective yields were as follows:

reactant	products	yield (%)
phenol	1,2-dihydroxybenzene	80.4 ± 12.1
	1,4-benzoquinone	3.7 ± 1.2
	2-nitrophenol	5.8 ± 1.0
<i>ortho</i> -cresol	1,2-dihydroxy-3-methylbenzene	73.4 ± 14.6
	methyl-1,4-benzoquinone	6.8 ± 1.0
	6-methyl-2-nitrophenol	6.8 ± 1.5
<i>meta</i> -cresol	1,2-dihydroxy-3-methylbenzene	68.6 ± 13.4
	1,2-dihydroxy-4-methylbenzene	9.7 ± 2.7
	methyl-1,4-benzoquinone	11.3 ± 2.5
	5-methyl-2-nitrophenol	4.4 ± 1.5
	3-methyl-2-nitrophenol	4.3 ± 1.6
<i>para</i> -cresol	1,2-dihydroxy-4-methylbenzene	64.1 ± 11.3
	4-methyl-2-nitrophenol	7.6 ± 2.2

The rate constants for the reaction of OH radicals with dihydroxy(methyl)benzenes and (methyl)benzoquinones were determined using the relative rate technique. All of the following data represent first-time determinations of the rate constants. At 1000 mbar total pressure and 300 ± 2 K, the following rate constants (in 10⁻¹¹ cm³ molecule⁻¹ s⁻¹) were obtained:

reactant	k _{OH}
1,2-dihydroxybenzene	10.4 ± 2.1
1,2-dihydroxy-3-methylbenzene	20.5 ± 4.3
1,2-dihydroxy-4-methylbenzene	15.6 ± 3.3
1,4-benzoquinone	0.46 ± 0.1
methyl-1,4-benzoquinone	2.35 ± 0.47

The following products and respective yields were observed from the NO₃ radical reaction with phenol and the cresol isomers:

reactant	products	yield (%) 1080 I	yield (%) EUPHORE
phenol	2-nitrophenol	24.2 ± 3.7	21.3 ± 3.3
	4-nitrophenol	50.0 ± 3.8	50.0 ± 10.0
	HNO ₃	89.7 ± 13.0	73.8 ± 8.3
<i>ortho</i> -cresol	6-methyl-2-nitrophenol	11.5 ± 0.8	-
	methyl-1,4-benzoquinone	4.4 ± 0.3	-
	HNO ₃	77.2 ± 6.3	95.9 ± 4.8
<i>meta</i> -cresol	3-methyl-2-nitrophenol	21.2 ± 1.4	22.3 ± 1.6
	3-methyl-4-nitrophenol	22.8 ± 1.8	25.4 ± 1.7
	5-methyl-2-nitrophenol	23.5 ± 1.8	22.4 ± 1.5
	methyl-1,4-benzoquinone	4.2 ± 0.7	-
	HNO ₃	72.3 ± 6.4	91.1 ± 6.3
<i>para</i> -cresol	4-methyl-2-nitrophenol	41.3 ± 3.7	44.3 ± 3.3
	HNO ₃	85.0 ± 10.2	86.2 ± 7.0

This work has vastly improved the knowledge on the distribution of oxidation products from the reaction of OH with phenol and the cresol isomers and also significantly improved it for the NO₃ reactions. The product studies have allowed the construction of tentative oxidation mechanisms for these selected aromatic compounds which are required for atmospheric chemical transport models.

Content

Chapter 1

1.1 Introduction.....	1
1.2 Phenol and cresols in the atmosphere	3
1.2.1 Sources and abundance.....	3
1.2.2 In situ formation and removal processes.....	5
1.3 Status of knowledge.....	7
1.3.1 Product and mechanistic studies on the reactions of the OH radical with phenols.....	7
1.3.2 Product and mechanistic studies on the reactions of the NO ₃ radical with phenols	10
1.4 Aim of the work.....	12

Chapter 2

Experimental section.....	13
2.1 Reaction chambers.....	13
2.1.1 1080 l quartz glass reactor	13
2.1.2 EUPHORE chamber.....	15
2.2 Generation of radicals	16
2.2.1 OH radicals.....	16
2.2.2 In situ generation of NO ₃ radicals.....	17
2.2.3 Cl radicals.....	17
2.3 Typical experimental procedure.....	17
2.3.1 Experiments in the 1080 l quartz glass reactor.....	17
2.3.1.1 Control experiments	18
2.3.1.2 OH radical experiments	19
2.3.1.2.1 Kinetic experiments on dihydroxy(methyl)benzenes and (methyl)benzoquinones	19
2.3.1.2.2 Gas-phase product study experiments.....	19
2.3.1.3 NO ₃ radical experiments	20
2.3.2 Experiments in the EUPHORE chamber.....	20

Chapter 3

Kinetic study of the reaction of OH radicals with dihydroxybenzenes and benzoquinones	23
3.1 Data evaluation and results.....	24
3.2 Discussion.....	28

Chapter 4

Mechanisms of the atmospheric oxidation of phenol.....	33
4.1 Product study of the photo-oxidation of phenol initiated by OH radicals.....	33
4.1.1 Experimental results	33
4.1.2 Discussion of the results	38
4.1.2.1 Discussion of the formation mechanism of 1,2-dihydroxybenzene	40
4.1.2.2 Discussion of the formation mechanism of benzoquinone and nitrophenol	41
4.1.2.3 Summary of results.....	42
4.2 Product study of the nitration of phenol by reaction with the NO ₃ radical	44
4.2.1 Experimental results	44
4.2.1.1 1080 l quartz glass reactor.....	44
4.2.1.2 EUPHORE chamber.....	48
4.2.3 Discussion of the results	51
4.2.3.1 Comparison of results.....	51
4.2.3.2 Discussion of the formation of 2-nitrophenol and 4-nitrophenol.....	52
4.2.3.3 Discussion of the formation of HNO ₃	54
4.2.3.4 Summary of results	55

Chapter 5

Mechanisms of the atmospheric oxidation of the cresol isomers.....	57
5.1 Product analyses of the OH initiated oxidation of the cresol isomers	57
5.1.1 General results	57
5.1.1.1 FT-IR spectral data from the reaction of OH with <i>ortho</i> -cresol.....	58
5.1.1.2 FT-IR spectral data from the reaction of OH with <i>meta</i> -cresol.....	60
5.1.1.3 FT-IR spectral data from the reaction of OH with <i>para</i> -cresol	62
5.1.1.4 Data evaluation	63
5.1.2 Discussion of the results	68
5.1.2.1 Discussion of the formation mechanism of dihydroxy(methyl)benzene in the OH-initiated oxidation of the cresol isomers.....	71
5.1.2.2 Discussion of the formation mechanism of nitrocresols.....	73
5.1.2.3 Discussion of the formation mechanism of methyl-1,4-benzoquinone.....	74
5.1.2.4 Reaction mechanisms	75
5.2 Product study of the nitration of cresol isomers by reaction with the NO ₃ radical.....	79
5.2.1 Experimental data.....	79
5.2.1.1 1080 l quartz glass reactor	79
5.2.1.1.1 FT-IR spectral data from the reaction of NO ₃ with <i>ortho</i> -cresol.....	80
5.2.1.1.2 FT-IR spectral data from the reaction of NO ₃ with <i>meta</i> -cresol	82
5.2.1.1.3 FT-IR spectral data from the reaction of NO ₃ with <i>para</i> -cresol.....	84
5.2.1.2 EUPHORE chamber.....	85
5.2.2.1.1 FT-IR spectral data from the reaction of NO ₃ with <i>meta</i> -cresol	86
5.2.2.1.2 FT-IR spectral data from the reaction of NO ₃ with <i>para</i> -cresol.....	88
5.2.2 Data evaluation.....	89
5.2.2.1 The 1080 l quartz glass reactor studies	89
5.2.2.2 The EUPHORE chamber studies	93
5.2.3 Discussion of the results	95
5.2.3.1 Comparison of results.....	95
5.2.3.2 Discussion of the formation mechanism of nitrocresols.....	97
5.2.3.3 Discussion of the formation mechanism of methyl-1,4-benzoquinone.....	99
5.2.3.4 Discussion of the formation of HNO ₃	100
5.2.4 Summary of results.....	101

<u>Chapter 6</u>	
Summary.....	103
<u>Appendix I</u>	
Syntheses.....	107
I.1 Synthesis of methyl nitrite (CH ₃ ONO).....	107
I.2 Synthesis of 6-methyl-2-nitrophenol.....	107
<u>Appendix II</u>	
Chamber wall loss rates for the compounds studied.....	108
<u>Appendix III</u>	
Gas-phase infrared absorption cross sections.....	109
III.1 Calibration method.....	109
III.2 FT-IR absorption cross sections and intergated cross sections of phenol and the cresol isomers.....	113
<u>Appendix IV</u>	
Correction of the formation yields of dihydroxy(methyl)benzene and (methyl)benzoquinone in the OH-initiated oxidation of phenol and cresol isomers.....	114
<u>Appendix V</u>	
Origin and purity of the chemicals and gases used.....	116
<u>References</u>	117

1.1 Introduction

Large quantities of volatile non-methane organic compounds (NMOCs) are emitted into the atmosphere from a variety of anthropogenic and biogenic sources. These emissions of organic compounds are involved in a complex series of chemical and physical transformation and removal processes in the atmosphere. The result of these processes is manifested in effects such as ozone formation in urban and rural areas as well as in changes of the global troposphere (Logan, 1985), long range transport of chemicals (Bidleman, 1988) and acid depositions (Schwartz, 1989). The formation of secondary particulate matter through gas/particle partitioning of both emitted chemical compounds and the atmospheric reaction products of NMOCs, nitrogen oxides, sulphur dioxide and organic-sulphur compounds (Pankow, 1987; Bidleman, 1988; Odum *et al.*, 1996; Odum *et al.*, 1997a, b) and global climate change (Atkinson, 1994) are also important effects of the physico-chemical transformation of all organic compounds emitted into the atmosphere.

In the troposphere, these NMOCs either undergo photolysis at wavelengths > 290 nm or can react with the hydroxyl (OH) and nitrate (NO_3) radicals and with ozone (O_3) (Atkinson, 1994). At certain times and locations reaction with the Cl atom may be important (Jobson *et al.*, 1994). Certain basic nitrogen-containing compounds (for example, amines) can react with gaseous nitric acid (HNO_3) to form the corresponding salts (Atkinson *et al.*, 1987).

Usually, organic compounds which are present in the atmosphere are partitioned between gas and particle phases, and the phase in which a chemical exists in the atmosphere can significantly influence its dominant tropospheric removal processes and lifetime (Bidleman, 1988; Finizio *et al.*, 1997).

A large amount of the experimental data concerning the chemical and physical behaviour of the organic compounds in the atmosphere has been obtained from laboratory and ambient air studies over the past three decades.

At the present stage of knowledge there exists an understanding, at varying levels of detail, of the atmospheric chemistry of the various classes of organic compounds emitted into the troposphere. As a result of intensive research over recent years, rate constants for the gas-phase reactions of a large number of NMOCs with OH radicals, NO₃ radicals and O₃ have been measured (Atkinson, 1986; Atkinson, 1989; Atkinson, 1991; Atkinson, 1994; Atkinson, 2000). Different methods (of varying reliability depending on the structure of the NMOCs) are available for the estimation of rate constants for NMOCs for which experimental data have not been obtained (Atkinson, 1987; Kwock and Atkinson, 1995).

In order to elucidate the effects of anthropogenic and biogenic emissions on the atmosphere, computer models incorporating the emissions rates, atmospheric chemistry and transport processes were developed (Carter, 1990; Stockwell *et al.*, 1997). Chemical mechanisms of varying levels of detail have been formulated and used as components of these computer modelling studies. The individual rate constants determined, reaction mechanisms proposed and product distributions from the multitude of elementary reactions which are supposed to occur in the atmosphere affect the accuracy of the chemical mechanisms used in different computer models (Derwent *et al.*, 1996).

A proper evaluation of the experimental laboratory studies (the results from theoretical and experimental studies of the kinetics, mechanisms and products analysis) should serve as a base of the current status of knowledge of atmospheric chemistry (Atkinson *et al.*, 1992b; Atkinson *et al.*, 1997). Using such reviews future experiments and/or theoretical studies should be designed. However, while the kinetics and mechanisms of the initial reaction of OH radicals, NO₃ radicals and O₃ with many NMOCs are understood, the products and mechanisms of the subsequent reactions of the initially-formed radicals are much less well understood (Atkinson, 1994).

In order to obtain a better understanding the impact of the emissions of NMOCs on the Earth's ecosystem, through effects such as deposition of NMOCs reaction products (including acidic species), in situ tropospheric formation of toxic air contaminants, the formation of photochemical air pollution on urban and regional scales, depletion of stratospheric ozone and the potential of atmospheric aerosols for global warming, new studies aimed at establishing the end reaction products and chemical mechanisms of the tropospheric degradation of NMOCs are necessary.

1.2 Phenol and cresols in the atmosphere

The occurrence of high levels of monocyclic aromatic hydrocarbons in the urban area are directly linked to anthropogenic activity. The importance of the contribution of aromatic hydrocarbons to problems of urban air pollution is well recognised today (Atkinson and Aschmann, 1994; Odum *et al.*, 1997a,b; Thürner *et al.*, 1998; Ciccioli *et al.*, 1999; Ackermann 2000; Calvert *et al.*, 2001).

Beside their carcinogenic and mutagenic effects on living organisms and human health (Shepson *et al.*, 1985; Dumdei *et al.*, 1988), the main importance of aromatic hydrocarbons with regard to air pollution is their role as precursors for the formation of photo-oxidants (Derwent *et al.*, 1996) and secondary organic aerosols (Odum *et al.*, 1997a,b; Forstner *et al.*, 1997; Kleindienst *et al.*, 1999; Hurley *et al.*, 2001). In a recent modelling study the contribution of aromatic hydrocarbons to the O₃ formation in Europe was estimated to be as high as 40% (Derwent *et al.*, 1998) which means that the aromatics should be considered as a very important hydrocarbon class with regard to photochemical O₃ formation.

Although the importance of aromatic hydrocarbons has been known for a considerable time, the mechanism of these reactions and the nature of the products formed are still the subject of extensive research efforts (Atkinson, 1994; Calvert *et al.*, 2001).

1.2.1 Sources and abundance

The major sources of phenol and cresol isomers into the atmosphere are from automobile exhaust, wood burning and industrial sources.

Emissions of 1900 and 2300 Tg yr⁻¹ phenol from automobile exhaust and wood burning, respectively, were estimated in 1985 (Lesh and Mead, 1985). Additionally, wood smoke (from fireplaces) and wood stoves contains high concentrations of phenol, cresols and semi-volatile and non-volatile methoxylated phenols (Hawthorne *et al.*, 1988; Hawthorne *et al.*, 1989). Since the total concentration of wood smoke phenols and methoxyphenols emitted from residential chimneys average ca 200 - 350 µg mg⁻¹ of particulate carbon (Hawthorne *et al.*, 1989), wood burning is expected to be the major source of atmospheric phenols in the winter. In a relatively recent study about collection and quantitation of semi- and non volatile phenolic compounds from winter urban air, a concentration of phenolic compounds in the range of 279 - 2410 ng m⁻³ was reported (Hawthorne *et al.*, 1992).

Rogozen *et al.* (1987) estimated an emission of 15 - 800 Tg yr⁻¹ phenol and cresols into the air from industrial sources. About 96% of the phenol produced in the USA and Europe is by oxidation of cumene, with estimated air emissions of, e.g. 1 Tg yr⁻¹ in California (Rogozen

et al., 1987). Phenol is used mainly in the manufacturing of phenolic resins (45%), bisphenol A (25%) and caprolactam (15%) (Grosjean, 1991).

Cresols are by-products of either tar distillation or naphtha cracking. A major source of indirect emissions of the cresols in the atmosphere is from coke ovens, since coal tar contains about 1% cresols. Industrial uses of cresols include the manufacturing of phenolic resin, tricresylphosphate and related products and pesticides. Cresols are also used as wire enamel solvents and as ingredients in disinfectants and cleaning products (Grosjean, 1991). Other uses include the manufacturing of food preservatives and anti-oxidants (*ortho*-cresol) and pesticides (*meta*- and *para*-cresol).

Information regarding ambient levels of phenol and cresols is very limited. Pellizzari (1979) measured up to 522 ppbC of phenol (mean value 102 ppbC) and 203 ppbC of *ortho*-cresol (mean value 42 ppbC) in Upland, Canada, in the vicinity of a phenolic resin factory. Similar values were obtained near industrial sources at several other locations in the USA, e.g. up to 2520 ppbC of phenol (mean value 468 ppbC) and 61.6 ppbC of *ortho*-cresol (mean value 26,6 ppbC) in El Paso, Texas (Pellizzari, 1979).

Recently, the emission data from road traffic indicated that phenol and the cresols account for less than 3% of the overall relative concentration of the VOCs measured for different locations and engine types (Kurtenbach *et al.*, 1999a; Kurtenbach *et al.*, 2000; Schmitz *et al.*, 2000). Table 1.1 shows the concentration of the oxygenated aromatic species which were measured in a traffic tunnel as well as in the city center of Wuppertal, Germany.

Table 1.1 Concentration of oxygenated aromatic compounds found in a tunnel and urban center of Wuppertal, Germany (Kurtenbach *et al.*, 1999a; Kurtenbach *et al.*, 2000).

oxygenated aromatic compounds	tunnel, ppbC	urban center, ppbC
phenol	0.3-17.5	0.12-2.16
<i>ortho</i> -cresol	≤ 1.8	≤ 0.98
<i>meta</i> -cresol	≤ 2.5	≤ 1.12
<i>para</i> -cresol	0.7-7.7	≤ 0.21

Urban values of these aromatic hydrocarbons are limited to data of Leuenberger *et al.* (1985) for Portland-Oregon, USA, of Kuwata *et al.* (1980) for Osaka, Japan, and of Hoshika and Muto (1978) for Nagoya, Japan. Results of these studies indicated a concentration in urban areas between 1.8 - 13.8 ppbC of phenol (mean 0.6 - 3.3 ppbC) and 0.35 ppbC of *ortho*-cresol (mean 0.21 ppbC). Information concerning abundance of *meta*- and *para*-cresol in urban areas are only available from Kurtenbach *et al.* (1999a,b) and Kurtenbach *et al.* (2000).

Phenol and the cresol isomers are polar molecules and have high solubilities in water, 18 - 82 g l⁻¹ at 25 °C (Lüttke and Levsen, 1997) and high vapour pressure, 0.12 - 0.34 torr at 25°C (Lüttke and Levsen, 1997), with high Henry's law constants, and are expected to be efficiently scavenged from the gas-phase by rain and fog. The study of Leuenberger *et al.* (1985) included simultaneous measurements of gas-phase, aerosol-phase and rainwater phenol concentrations. Values ranging between 0.2 - 9 µg l⁻¹ were measured for phenol in the rainwater at different locations (Leuenberger *et al.*, 1985; Kawamura and Kaplan, 1983; Kawamura and Kaplan, 1986; Lüttke *et al.*, 1997) and the concentration of cresols in the rainwater was estimated to be about 0.38 - 2 µg l⁻¹ (Leuenberger *et al.*, 1985). With a typical concentration of 2 - 9 µg l⁻¹, phenols are among the most abundant organic compounds in rainwater (Richartz *et al.*, 1990; Grosjean, 1991; Belloli *et al.*, 1999).

1.2.2 In situ formation and removal processes

Phenol and cresols can be formed in the atmosphere by gas-phase and liquid-phase reactions involving alkylbenzenes. Unfortunately, the importance of these reactions in urban air has not yet been assessed by means of direct field measurements, only laboratory studies of reaction kinetics and products are available (Atkinson, 1994).

Phenol is a major product of the reaction of OH with benzene in the gas phase with a molar yield of about 25% (Atkinson *et al.*, 1989; Bjergbakke *et al.*, 1996; Berndt *et al.*, 1999). It is followed by nitrobenzene (3.36% molar yield) (Atkinson *et al.*, 1989) and ring-opening products such as glyoxal (21% molar yield) (Tuazon *et al.*, 1986). Unpublished results indicate that the actual yield of phenol from the oxidation of benzene may be as high 50% and that other measurements may have been affected by the high concentrations of NO used in the systems (Volkamer *et al.*, 2001). This result still has to be validated by further investigation.

Cresol has been reported to account for 15 - 42% of the products from the reaction of the OH radical with toluene (Atkinson *et al.*, 1989; Klotz *et al.*, 1998; Smith *et al.*, 1998) with the 3 most recent publications agreeing on a value of about 20%. Because of the *ortho* - *para* orientation effect of the CH₃ group, addition of OH to the toluene aromatic ring takes place preferentially at the C₂ (*ortho*) and C₄ (*para*) carbon atoms. The expected relative abundance of the three cresol isomers is thus *ortho* > *para* > *meta*. While *ortho*-cresol has indeed been identified as a major reaction product of toluene by several groups, little data exists concerning the yields of the other two isomers. The available information concerning the cresol isomers distribution is summarised in Table 1.2. *Ortho*-cresol accounts for about 80% of the total cresols formed in the toluene - OH reaction.

The precursor of cresols in the polluted atmosphere, toluene, is one of the most abundant aromatic compounds in urban air, accounting for approximately 6% of the observed

non-methane hydrocarbons (Jeffries, 1995). This reflects, to some extent, the high aromatic content of unleaded fuels. Recent studies of ambient levels of hydrocarbons in the USA and West Europe (Fujita *et al.*, 1997; Kurtenbach *et al.*, 1999a; Kurtenbach *et al.*, 2000) shows a toluene concentration of 19 - 33 ppbC. With reported cresol yields of 15 - 42% of the reacted toluene, 2.8 - 14 ppbC per day of cresols may be produced in situ during smog episodes.

Table 1.2 Cresol isomer distribution from toluene.

reference	<i>ortho</i> -cresol	<i>meta</i> -cresol	<i>para</i> -cresol
Atkinson <i>et al.</i> , 1980	+ ^a	n.d.	n.d.
Atkinson <i>et al.</i> , 1989	81%	(<i>m+p</i>) unresolved = 19%	
Smith <i>et al.</i> , 1998	80%	-	20%
Klotz <i>et al.</i> , 1998	67%	15%	18%

^a identified, isomer yield not reported;
n.d. undetermined.

Table 1.3 gives an overview of the rate constants of the potential atmospheric loss processes of phenolic compounds, i.e. reaction with OH and NO₃ radicals, reaction with O₃.

Table 1.3 Room temperature rate constants for the gas-phase reactions of OH and NO₃ radicals and O₃ with phenol and with cresols (Calvert *et al.*, 2001).

	OH		NO ₃		O ₃	
	k x 10 ¹¹ cm ³ molecule ⁻¹ s ⁻¹	τ h	k x 10 ¹² cm ³ molecule ⁻¹ s ⁻¹	τ min	k x 10 ¹⁹ cm ³ molecule ⁻¹ s ⁻¹	τ d
phenol	2.7	6.4	3.8	8.1	-	-
<i>ortho</i> -cresol	4.1	4.2	14	2.2	3	18
<i>meta</i> -cresol	6.8	2.5	11	2.8	2	24
<i>para</i> -cresol	5.0	3.4	11	2.8	5	10

Using the kinetic data in Table 1.3, in combination with an average tropospheric OH radical concentration of [OH] = 1.6 x 10⁶ cm⁻³ (Crutzen and Zimmermann, 1991; Prinn *et al.*, 1992) and a NO₃ radical concentration of [NO₃] = 5.4 x 10⁸ cm⁻³ (Platt and Heintz, 1994) estimated atmospheric residence times τ of phenols due to reaction with OH during the daytime and with NO₃ during the night-time, can be calculated. The residence times thus obtained are presented in Table 1.3. Thus, phenol and cresol isomers, are expected to be rapidly removed from the atmosphere by their reaction with OH and NO₃ radicals. Removal by reaction with O₃ is of minor importance, accounting for only up to 5% of the total cresol removal processes at O₃ levels of ≥ 0.1 ppm. Photolysis of phenol and cresols is negligible.

An additional sink of phenolic compounds in the atmosphere is removal by wet and dry deposition. The partitioning of phenol between gas, liquid and particulate phases has been investigated in theoretical studies and in field measurements (Pankow, 1987; Schwarzenbach *et al.*, 1988; Lüttke and Levsen, 1997).

1.3 Status of knowledge

1.3.1 Product and mechanistic studies on the reactions of the OH radical with phenols

In the literature, observations of nitrophenols, pyruvic acid, acetaldehyde, formaldehyde (HCHO), acetyl peroxyxynitrate (PAN) and various particulate nitro-aromatic products have been reported from the OH radical initiated oxidation of phenols (Grosjean, 1984; Grosjean, 1985; Atkinson *et al.*, 1992a). Most of the reported product yields are very low, with the nitro compounds accounting for a maximum of 10% of the oxidation products. The major products of the OH-initiated oxidation of phenols are consequently still unknown. Formation yields are available mostly for one class of products, nitrophenols. Tables 1.4 gives an overview of the published product data from studies on the OH radical initiated oxidation of phenol and the cresol isomers.

Table 1.4 Molar yields of gas-phase products from the reaction of OH radicals with phenolic compounds.

reactant	product	yield (%)	reference
phenol	2-nitrophenol	6.7 ± 1.5	Atkinson <i>et al.</i> , (1992a)
<i>ortho</i> -cresol	pyruvic acid	0.8	Grosjean, (1984)
	carbonyl compounds ^a	$5 \div 11$	Grosjean, (1984)
	6-methyl-2-nitrophenol	identified	Grosjean, (1984)
	nitrocresols ^b	5.1 ± 1.5	Atkinson <i>et al.</i> , (1992a)
<i>meta</i> -cresol	4-methyl-2-nitrophenol	$4.9 \div 11$	Grosjean, (1985)
	3-methyl-2-nitrophenol	1.6 ± 1.0	Atkinson <i>et al.</i> , (1992a)
	5-methyl-2-nitrophenol	1.6 ± 1.0 ^c	Atkinson <i>et al.</i> , (1992a)
<i>para</i> -cresol	4-methyl-2-nitrophenol	10 ± 4	Atkinson <i>et al.</i> , (1992a)

^a sum of acetaldehyde, formaldehyde and acetyl peroxyxynitrate; ^b sum of 6-methyl-2-nitrophenol (major) and 6-methyl-4-nitrophenol (minor); ^c estimated yield.

It can be observed from Table 1.4 that the formation yields of the nitrophenols are low. Although, it is conceivable that they are formed in the OH radical initiated oxidation of phenols, they may also be artefacts of the fast reaction of phenols with NO_3 radicals. NO_3 radicals can be formed in significant quantities in aromatic hydrocarbon- NO_x photo-oxidation systems (Carter *et al.*, 1981; Grosjean, 1984; Klotz *et al.*, 1998).

Under the conditions of the Grosjean (1984) study, a computer simulation study of the experimental data of a *ortho*-cresol- NO_x mixture, using the model of Leone and Seinfeld (1984) indicated about 65% removal by reaction with OH, about 30% by reaction with NO_3 and about 5% by reaction with O_3 .

The experiments of Atkinson *et al.* (1992a) employed $\text{CH}_3\text{ONO-NO}$ -aromatic-air mixtures, and the conditions for which NO_3 became important were easy to identify. Under tropospheric conditions of low NO_x concentrations (in contrast to most laboratory studies), nitrophenols are not expected to be formed in significant yields.

Atkinson *et al.* (1992a) concluded from a product study together with the estimated rate constant for H-atom abstraction from the OH group of phenol that the OH initiated photo-oxidation of phenol in the presence of NO_x proceeds by both OH radical addition to the aromatic ring and by H-atom abstraction from the substituent OH. Figure 1.1 shows the postulated reaction mechanism for the oxidation of phenol by OH radicals. The percentages given for the two reaction pathways are those calculated by Atkinson (1989) at 298 K.

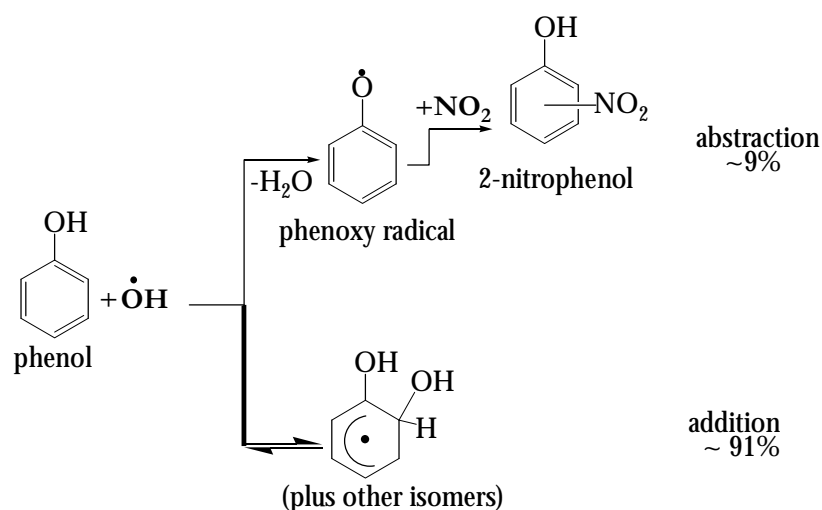


Figure 1.1 The OH-initiated photo-oxidation of phenol

Nitrophenol formation can occur essentially only from the phenoxy radical. By analogy with the OH initiated oxidation of benzene, toluene and the xylene isomers in the presence of NO_x (Atkinson *et al.*, 1989; Atkinson *et al.*, 1991), nitrophenol formation

subsequent to OH radical addition to phenol and the cresols is expected to be of minor importance and may be expected to give non-*ortho* nitro-substituted isomers (Atkinson, 1989).

The sequences of reactions initiated by reaction of OH with *ortho*-cresol is given in Figure 1.2 which summarises a tentative mechanism based largely on experimental and computer kinetic modeling studies of the toluene-NO_x system. It is postulated to apply to *ortho*-cresol as well (Grosjean, 1991).

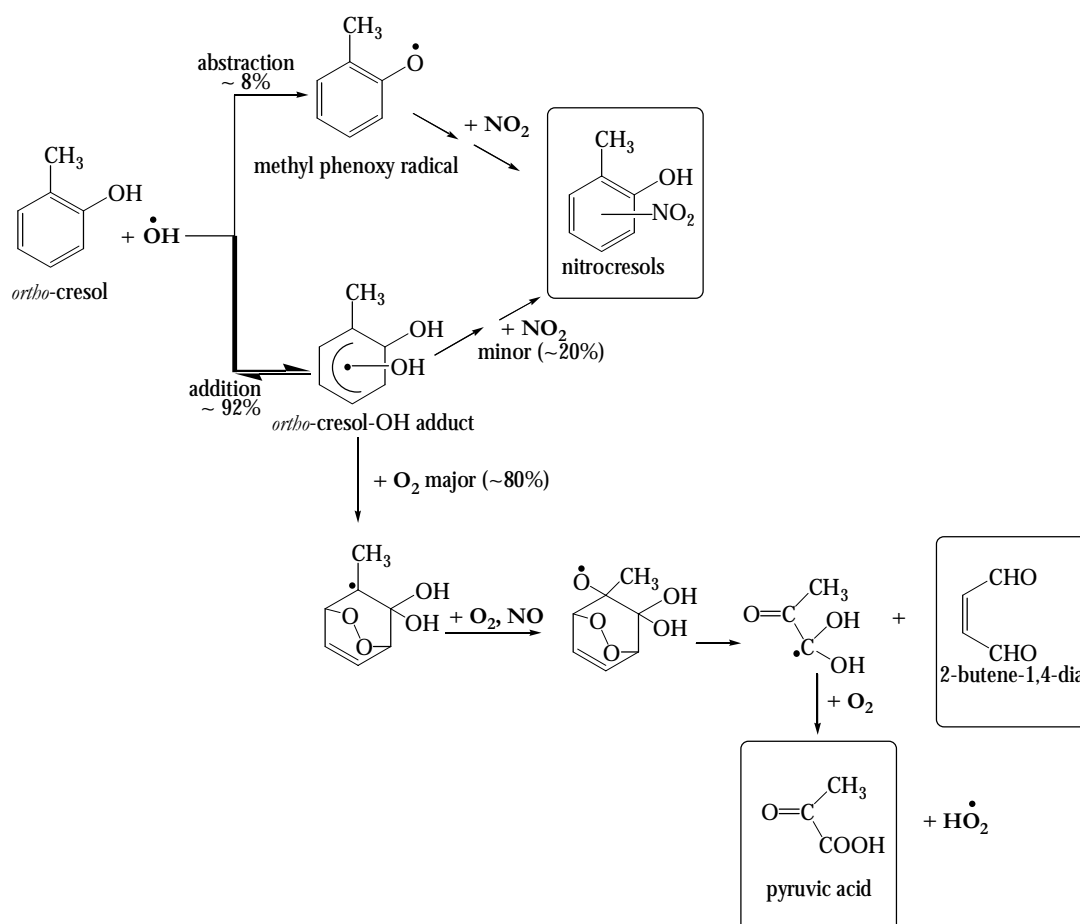


Figure 1.2 Tentative photo-oxidation mechanism for *ortho*-cresol.

At ambient temperatures, OH addition to the aromatic ring, with predicted OH addition preferentially on the hydroxy-substituted carbon atom, is thought to account for about 90% of the overall OH-radical reactions with *ortho*-cresol (Grosjean 1984). Further reactions of the OH - *ortho*-cresol adduct include reaction with NO₂ (minor, about 20%) to form nitrocresols and reaction with molecular oxygen (major, about 80%) to form a bicyclic peroxy alkyl radical. By analogy with other alkyl radicals, the bicyclic peroxy alkyl radical is expected to react with oxygen to form a bicyclic peroxy alkyl peroxy radical, which in turn reacts with NO to form NO₂ and a bicyclic peroxy alkoxy radical. Further reactions of the bicyclic peroxy alkoxy radical include β-scission fragmentations of the aromatic ring, leading

to the aliphatic carbonyl products *Z*-2-butene-1,4-dial (CHOCH=CHCHO) and pyruvic acid (CH₃C(O)COOH). As noted above, there is still considerable uncertainty regarding the exact nature and relative importance of the pathways leading to “ring-retaining” and “ring-cleavage” products.

Abstraction pathway kinetic studies at 298 K, indicate that the H-atom abstraction process accounts for about 7 - 8% of the overall OH radical reaction for *ortho*-cresol (Atkinson, 1989).

1.3.2 Product and mechanistic studies on the reactions of the NO₃ radical with phenols

Observation of nitrophenol formation from the NO₃ radical initiated oxidation of phenols has previously been reported by Grosjean (1985), Atkinson *et al.* (1992a) and Bolzacchini *et al.* (2001). Table 1.5 gives an overview of the formation yields of the nitrophenols identified in studies on the reaction of the NO₃ radical with phenol and the cresol isomers.

Table 1.5 Molar product yields from the reaction of NO₃ radicals with phenolic compounds.

reactant	product	yield (%)	reference
phenol	2-nitrophenol	25.1 ± 5.1	Atkinson <i>et al.</i> , (1992a)
		58.8 ± 9.4	Bolzacchini <i>et al.</i> , (2001)
	4-nitrophenol	27.6 ± 7.9	Bolzacchini <i>et al.</i> , (2001)
<i>ortho</i> -cresol	6-methyl-2-nitrophenol	2.4 ÷ 22.7 ^a	Grosjean, (1985)
	6-methyl-4-nitrophenol		
	6-methyl-2-nitrophenol	12.8 ± 2.8	Atkinson <i>et al.</i> , (1992a)
	6-methyl-2,4-dinitrophenol	detected	Grosjean, (1985)
<i>meta</i> -cresol	3-methyl-2-nitrophenol	16.8 ± 2.9	Atkinson <i>et al.</i> , (1992a)
	5-methyl-2-nitrophenol	19.6 ± 3.6	Atkinson <i>et al.</i> , (1992a)
<i>para</i> -cresol	4-methyl-2-nitrophenol	74 ± 16	Atkinson <i>et al.</i> , (1992a)

^asum of 6-methyl-2-nitrophenol and 6-methyl-4-nitrophenol

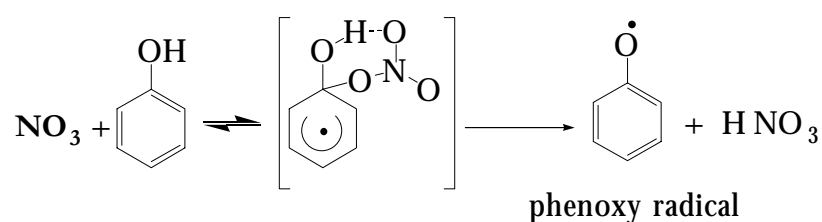
As seen from Table 1.5, where comparison is possible, there are significant differences in the reported nitrophenol yields between the three studies. From Table 1.5 it can be seen that, with the exception of phenol and *para*-cresol, the observed products account for only a modest fraction of the loss of the parent aromatic compound.

Grosjean (1985) observed a combined yield of 6-methyl-2-nitrophenol and 6-methyl-4-nitrophenol in the NO_3 +*ortho*-cresol reaction which varied over the range 2.4 to 22.7%. In this study no information was given concerning the individual yields of the two methyl-nitrophenol isomers. Detection of a dinitrocresol (2-methyl-4,6-dinitrophenol), 6-methyl-2-nitrophenol and 6-methyl-4-nitrophenol in the aerosol phase was also reported by Grosjean (1985).

Atkinson *et al.* (1992a) reported the formation of 2-nitrophenol (from phenol), 6-methyl-2-nitrophenol (from *ortho*-cresol), 3-methyl-2-nitrophenol and 5-methyl-2-nitrophenol (from *meta*-cresol) and 4-methyl-2-nitrophenol (from *para*-cresol).

In the study of Bolzacchini *et al.* (2001) on the NO_3 -radical initiated oxidation of phenol, identification of the oxidation products was performed using FT-IR spectroscopy. Two different NO_3 radical sources were used in this work: the thermal decomposition of N_2O_5 and in situ NO_3 radical generation by reaction of O_3 with NO_2 . Bolzacchini *et al.* (2001) observed differences in the product formation when using the 2 different means of generating NO_3 . They observed 2-nitrophenol as major product with a yield of $(58.8 \pm 9.4)\%$ when the thermal decomposition of N_2O_5 was used as a source of NO_3 radicals. When the reaction of the O_3 with NO_2 was used as an in situ NO_3 radical source they also observed formation of 4-nitrophenol but with a yield of $(27.6 \pm 7.9)\%$. Bolzacchini *et al.* (2001) concluded that the formation of the 2-nitrophenol isomer is favoured compared to the 4-nitrophenol isomer and, moreover, the formation of the 4-nitrophenol is only observed when O_3 is present in the reaction mixture.

The NO_3 radical reactions with phenols have been postulated to proceed via an overall H-atom abstraction mechanism which occurs after NO_3 radical addition to the aromatic ring, through the intermediacy of a six-membered transition state (Atkinson *et al.*, 1992a):



The initial NO_3 radical addition to the aromatic ring is expected to be reversible because of the short lifetime of the NO_3 -adduct with respect to its thermal decomposition back to reactants (Atkinson *et al.*, 1990). A decomposition rate for the NO_3 -monocyclic aromatic adducts of $\sim 5 \times 10^8 \text{ s}^{-1}$ at 298 K has been estimated (Atkinson, 1991).

As discussed by Atkinson *et al.* (1992a), from the simple mechanistic picture presented above one would expect to observe nitrophenolic products in a combined yield of 100%. As seen from Table 1.5, with the exception of the product study of phenol and *para*-cresol, this is

not found. These observations indicate that the NO_3 radical reaction with phenols are more complex than previously thought and that other reaction pathways, possibly involving ring cleavage, occur. Clearly, there are one or more significant reaction channels (perhaps involving opening of the ring) which are unknown at present.

1.4 Aim of the work

The occurrence of phenol and the cresols in the urban atmosphere are mainly linked to anthropogenic activity with recent studies showing substantial emissions from automobile exhaust. In situ formation of phenolic compounds (from benzene, toluene, xylene isomers, mesitylene, i.e. BTXM) is also an important source in polluted air. However, both phenol and the cresol isomers are rapidly removed by reaction with OH and with NO_3 radicals.

Since phenols are important products of the OH radical initiated oxidation of benzene and its methylated derivatives, the gas phase reaction of the phenolic compounds with both OH and NO_3 radicals have been studied only to a limited extent and the reaction pathways and the products are still uncertain.

Due to the importance of phenol and the cresols as oxidation products of benzene and toluene, respectively, and the lack of information on their subsequent fate, further investigations on their atmospheric chemistry are needed. To address these needs the following investigations have been performed:

- Kinetic investigations on the reaction of the OH radical with dihydroxy(methyl)benzenes and (methyl)benzoquinones which are expected oxidation products of the photo-oxidation of phenols.
- Investigations of the product distribution from the OH and NO_3 radicals initiated oxidation of phenol and the cresol isomers under simulated atmospheric conditions.

Experimental section

The experiments were carried out in an 1080 l quartz glass reactor at the University of Wuppertal and in the European photoreactor EUPHORE, Valencia/Spain, a large volume outdoor smog chamber which is operated under conditions similar to those in the real atmosphere.

The photolysis of methyl nitrite (CH_3ONO) was used as the OH radical source. The reaction of O_3 with NO_2 was used to generate NO_3 radicals. The chemicals were used without further purification.

2.1 Reaction chambers

2.1.1 1080 l quartz glass reactor

A detailed description of the 1080 l quartz glass reactor can be found in the literature (Barnes *et al.*, 1994). Only a brief description of the chamber is given below. Figure 2.1 shows a schematic representation of the reaction chamber.

The reactor consists of two tubes connected by a central flange, has a length of 6.2 m and an inner diameter of 0.47 m and is closed at both end by aluminium flanges. The reactor can be evacuated to a pressure of $< 10^{-3}$ mbar by a turbo molecular pump system. To ensure

homogeneous mixing of the reactants, three fans with Teflon blades are mounted inside the reactor.

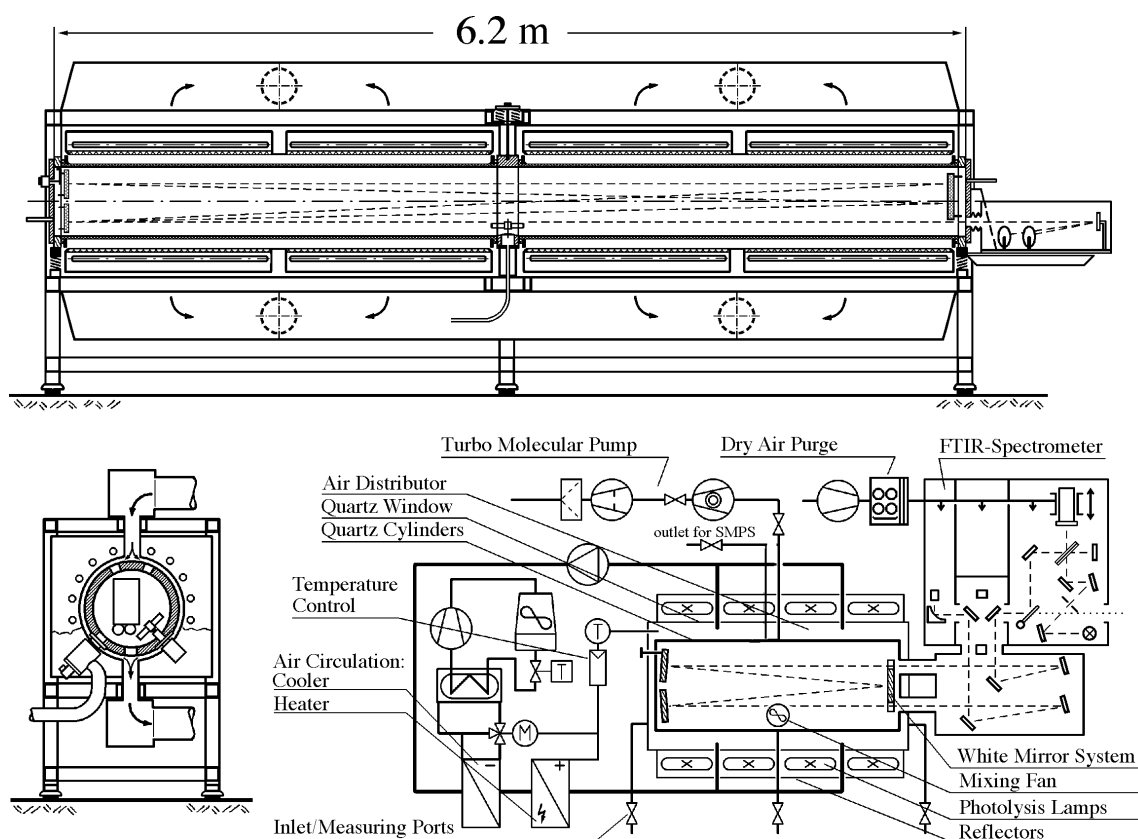


Figure 2.1 Schematic representation of the 1080 l quartz glass reactor.

For the photolysis, 32 superactinic fluorescent lamps (Philips TL 0.5 W), which are evenly spaced around the reaction vessel, were employed. These lamps emit light in the wavelength region from 320 nm to 480 nm, with a maximum intensity at 360 nm. The chamber is equipped with a White type multiple-reflection mirror system with a base length of (5.91 ± 0.01) m for sensitive in situ long path absorption monitoring of reactants and products in the IR spectral range. The White system was operated at 82 traverses, giving a total optical path length of (484.7 ± 0.8) m. The IR spectra were recorded with a spectral resolution of 1 cm^{-1} using a Bruker IFS 88 FT-IR spectrometer, equipped with a liquid nitrogen cooled mercury-cadmium-tellurium (MCT) detector.

Both end flanges contain inlet systems for reactants and bath gases, pressure and temperature measuring instruments. An outlet port for particle sampling is located in the central flange of the reactor.

2.1.2 EUPHORE chamber

The European photoreactor (EUPHORE), a large scale outdoor smog-chamber is integrated into the Centro de Estudios Ambientales del Mediterraneo (CEAM) in Valencia (Spain). A detailed description of the European photoreactor (EUPHORE) facilities can be found elsewhere (Becker, 1996). A brief description of the chambers, including only the analytical instrumentation used in the present work, is given below.

Figure 2.2 shows chamber A from the EUPHORE facility. Each chamber consists of a half spherical FEP (fluorine ethene propene) foil mounted on aluminium floor panels and each has a volume of about 204 m³. The foil is highly transparent even to short wavelength sunlight, with transmissions ranging from 85% in the range 500 - 320 nm to > 75% at 290 nm. In order to avoid unwanted heating of the chamber, the aluminium floor panels are fitted with an active cooling system designated to keep their temperature constant even during long irradiation periods in summer time. This allows realistic atmospheric temperature conditions to be maintained during experiments.

When not in use or for dark chemistry experiments, the chambers are protected by hydraulically operated steel housings.

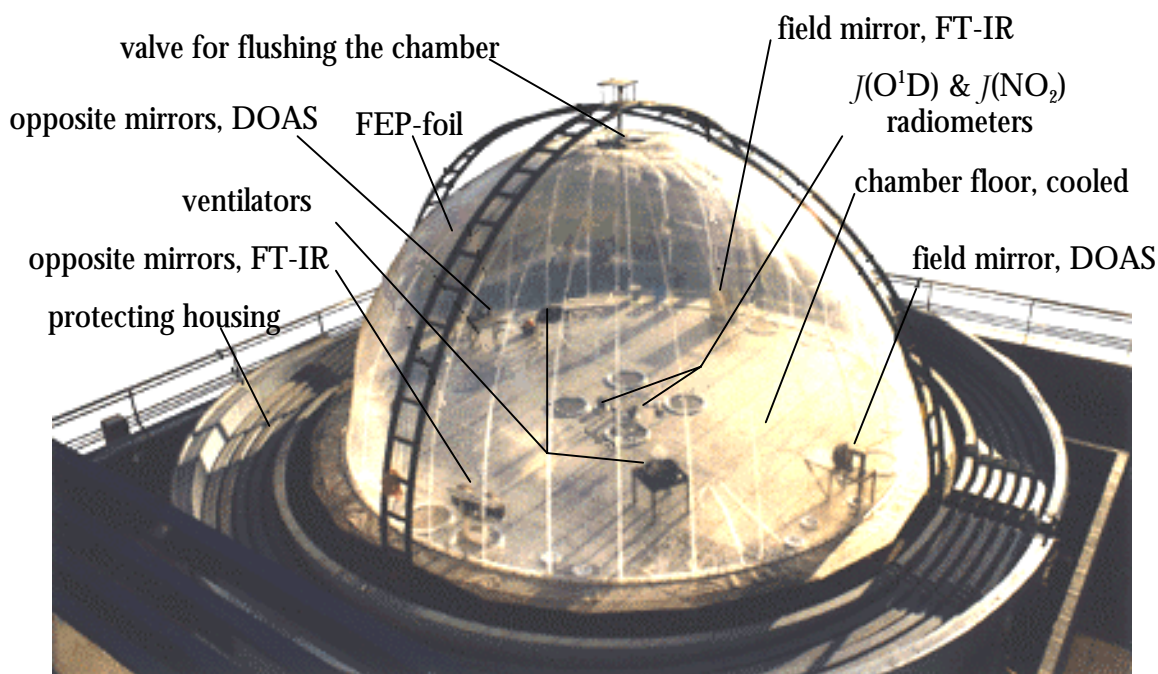


Figure 2.2 The EUPHORE photoreactor (chamber A).

The inlet and outlet ports and other accessories (mixing fans, analytical instruments, mechanical excess pressure valves) are located on the floor in order that the chamber surface is free for light entry. Integrated on the flanges are ports for the input of reactants and sampling lines for the different analytical instruments.

Each chamber can be filled with air from a separate air purification system. A screw compressor (Mannesmann, Type Ralley 110 AS) is used for pressurising. After the compressor, the air is passed through a condensate trap to separate the air from oil and water. The air is dried in adsorption dryers (Zander, Type HEA 1400) with an air throughput of ca. 500 m³ h⁻¹. With this procedure a dew point of - 70°C is reached and the CO₂ content is reduced. With help of a special charcoal adsorber NO_x (NO_x = NO + NO₂) is eliminated and oil vapour and non-methane hydrocarbons are reduced to ≤ 0.0003 mg m⁻³. The air flow into the chamber is controlled with a magnetic valve and is measured with help of a volumetric meter.

In addition to conventional analytical instrumentation (GC, GC-MS, HPLC, O₃, NO_x and NO_y analysers, actinometers for *J*(O¹D) and *J*(NO₂)) the chamber is equipped with state-of-the-art in situ measurement techniques (DOAS – Differential Optical Absorption Spectroscopy; FT-IR – Fourier Transform InfraRed Spectroscopy with long path absorption; TDL – Tuneable Diode Laser). The long path absorption system is a White arrangement with a base length of 8.17 m, giving a total optical path length of 326.8 m in Chamber A and 550 m in Chamber B.

Aerosol formation can be monitored by using a Scanning Mobility Particle Sizer (SMPS) instrument (TSI 3934), consisting of an electrostatic classifier (TSI 3071 A) and a condensation particle counter (TSI 3022 A). The sample line is a straight ¼ inch stainless steel tube of 1.5 m length. The sampling site is located ca 0.5 m above the chamber floor and about 1 m away from the FEP wall.

2.2 Generation of radicals

2.2.1 OH radicals

The photolysis of CH₃ONO-NO-air mixtures was used as the OH radical source in the experiments performed in the 1080 l quartz glass reactor.

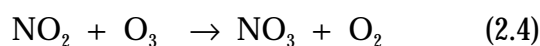
The photolysis of methyl nitrite (CH₃ONO), in the wavelength region 300-400 nm, in the presence of NO leads to the production of OH radicals through the reaction sequence:



Using the photolysis of methyl nitrite, OH radical concentrations of about 1×10^8 molecule cm^{-3} can be readily obtained for time scales of 10 min or more (the time being limited by the photolytic lifetime of methyl nitrite (Atkinson, 1998). The advantage of CH_3ONO as an OH radical precursor is that methyl nitrite is easy to synthesise in pure form. It can be readily stored for indefinite periods of time (see Appendix I.1 for the procedure of synthesis). Inclusion of NO in the reaction mixture is generally used to enhance OH production and to suppress the formation of O_3 and, hence, of NO_3 radicals.

2.2.2 In situ generation of NO_3 radicals

Reaction of O_3 with NO_2 , leading to NO_3 radical formation:



was used for in situ generation of NO_3 radicals in both the 1080 l quartz glass reactor and the EUPHORE chamber. O_3 was produced by a corona discharge in O_2 using commercial ozone generators.

2.2.3 Cl radicals

In order to elucidate the importance of particular pathways some additional experiments with chlorine atoms were performed. Photolysis of Cl_2 using superactinic fluorescent lamps (Philips TL 05/40W: $320 < \lambda < 480\text{nm}$, $\lambda_{\text{max}} = 360\text{nm}$) was employed as the source of Cl atoms:



2.3 Typical experimental procedure

2.3.1 Experiments in the 1080 l quartz glass reactor

The reactants can be introduced into the reaction chamber by two different inlets, depending mostly on their state (solid, liquid and gaseous) and on their vapour pressure. The liquid and gaseous reactants (see Appendix V) were injected directly into the reaction chamber using calibrated gas-tight syringes via inlet ports located on one of the flanges. Solid compounds (see Appendix V) were introduced into the chamber by using a special inlet

system which is also located on an end flange. This inlet system consists of a long glass tube, which has a small glass container attached in the middle where weighed amounts of the substances can be added. One port of this inlet system is connected to the synthetic air or nitrogen bottle by a Teflon tube and the second port is connected to the reaction chamber through a steel tube and special valve. The solid compounds are then heated in the small glass container until a certain pressure is reached. The content of the glass container is then added into the evacuated reaction chamber by opening the valve and helped with a slow flow of the diluent gas (synthetic air or N₂). In order to avoid condensation of these semi-volatile compounds onto the inlet system, the inlet system was heated using an electrical heating band.

The concentrations of compounds were determined by computer-aided subtraction of reference calibrated spectra. The infrared spectral range where the compounds were monitored are presented in Appendix III. The values of the FT-IR absolute and/or integral cross sections that have been used in the quantification procedure are also given in Appendix III.

The source of the chemicals used and their stated purity are presented in Appendix V. Not all the products identified in this work were commercially available, i.e. 6-methyl-2-nitrophenol. The synthesis of 6-methyl-2-nitrophenol is described in Appendix I.2.

2.3.1.1 Control experiments

In order to calculate the yield of the products formed in oxidation mixtures, it is necessary to know how much of the parent compounds and oxidation products are lost by chemical reactions which occur in the system and how much by other additional loss processes.

For all the investigated compounds control experiments have been performed. These experiments were designed to measure the wall loss rate and/or the combined loss rate for wall deposition and photolysis. Typically the desired amount (about 0.5 ppm) of the compound was introduced alone into the reaction chamber, synthetic air as diluent gas was added to a total pressure of around 1000 mbar. The gas mixture inside the chamber was then left for 1 min to ensure homogeneous mixing of the reactants.

The decay of the compound was monitored using its IR absorption. Spectra were recorded by co-adding 128 scans per spectrum over a period of 2 min and collecting 15 such spectra during 30 min with and without light. The results of these types of experiments are presented in Appendix II.

2.3.1.2 OH radical experiments

2.3.1.2.1 Kinetic experiments on dihydroxy(methyl)benzenes and (methyl)benzoquinones

All of the experiments aimed at the determination of rate constants were performed at 1000 mbar total pressure of synthetic air and temperatures of 300 ± 2 K. The photolysis of CH_3ONO in the presence of NO and synthetic air was used as the OH radical source. As reference organic compounds isoprene, 1,3-butadiene and *E*-2-butene have been used.

Starting concentrations were typically 5×10^{13} molecule cm^{-3} for CH_3ONO and 2.5×10^{14} molecule cm^{-3} for NO. NO was added in high concentrations in order to eliminate any possible formation of O_3 and NO_3 radicals. Both O_3 and NO_3 radicals would significantly falsify the results of the kinetic study, since O_3 is known to react with the reference hydrocarbons, notably *E*-2-butene, while NO_3 radicals are known to react rapidly with hydroxylated aromatic hydrocarbons.

The starting concentrations of the reactants (1,2-dihydroxybenzene, 1,2-dihydroxy-3-methylbenzene, 1,2-dihydroxy-4-methylbenzene, 1,4-benzoquinone, methyl-1,4-benzoquinone) and the organic reference compounds were in the range from 2 to 6×10^{13} molecule cm^{-3} .

The concentration-time behaviour of the studied compounds and the organic reference compounds was followed over 30 min time periods by FT-IR spectroscopy. Spectra were obtained by co-adding 128 scans which yielded a time resolution of 2 min.

2.3.1.2.2 Gas-phase product study experiments

The experiments to determine the gas-phase oxidation product from the OH radical initiated oxidation of phenol and cresol isomers were performed at 1000 mbar total pressure synthetic air and 298 ± 2 K.

The experimental procedure was as follows. After the background was recorded, the chamber was evacuated and flushed using synthetic air. Reaction mixtures consisting of phenol (or cresol isomers), CH_3ONO and NO in 1000 mbar of synthetic air were introduced into the chamber using the inlet systems presented in Section 2.3.1 and the photo-oxidation initiated by switching on the lamps. Reactants and products were monitored by FT-IR over a time period of 30 min.

2.3.1.3 NO₃ radical experiments

Nitrate radical reactions were carried out at 298 ± 2 K and atmospheric pressure. NO₃ radicals were generated in situ as was described in Section 2.2.2. O₃ was produced by photolysis of O₂ at 184.9 nm using an ozone generator with a quartz glass envelope.

After the background was recorded, the chamber was evacuated and flushed using synthetic air. Reaction mixtures consisting of phenol (or cresol isomers) and NO₂ in 1000 mbar of synthetic air were first introduced into the chamber. Monitoring of the reactants with the in situ FT-IR system was then commenced. Spectra were derived from 64 co-added interferograms. After one recorded spectrum, which yielded a time resolution of 1 min, O₃ was added for 1 min directly into the chamber through a Teflon line. The experiment runs were over 30 min time periods.

2.3.2 Experiments in the EUPHORE chamber

In September 1998 and May 1999 eight dark experiments were performed on the NO₃ radical initiated oxidation of phenol and cresol isomers to identify the oxidation products: phenol (3 experiments), *ortho*-cresol (2 experiments), *meta*-cresol (one experiment) and *para*-cresol (2 experiments). These experiments were performed in chamber A of EUPHORE.

The experimental procedure was as follows. First, the chamber was flushed with purified air for approximately 12 - 15 h before the start of the experiment in order to clean the chamber after the last experiment. Before starting to record the background spectrum the chamber valve was closed and the mixing fans were switched on. In order to measure the temperature, pressure, NO_x concentration and ozone, all the analytical instruments collecting data were started. All data were collected by a data acquisition system. A background spectrum was obtained under this condition. The background spectrum was derived from 600 co-added interferograms.

NO₂ was injected by means of a syringe into a glass tube (impinger) connected to the chamber by a Teflon line. The gaseous compound was introduced into the chamber by flowing 4 l min⁻¹ of purified air through the glass tube. O₃, produced by the photolysis of O₂ at 184.9 nm using a Pen-ray low-pressure mercury lamp, was added directly to the chamber through a Teflon line.

The phenolic compounds were added to the chamber using a spray inlet system. Prior to injection a weighed amounts of phenol (or cresol isomers) was first dissolved in 5 ml CH₃CN.

Each experiment on a phenol(or cresol)-NO₂-O₃ mixture was carried out over a period of approximately 5 - 7h in darkness using in situ FT-IR absorption. Infrared spectra were derived from 210 scans which yielded a time resolution of 3.5 min.

An additional sink for the phenolic compounds and their oxidation products in the chamber was surface deposition. The surface deposition rates were determined for phenol (or cresol isomers) by observing the decay of their IR absorption feature prior to addition of O₃ and NO₂. The oxidation product surface deposition rates were determined by observing the decay of their IR absorption feature after the experiments were concluded by adding a large amount of NO (~ 400 ppm) in order to ensure that O₃ and NO₃ radicals were removed from the reaction mixture.

Kinetic study of the reaction of OH radicals with dihydroxybenzenes and benzoquinones

The major products of the OH radical initiated oxidation of phenols are still unknown (Calvert *et al.*, 2001). It may be expected that, in analogy to the gas-phase formation of phenols from benzene, toluene and other methylated benzenes, the OH-initiated oxidation of these phenols leads to further hydroxylation of the aromatic ring (Atkinson *et al.*, 1989; Atkinson, *et al.*, 1991). This reaction would result in the formation of dihydroxybenzenes. Given the strongly *ortho*-directing effect of the HO groups of phenols, the predominant dihydroxybenzene isomers expected to be formed are 1,2-dihydroxybenzenes, also known as catechols.

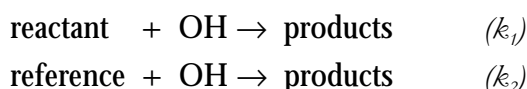
Essentially nothing is presently known about the atmospheric chemistry of 1,2-dihydroxybenzenes. The formation of benzoquinones has recently been observed in a chamber study of the photo-oxidation of alkylbenzenes, using GC-MS for detection of the products (Yu *et al.*, 1997). These (methyl)benzoquinones have been identified to be ring-retaining products from the OH radical initiated photo-oxidation of phenolic compounds in this work.

In order to determine the yields of the dihydroxy(methyl)benzenes which were found to be an important ring-retaining product in the OH radical initiated photo-oxidation of the phenolic compounds (this work), it was necessary to determine rate constants for the reaction of OH radicals with these compounds. In the present study the OH radical reaction rate constants of the other important products 1,4-benzoquinone and methyl-1,4-benzoquinone were also determined.

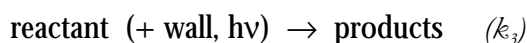
3.1 Data evaluation and results

In order to determine rate constants of the OH radical reaction with the dihydroxy(methyl)benzene and (methyl)benzoquinone compounds a relative rate method was used. The disappearance rates of the aromatic compounds and reference compounds were measured in the presence of OH radicals.

The OH radicals generated in the photolysis of CH₃ONO react with the reactant and the reference organic compounds in the reaction mixture.



Control experiments have shown that the reactants are also subject to losses in the absence of OH radicals, probably due to wall adsorption, with a possible minor contribution from photolysis.



No wall deposition and photolysis losses were observed for the reference hydrocarbons. Taking the above reactions into consideration results in the following rate laws for the compounds under investigation:

$$-\frac{d[\text{reactant}]}{dt} = k_1[\text{OH}][\text{reactant}] + k_3[\text{reactant}] \quad (3.1)$$

$$-\frac{d[\text{reference}]}{dt} = k_2[\text{OH}][\text{reference}] \quad (3.2)$$

Integration and combination of Equations (3.1) and (3.2) leads to:

$$\ln \frac{[\text{reactant}]_{t_0}}{[\text{reactant}]_t} - k_3(t - t_0) = \frac{k_1}{k_2} \ln \frac{[\text{reference}]_{t_0}}{[\text{reference}]_t} \quad (3.3)$$

where k_1 and k_2 are the rate constants for the reactions of the reactant and reference compounds with OH radicals, respectively. The terms $[\text{reactant}]_{t_0}$, $[\text{reactant}]_t$, $[\text{reference}]_{t_0}$ and $[\text{reference}]_t$ give the concentrations of the reactant and reference hydrocarbons at times t_0 (initial concentration) and t (during experiment).

Thus, plots of $\ln([\text{reactant}]_{t_0}/[\text{reactant}]_t) - k_3(t - t_0)$ as a function of $\ln([\text{reference}]_{t_0}/[\text{reference}]_t)$ for each individual reactant and reference hydrocarbon should yield a straight line with a slope k_1/k_2 . Hence, the rate constant, k_1 can be placed on an absolute basis using the known rate constant k_2 for the reference hydrocarbon.

Since several reference hydrocarbons have been employed in this study, realigning Equation (3.3) to give (3.4) appears to be useful:

$$\ln \frac{[\text{reactant}]_{t_0}}{[\text{reactant}]_t} - k_3(t - t_0) = k_1 \ln \frac{[\text{reference}]_{t_0}}{[\text{reference}]_t} / k_2 \quad (3.4)$$

According to this equation, a plot of $\ln([\text{reactant}]_{t_0}/[\text{reactant}]_t) - k_3(t - t_0)$ as a function of $\ln([\text{reference}]_{t_0}/[\text{reference}]_t)/k_2$ gives a straight line directly yielding k_1 as the slope.

Equation (3.4) allows the data for all reference hydrocarbons employed for one reactant to be plotted and evaluated simultaneously and gives a direct visual view of the quality of the agreement of the experimental data obtained from the different reference compounds.

In the present study three reference hydrocarbons have been employed: isoprene, 1,3-butadiene and *E*-2-butene. For the reaction rate constants of these compounds with OH radicals, values of $k_2 = (1.01 \pm 0.20) \times 10^{-10}$, $(6.69 \pm 1.34) \times 10^{-11}$ and $(6.32 \pm 1.26) \times 10^{-11} \text{ cm}^3 \text{ molecule}^{-1} \text{ s}^{-1}$ were used for isoprene, 1,3-butadiene and *E*-2-butene, respectively (Atkinson, 1994). These rate constants were assumed to be correct to within an error of $\pm 20\%$, as recommended by Atkinson (1994).

The rate constants k_1 were determined from the slopes of the straight lines plotted in Figures 3.1 to 3.5. All of the plots show good linearity. Generally, the corrections for wall loss were approximately 30% compared to reaction with OH. Compared to the walls loss, losses due to photolysis were negligible ($\sim 3 - 5\%$).

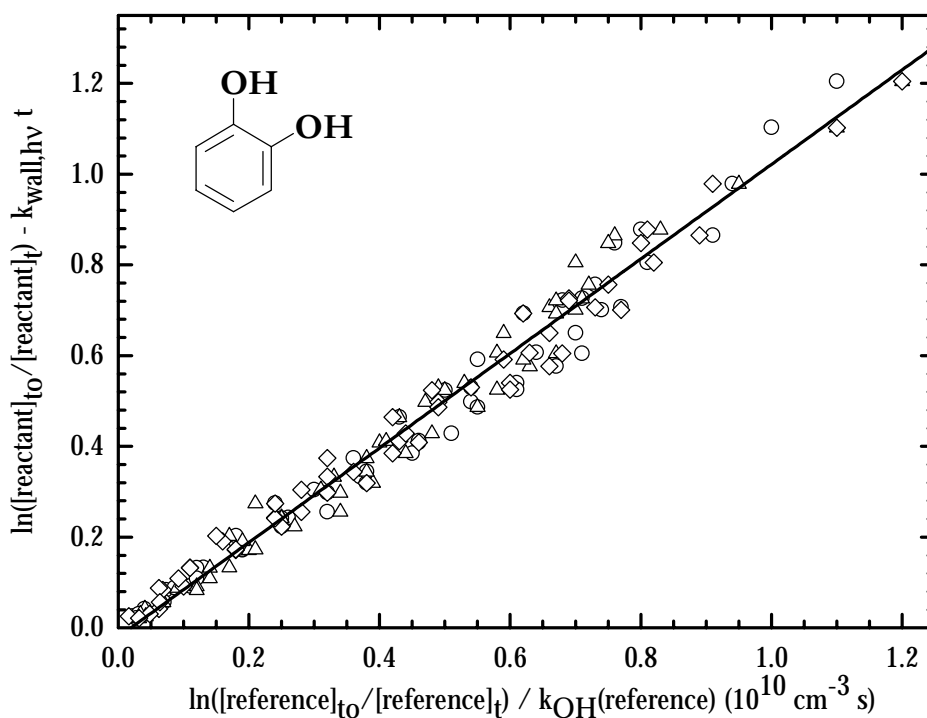


Figure 3.1 Plot according to eq. (3.4) for the reaction of 1,2-dihydroxybenzene with OH radicals. Reference hydrocarbons are: (○)-isoprene; (Δ)-1,3-butadiene; (◇)-*E*-2-butene.

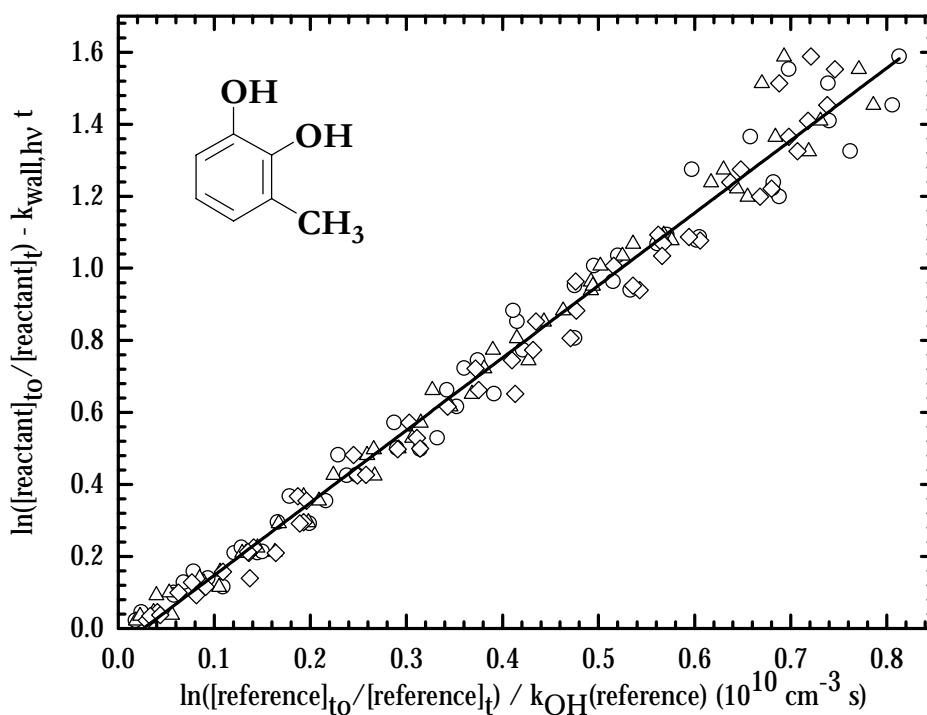


Figure 3.2 Plot according to eq. (3.4) for the reaction of 1,2-dihydroxy-3-methylbenzene with OH radicals. Reference hydrocarbons are: (○)-isoprene; (△)-1,3-butadiene; (◇)-E-2-butene.

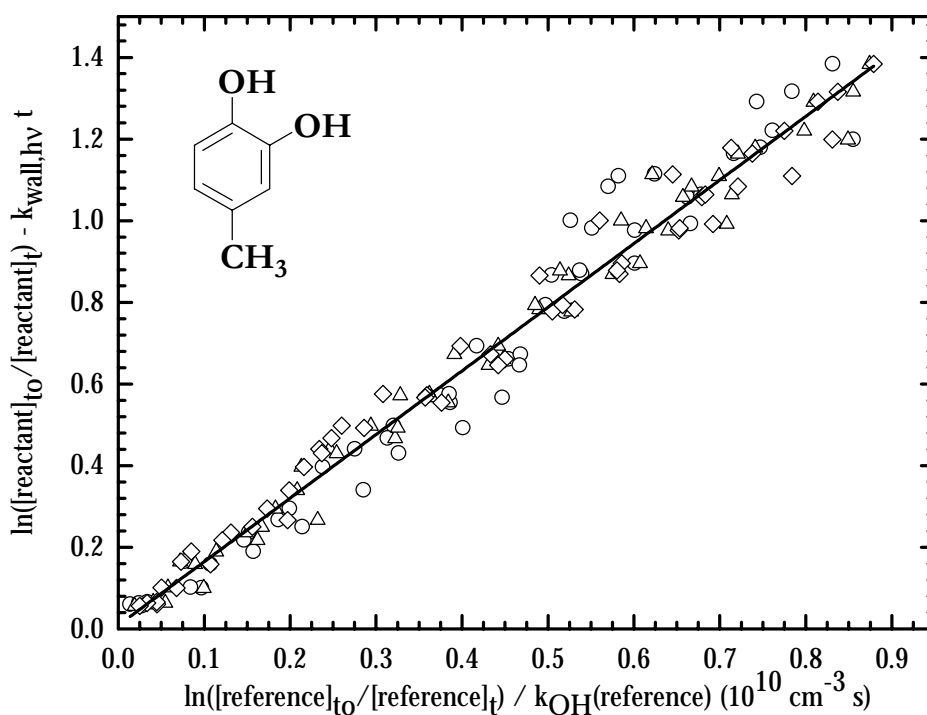


Figure 3.3 Plot according to eq. (3.4) for the reaction of 1,2-dihydroxy-4-methylbenzene with OH radicals. Reference hydrocarbons are: (○)-isoprene; (△)-1,3-butadiene; (◇)-E-2-butene.

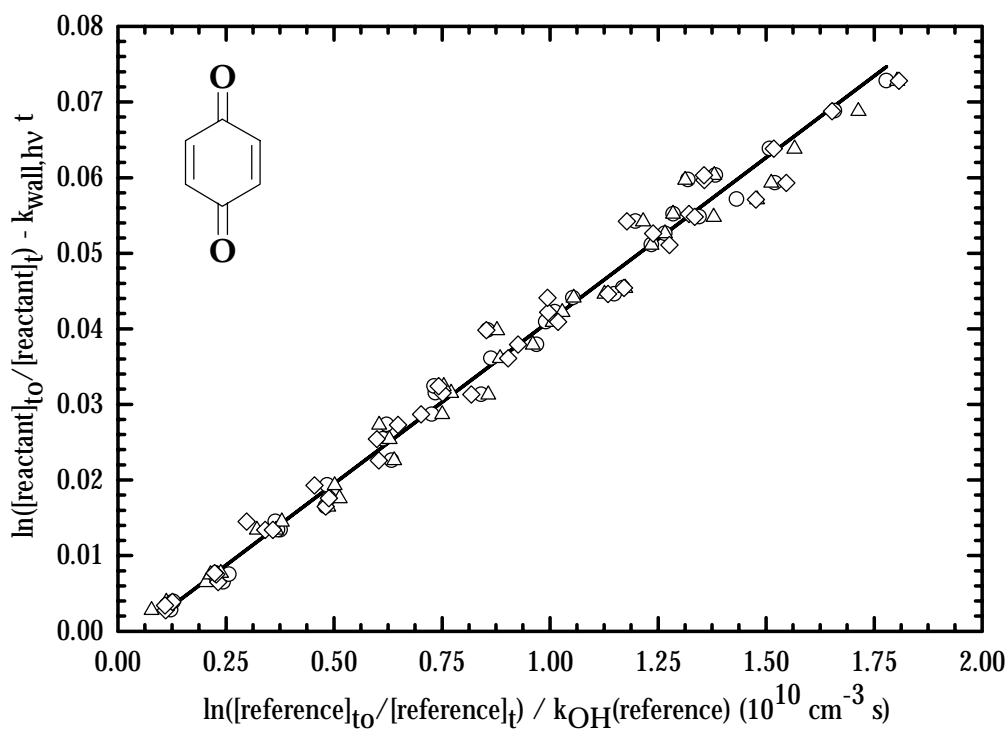


Figure 3.4 Plot according to eq. (3.4) for the reaction of 1,4-benzoquinone with OH radicals. Reference hydrocarbons are: (○)-isoprene; (△)-1,3-butadiene; (◇)-E-2-butene.

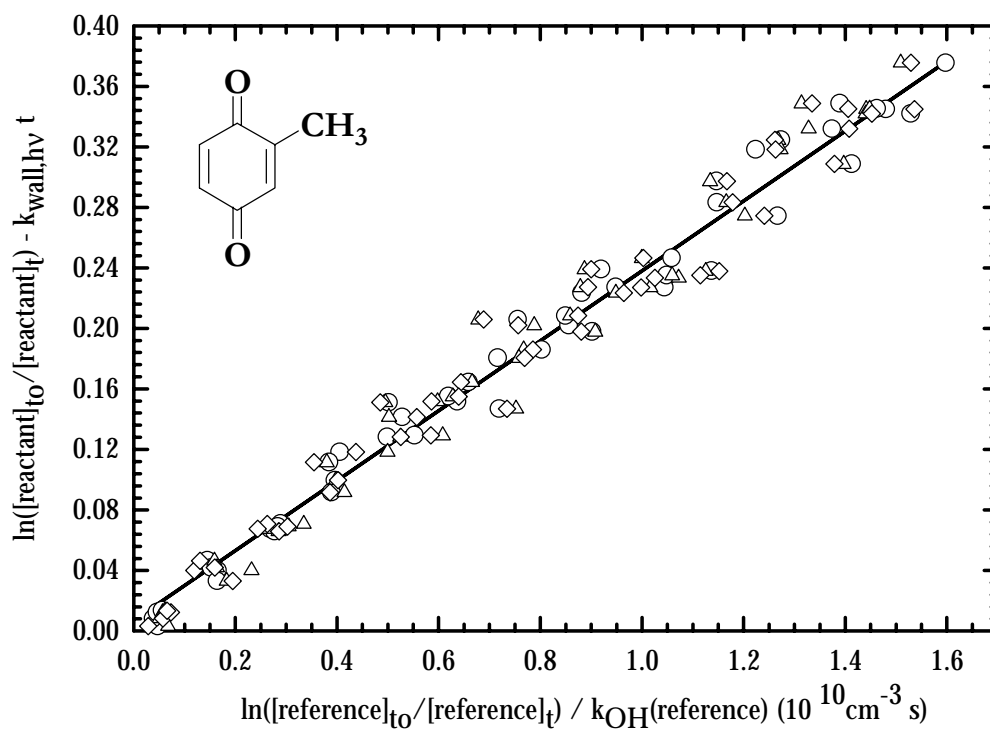


Figure 3.5 Plot according to eq. (3.4) for the reaction of methyl-1,4-benzoquinone with OH radicals. Reference hydrocarbons are: (○)-isoprene; (△)-1,3-butadiene; (◇)-E-2-butene.

Table 3.1 lists the reference compounds used, the measured ratios k_1/k_2 obtained from analysis of the data according to Equation (3.3) and the rate constants for the reaction of OH radicals with the studied compounds, as determined according to Equation (3.4). The errors quoted in Table 3.1 are a combination of the 2σ statistical errors from the linear regression analysis and the 20% errors given for the recommended values of the rate constants of the OH radical reaction with the reference compounds in the literature. The experimental data for the investigated substances were taken from a minimum of five experiments for the dihydroxybenzenes and four for the benzoquinones.

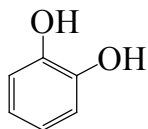
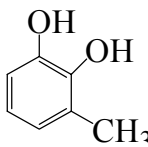
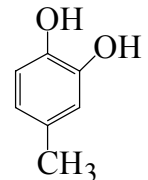
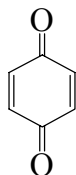
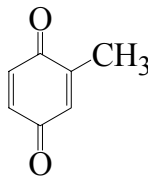
3.2 Discussion

It is evident from the data shown in Table 3.1, that the reactivity of the 1,2-dihydroxybenzenes follows the order $k_{\text{OH}}(1,2\text{-dihydroxybenzene}) < k_{\text{OH}}(1,2\text{-dihydroxy-4-methylbenzene}) < k_{\text{OH}}(1,2\text{-dihydroxy-3-methylbenzene})$. This order would be expected from a consideration of the structure of the compounds. The faster rate constants for the reactions of the methylated 1,2-dihydroxybenzenes compared to 1,2-dihydroxybenzene can be attributed to the presence of the CH_3 group. The CH_3 group adds to the already large activation of the ring towards electrophilic addition of the OH radical from the HO groups. The reaction of the dihydroxybenzenes with OH radicals is expected to proceed predominantly via electrophilic addition of OH to the aromatic ring (Atkinson, 1994). This conclusion is drawn from an analogy with the known behaviour of mono-hydroxylated benzenes. The reaction of OH radicals with phenol and *ortho*-, *meta*- and *para*-cresol proceeds mainly by addition of OH to the aromatic ring. For phenol, only about 9% of the reaction is thought to occur via H-atom abstraction from the HO group and for *ortho*-cresol, about 7% of the overall reaction is assumed to be H-atom abstraction from the OH and CH_3 groups (Atkinson, 1994).

Using the kinetic data obtained in this study, in combination with an average tropospheric OH radical concentration of $[\text{OH}] = 1.6 \times 10^6 \text{ cm}^{-3}$ (Crutzen and Zimmermann, 1991; Prinn *et al.*, 1992) an estimated atmospheric residence time τ_i of a compound i due to reaction with OH radicals can be calculated according to the relationship: $\tau_i = (k_i [\text{OH}])^{-1}$. The residence times thus obtained are presented in Table 3.1. The 1,2-dihydroxybenzenes will have very short atmospheric lifetimes and can influence the photochemical oxidant formation only on a local scale, whereas the benzoquinones with their significantly longer lifetimes will have a more regional influence.

This study represents the first determination of the rate constants for the reaction of OH radicals with 1,2-dihydroxybenzene, 1,2-dihydroxy-4-methylbenzene and 1,2-dihydroxy-3-methylbenzene and, therefore, a comparison with literature values is not possible.

Table 3.1 Rate constants for the reaction of OH radicals with 1,2-dihydroxybenzene, 1,2-dihydroxy-3-methylbenzene, 1,2-dihydroxy-4-methylbenzene, 1,4-benzoquinone and methyl-1,4-benzoquinone at 1000 mbar total pressure synthetic air and 300 ± 2 K.

compound	reference	k_1/k_2	$k_1 \times 10^{11}$	$k_{1(\text{average})} \times 10^{11}$	τ_i
 1,2-dihydroxybenzene	isoprene	1.02 ± 0.04	10.3 ± 2.06		
	1,3-butadiene	1.60 ± 0.052	10.8 ± 2.16	10.4 ± 2.1	100 min
	<i>E</i> -2-butene	1.60 ± 0.05	10.2 ± 2.04		
 1,2-dihydroxy-3-methylbenzene	isoprene	1.92 ± 0.07	20.4 ± 4.28		
	1,3-butadiene	3.02 ± 0.09	20.3 ± 4.26	20.5 ± 4.3	51 min
	<i>E</i> -2-butene	3.15 ± 0.1	21.0 ± 4.41		
 1,2-dihydroxy-4-methylbenzene	isoprene	1.61 ± 0.07	16.3 ± 3.2		
	1,3-butadiene	2.31 ± 0.05	15.5 ± 3.1	15.6 ± 3.3	67 min
	<i>E</i> -2-butene	2.37 ± 0.05	15.1 ± 3.02		
 1,4-benzoquinone	isoprene	0.047 ± 0.001	0.47 ± 0.09		
	1,3-butadiene	0.069 ± 0.002	0.46 ± 0.09	0.46 ± 0.09	37 h
	<i>E</i> -2-butene	0.073 ± 0.002	0.46 ± 0.09		
 methyl-1,4-benzoquinone	isoprene	0.23 ± 0.01	2.32 ± 0.47		
	1,3-butadiene	0.36 ± 0.01	2.40 ± 0.49	2.35 ± 0.47	7.4 h
	<i>E</i> -2-butene	0.37 ± 0.01	2.33 ± 0.47		

units: $\text{cm}^3 \text{ molecule}^{-1} \text{ s}^{-1}$

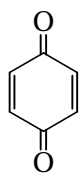
The rate constant for the reaction of OH with 1,2-dihydroxybenzene ($k_{\text{OH}} = 10.4 \pm 2.1 \times 10^{-11} \text{ cm}^3 \text{ molecule}^{-1} \text{ s}^{-1}$) (Olariu *et al.*, 2000a) is about a factor of 4 higher than that for phenol ($k_{\text{OH}} = 2.7 \pm 0.6 \times 10^{-11} \text{ cm}^3 \text{ molecule}^{-1} \text{ s}^{-1}$) (Calvert *et al.*, 2001).

For 1,2-dihydroxy-3-methylbenzene, the rate constant determined ($k_{\text{OH}} = 20.5 \pm 4.3 \times 10^{-11} \text{ cm}^3 \text{ molecule}^{-1} \text{ s}^{-1}$) (Olariu *et al.*, 2000a) is factors of 5 and 3 higher than those for *ortho*-cresol ($k_{\text{OH}} = 4.1 \pm 1.2 \times 10^{-11} \text{ cm}^3 \text{ molecule}^{-1} \text{ s}^{-1}$) and *meta*-cresol ($k_{\text{OH}} = 6.8 \pm 2.3 \times 10^{-11} \text{ cm}^3 \text{ molecule}^{-1} \text{ s}^{-1}$) (Calvert *et al.*, 2001), respectively. For 1,2-dihydroxy-4-methylbenzene, the rate constant ($k_{\text{OH}} = 15.6 \pm 3.3 \times 10^{-11} \text{ cm}^3 \text{ molecule}^{-1} \text{ s}^{-1}$) (Olariu *et al.*, 2000a) is factors of 2 and 3 higher than those for *meta*-cresol ($k_{\text{OH}} = 6.8 \pm 2.3 \times 10^{-11} \text{ cm}^3 \text{ molecule}^{-1} \text{ s}^{-1}$) and *para*-cresol ($k_{\text{OH}} = 5.0 \pm 1.5 \times 10^{-11} \text{ cm}^3 \text{ molecule}^{-1} \text{ s}^{-1}$) (Calvert *et al.*, 2001), respectively.

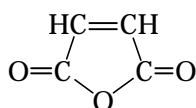
On average, the addition of the second HO group to phenol and the cresols to form 1,2-dihydroxybenzenes increases the reactivity of the compounds towards OH radical attack by a factor of about 3 to 4. The observed differences in reactivity can be ascribed to the activating effect of the hydroxyl groups towards electrophilic reactions, the magnitude of the *ortho*- and *para*-site directing strength of the substituents and the availability of the site for addition.

The reaction of OH radicals with 1,4-benzoquinone and methyl-1,4-benzoquinone is also expected to proceed almost exclusively by electrophilic addition of OH to the double bonds. The comparably low reactivity of 1,4-benzoquinone towards OH radicals (see Table 3.1) is probably due to a strong deactivating effect of the two carbonyl groups flanking each side of the double bonds. As expected, the presence of a CH_3 group attached to one of the double bonds in methyl-1,4-benzoquinone increases the reactivity towards OH radical attack quite considerably. This is due to the strong positive inductive effect of this group. The observed increase of the reactivity of methyl-1,4-benzoquinone with a factor of approximately 5 over 1,4-benzoquinone is significantly higher than what is generally observed for CH_3 substitution at the double bond of straight chain alkenes, but consistent with the effect of the addition of a CH_3 group to benzene to give toluene (Atkinson, 1989; Atkinson, 1994).

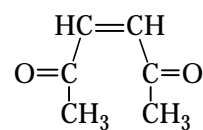
A comparison can be made between the rate constant for 1,4-benzoquinone and those for maleic anhydride ($k = 1.5 \times 10^{-12} \text{ cm}^3 \text{ molecule}^{-1} \text{ s}^{-1}$) and *Z*-hexene-2,5-dione ($k = 6.9 \times 10^{-11} \text{ cm}^3 \text{ molecule}^{-1} \text{ s}^{-1}$) (Bierbach *et al.*, 1994), which both contain the $-\text{CO}-\text{CH}=\text{CH}-\text{CO}-$ entity in *Z*-configuration.



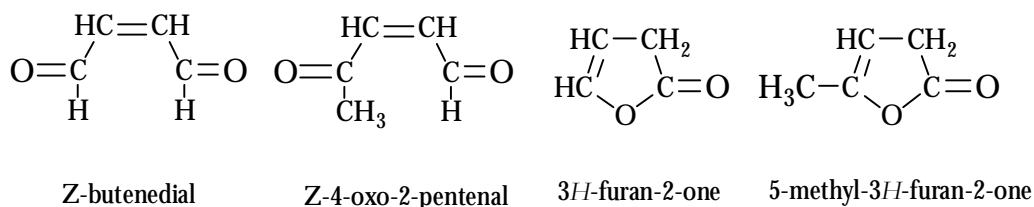
1,4-benzoquinone



maleic anhydride

*Z*-hexene-2,5-dione

Other unsaturated 1,4-dicarbonyls have OH reaction rate constants similar to that of *Z*-hexene-2,5-dione: *Z*-butenedial ($k_{\text{OH}} = 5.21 \times 10^{-11} \text{ cm}^3 \text{ molecule}^{-1} \text{ s}^{-1}$), *Z/E*-4-oxo-2-pentenal ($k_{\text{OH}} = 5.58 \times 10^{-11} \text{ cm}^3 \text{ molecule}^{-1} \text{ s}^{-1}$), 3*H*-furan-2-one ($k_{\text{OH}} = 4.45 \times 10^{-11} \text{ cm}^3 \text{ molecule}^{-1} \text{ s}^{-1}$), 5-methyl-3*H*-furan-2-one ($k_{\text{OH}} = 6.9 \times 10^{-11} \text{ cm}^3 \text{ molecule}^{-1} \text{ s}^{-1}$) (Bierbach *et al.*, 1994).



The rate constant for the reaction of the OH radical with 1,4-benzoquinone is about a factor of 3 higher than that for maleic anhydride, but between 10 to 15 times lower than those for the non-cyclic unsaturated 1,4-dicarbonyls mentioned above. A faster reaction of 1,4-benzoquinone with OH radicals compared to maleic anhydride might have been expected due simply to the presence of a second double bond available for OH addition in the former compound. The reason why the non-cyclic unsaturated 1,4-dicarbonyls are more than an order of magnitude more reactive than maleic anhydride and the benzoquinones is not immediately obvious. It appears that both the 2-oxa-propan-1,3-dial-1,3-diyl (-CO-O-CO-, carboxylic acid anhydride) and the *Z*-but-2-en-1,4-dial-1,4-diyl (-CO-CH=CH-CO-) moieties have similarly strong deactivating effects when attached between the 1- and 2- positions of a double bond.

Mechanisms of the atmospheric oxidation of phenol

Studies relevant to the atmospheric degradation of phenol, with regard to the observation of its gas-phase oxidation products, were carried out using smog chamber systems at Wuppertal University and the European photoreactor, EUPHORE Valencia/Spain.

Studies aimed at clarifying the oxidation mechanism of phenol due to the reactions with OH (conditions which characterise the day-time photochemistry) and NO₃ radicals (conditions which characterise the night-time chemistry) were performed.

4.1 Product study of the photo-oxidation of phenol initiated by OH radicals

4.1.1 Experimental results

The products of the OH radical initiated oxidation of phenol were investigated in the 1080 l quartz glass reactor study using the photolysis of CH₃ONO as OH radical source at 1000 mbar synthetic air and a temperature of 298 ± 2 K.

The initial and final concentrations of the reactants employed during the experiments are given in Table 4.1. The main products observed in the OH radical initiated oxidation of phenol using FT-IR include 1,2-dihydroxybenzene, 1,4-benzoquinone and 2-nitrophenol.

Table 4.1 Initial and final reactant concentrations (ppmv) employed in experiments of OH radical initiated oxidation of phenol in the 1080 l quartz glass reactor.

experiment	initial concentrations (ppmv)				final concentrations (ppmv)		
	phenol	CH ₃ ONO	NO	NO ₂	phenol	NO	NO ₂
PHE01	2.98	0.73	1.18	0.27	1.80	0.24	1.36
PHE02	2.32	0.86	0.80	0.72	1.30	0.25	1.35
PHE03	4.36	0.72	0.95	0.62	2.80	0.22	1.41
PHE04	4.41	0.49	1.15	0.49	2.36	0.27	1.28
PHE05	2.35	0.67	1.63	0.14	1.35	0.97	0.99
PHE06	1.06	0.72	1.58	0.13	0.52	1.09	0.83
PHE07	1.40	0.82	1.70	0.17	0.61	1.08	0.95
PHE08	3.77	0.73	1.53	0.15	2.23	0.66	1.07

Figure 4.1 shows an example of the FT-IR spectral data from a typical experiment on phenol photo-oxidation.

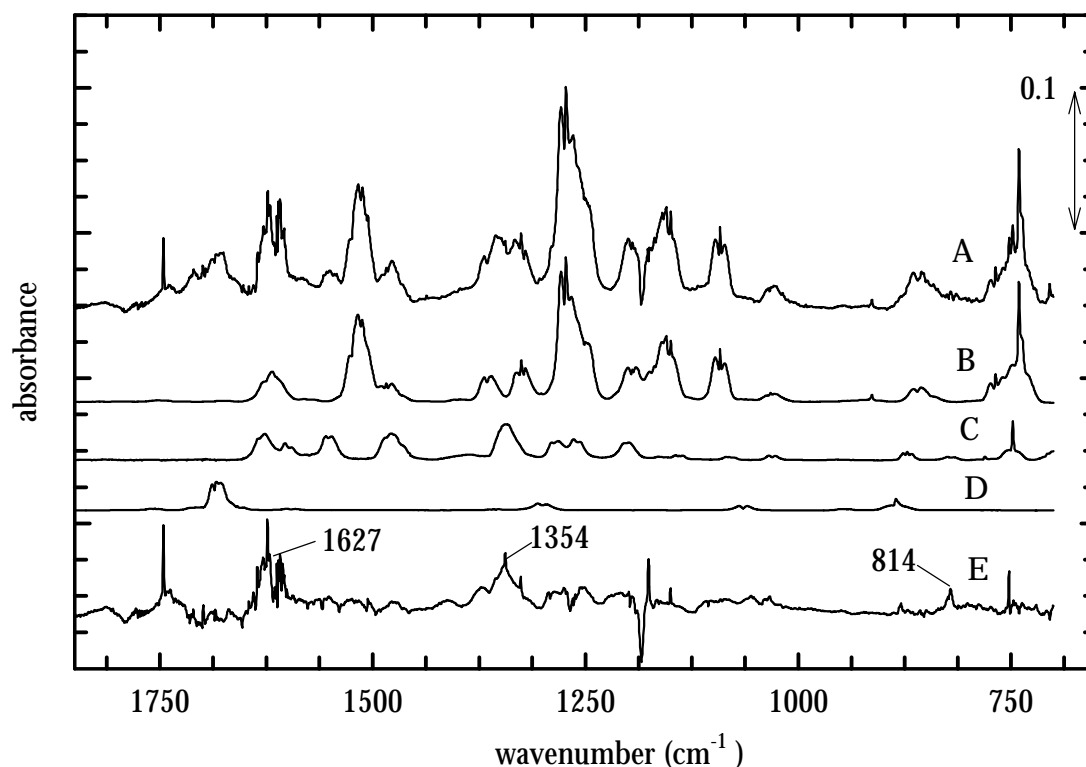


Figure 4.1 Infrared absorption spectra from the photo-oxidation of phenol in the range 700-1800 cm⁻¹: A-product spectrum of a phenol-CH₃ONO-NO-NO₂-air mixture after 12 min of irradiation with VIS lamps; B-reference spectrum for 1,2-dihydroxybenzene; C-reference spectrum for 2-nitrophenol; D-reference spectrum for 1,4-benzoquinone; E-residual spectrum after subtraction of the absorptions of all identified products.

In Figure 4.1, spectrum A represents the product spectrum obtained after subtraction of the spectral features belonging to water, reactants and some of the other known organic and inorganic co-products (e.g. H_2CO , HCOOH , CH_3OH , HNO_3 , CH_3NO_3 , HONO). The shown spectrum represents the result of the subtraction procedure from a spectrum which was recorded after approximately 12 min of irradiation. In this spectrum features of the most important identified product, 1,2-dihydroxybenzene, can be clearly seen. Spectra B, C and D are calibrated reference spectra for 1,2-dihydroxybenzene, 2-nitrophenol and 1,4-benzoquinone, respectively. The spectral features of 1,4-benzoquinone and 2-nitrophenol only become evident after subtraction of 1,2-dihydroxybenzene. The residual spectrum resulting from subtraction of absorptions due to 1,2-dihydroxybenzene, 2-nitrophenol and 1,4-benzoquinone from spectrum A is shown in E.

Of the identified products, 1,2-dihydroxybenzene and 1,4-benzoquinone have been observed and quantified for the first time. No information exists in the literature concerning their formation in the oxidation of phenol.

In order to check for the possible formation of other dihydroxybenzene, benzoquinone and nitrophenol isomers, the residual spectrum was compared with available reference spectra. Reference spectra were available for the other possible dihydroxybenzene isomers from phenol: 1,3-dihydroxybenzene and 1,4-dihydroxybenzene. Apart from the 1,2-dihydroxybenzene production there was no indication in the product spectrum for the formation of the other dihydroxybenzene isomers. Therefore, if the other isomers are formed, their yields will be minor.

Not all of the possible isomers for benzoquinone are commercially available. From the photo-oxidation of phenol production of 1,2-benzoquinone could also occur. The product 1,2-benzoquinone is expected to be thermally unstable. From the literature data (Patai, 1974), it is known that *ortho*-benzoquinones generally absorb at higher wave numbers than the corresponding *para*-benzoquinones, if the substituents are the same. The stretching vibrations of the carbonyl bond for 1,2-benzoquinone (in solution) are at 1680 and 1658 cm^{-1} (Thomson, 1971). The residual absorption spectrum (spectrum E, Figure 4.1) does not show any absorption in the region 1700-1600 cm^{-1} , which can be attributed to carbonyl vibrations. Taking into account the available literature spectroscopic data on the IR spectral features of 1,2-benzoquinone (Patai, 1974) and the residual product spectrum presented in Figure 4.1, suggests that 1,2-benzoquinone is not formed under the conditions employed in the experiments. If it is formed it will be a minor product.

Reference spectra were available for the other two possible nitrophenol isomers, 3-nitrophenol and 4-nitrophenol. A direct comparison of the residual spectrum (spectrum E, Figure 4.1) with the available reference spectra of the nitrophenol isomers supports that these isomers are not formed in significant concentrations.

After the subtraction procedure of all known and newly identified products the residual absorption bands shown in Figure 4.1 remained. From the residual spectrum it is evident that some minor products have not been identified. In the residual spectrum absorption bands around 1630, 1350 and 800 cm^{-1} can be observed, which are characteristic for nitrates (Roberts, 1990).

The concentration-time profiles of phenol and its identified oxidation products are presented in Figure 4.2.

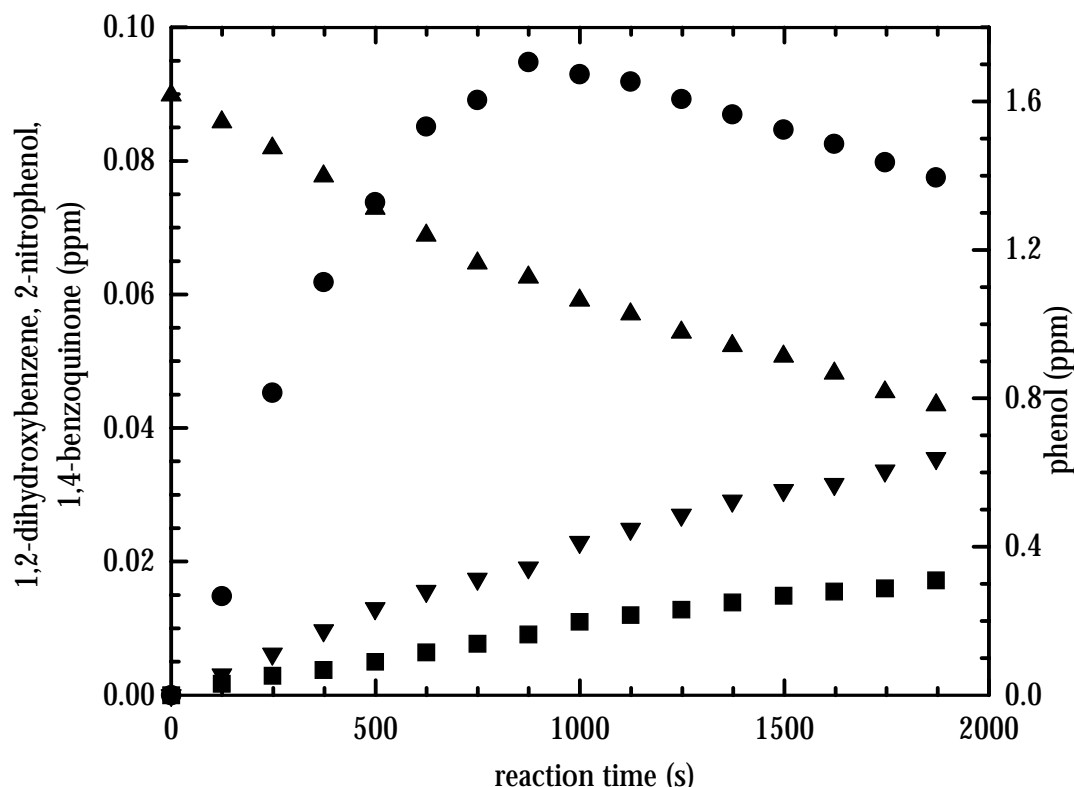


Figure 4.2 Concentration-time profiles of phenol and products identified in its OH initiated oxidation in the presence of NO_x : (▲)-phenol; (●)-1,2-dihydroxybenzene; (▼)-2-nitrophenol; (■)-1,4-benzoquinone.

The plots of the concentration of the identified products versus time show that secondary reaction of the primary products occurred during the experiment. The shapes of the product curves are determined by their production from phenol oxidation and loss processes such as reaction with OH, wall loss and photolysis. Since the 1,4-benzoquinone and 2-nitrophenol curves do not show a strong curvature, it would appear that these compounds are not strongly influenced by loss processes. It was determined that wall deposition of the identified compounds is an important loss processes. First order loss rates obtained in the dark experiments were measured for all these compounds. The average wall loss rate constants which were obtained are listed in Table II. 1, Appendix II. The photolysis rate constants of all identified compounds were determined to be negligible compared with wall deposition

processes. The identified compounds are also expected to react rapidly with NO_3 radicals (Atkinson *et al.*, 1984; Atkinson, 1994). In the present work, the NO concentrations were sufficiently high during these experiments (see Table 4.1) to suppress the formation of O_3 and hence of NO_3 radicals.

The measured concentrations of the products were corrected by taking into account these loss processes. Corrections were performed using the mathematical formalism proposed by Tuazon *et al.* (1986) which is presented in Appendix IV.

Examples of the corrected ring retaining-product concentrations versus the consumed amount of phenol are presented in Figure 4.3.

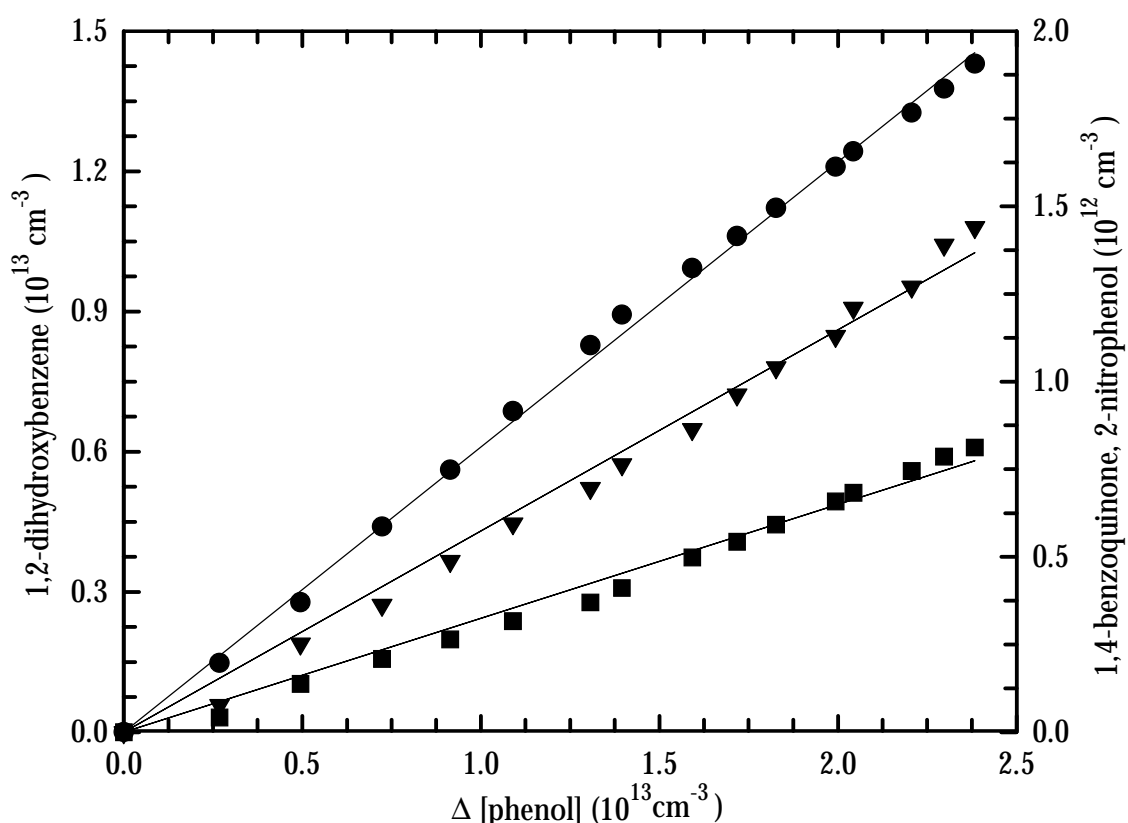


Figure 4.3 Plots of the corrected concentrations of (●)-1,2-dihydroxybenzene, (▼)-2-nitrophenol and (■)-1,4- benzoquinone versus the amount of consumed phenol.

The corrected yields of the identified ring-retaining products (1,2-dihydroxybenzene, 1,4-benzoquinone and 2-nitrophenol) determined from eight individual experiments on the OH-radical initiated oxidation of phenol are listed in Table 4.2. These yields were derived from the least squares analysis of plots such as those presented in Figure 4.3. The errors quoted in Table 4.2 are a combination of the 2σ statistical errors from the regression analysis and the errors from the spectral subtraction procedure and the error introduced by the correction procedure from the rate constants of the products with OH radicals.

It was observed that the multiplicative correction factor, increases with the rate constant ratio $k(\text{OH}+\text{product})/k(\text{OH}+\text{phenol})$ and with the extent of reaction. The maximum values of the correction factors were determined to be about 5 for 1,2-dihydroxybenzene. The correction factors for the 2-nitrophenol and 1,4-benzoquinone were negligible and the yields have therefore not been corrected.

Table 4.2 Molar yields of ring retaining products formed in the reaction of OH radicals with phenol at 1000 mbar total pressure and 298 ± 2 K.

experiment	product molar yields (%)		
	1,2-dihydroxybenzene	1,4-benzoquinone	2-nitrophenol
PHE01	89.3 ± 12.1	5.5 ± 0.4	6.4 ± 0.3
PHE02	67.5 ± 10.1	4.6 ± 0.4	7.5 ± 0.3
PHE03	80.3 ± 12.1	2.4 ± 0.2	6.1 ± 0.3
PHE04	76.1 ± 11.4	1.8 ± 0.2	6.0 ± 0.3
PHE05	85.7 ± 12.8	3.1 ± 0.3	4.6 ± 0.2
PHE06	80.4 ± 12.1	5.0 ± 0.5	6.0 ± 0.3
PHE07	78.0 ± 11.7	3.9 ± 0.4	5.4 ± 0.2
PHE08	86.0 ± 13.0	3.4 ± 0.3	4.7 ± 0.2
average yield	80.4 ± 12.1	3.7 ± 1.2	5.8 ± 1.0

4.1.2 Discussion of the results

Taking into account the above observations about removal processes of the identified products and phenol as well, it can be concluded that the dominant removal processes throughout the irradiation period were mainly by reaction with OH radical and wall loss.

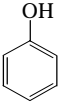
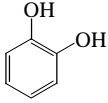
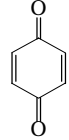
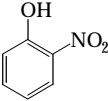
Table 4.3 gives an overview of the obtained molar formation yields of the products identified in the photo-oxidation of phenol. In this table yields available for nitrophenol from the literature are also included.

The formation of 1,2-dihydroxybenzene and 1,4-benzoquinone from the gas-phase OH-radical initiated oxidation of phenol has not been previously reported. Therefore, a direct comparison of the formation yields of these compounds, as obtained in the present study, with other available literature data is not possible.

From the results obtained within the present study it can be concluded that 1,2-dihydroxybenzene is certainly the major gas-phase reaction product (Olariu *et al.*, 2000b). The

formation yield of 2-nitrophenol, as determined in the present work is in reasonable agreement with that reported by Atkinson *et al.* (1992a).

Table 4.3 Molar formation yields of the products identified in the OH-radical initiated photo-oxidation of phenol.

reactant	product	yield (%) (this work)	yield (%) (literature)
 phenol	 1,2-dihydroxybenzene	80.4 ± 12.1	-
	 1,4-benzoquinone	3.7 ± 1.2	-
	 2-nitrophenol	5.8 ± 1.0	6.7 ± 1.5 ^a

^a Atkinson *et al.*, (1992a).

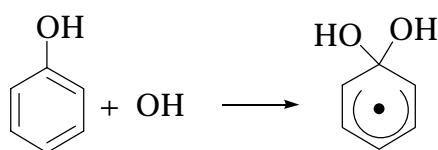
From the results of the present work it can be concluded that the observed ring-retaining products account for approximately 89% carbon in the OH radical initiated oxidation of phenol. As noted in Section 4.1.1 the yields of other dihydroxybenzene and nitrophenol isomers, if formed, are very minor. Therefore, presently it can only be speculated that the majority of missing carbon is probably in the form of ring-fragmentation products and/or aromatic nitrates.

It is interesting at this point, to note that the yields of 1,2-dihydroxybenzene from the reaction of OH with phenol are much higher than the yields of phenol formed in the reaction of OH with benzene. The yield of phenol from the OH + benzene reaction is approximately 25% (Calvert *et al.*, 2001) while that of 1,2-dihydroxybenzene from OH + phenol reaction is approximately 80%. This difference obviously reflects a major difference in the oxidation pathways of phenol compared to its precursor benzene. Whereas in the OH-radical initiated photo-oxidation of benzene about 30% of the reaction leads to ring-retaining products and about 70% to ring-fragmentation products, in the case of phenol it appears from this study that the yield of ring-retaining products is at least 89% or more. From the results obtained in

the present work it can be concluded that the yield of the ring-retaining compounds is, within the experimental error limits, close to unity.

4.1.2.1 Discussion of the formation mechanism of 1,2-dihydroxybenzene

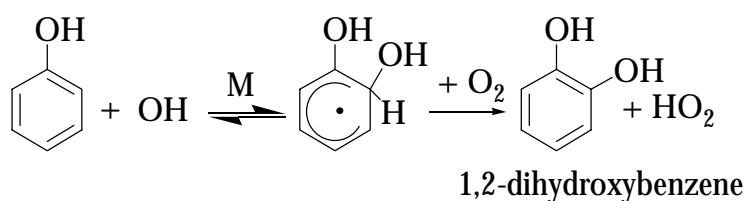
The major oxidation product of phenol, 1,2-dihydroxybenzene, can only be formed via an OH radical addition reaction pathway. For phenol there are several distinct addition sites for the OH radical with formation of an OH-aromatic adduct. Theoretical calculations have predicted that addition of the OH radical at the *ipso* position forms the most thermochemically favourable adduct (Benson, 1976).



Previous mechanistic considerations of the OH radical initiated oxidation of phenol (Grosjean, 1991; Atkinson *et al.*, 1992a) have often considered the *ipso* addition as the only pathway for subsequent mechanistic development. However, the large formation yield of 1,2-dihydroxybenzene, obtained in the present study, supports that addition of the OH radical at the *ortho* position to the OH substituent dominates.

In the system the OH - adduct can react with O₂ or NO₂. Rate constants for the reaction of the OH-phenol adduct with O₂ or NO₂ are known at 330 K with $k_{(\text{OH-phenol} + \text{O}_2)} = 3 \times 10^{-14} \text{ cm}^3 \text{ molecule}^{-1} \text{ s}^{-1}$ and $k_{(\text{OH-phenol} + \text{NO}_2)} = 3.6 \times 10^{-11} \text{ cm}^3 \text{ molecule}^{-1} \text{ s}^{-1}$ (Zetzsch *et al.*, 1997). For the benzene - OH adduct, rate constants of $k_{(\text{OH-benzene} + \text{O}_2)} = 2.1 \times 10^{-16} \text{ cm}^3 \text{ molecule}^{-1} \text{ s}^{-1}$ at 298 K and $k_{(\text{OH-benzene} + \text{NO}_2)} = 2.5 \times 10^{-11} \text{ cm}^3 \text{ molecule}^{-1} \text{ s}^{-1}$ at 333 K were determined (Knispel *et al.*, 1990; Bohn and Zetzsch, 1999). It is clear that while the reaction rate constants with NO₂ are not significantly higher for the phenol - OH adduct than for OH - benzene adduct, the rate constants for the O₂ reactions are more than 2 orders of magnitude faster for OH - phenol compared to OH - benzene. This may explain the high yield of 1,2-dihydroxybenzene observed in the OH initiated oxidation of phenol. The isomerisation of peroxy radicals, OH - aromatic - O₂, formed by the addition of O₂ to the OH - aromatic adducts, is expected to result in the ring-fragmentation products observed in aromatic hydrocarbon photo-oxidation systems, see for example Calvert *et al.* (2001). The rate constant for this unimolecular isomerisation is not expected to depend significantly on the substituents of the aromatic hydrocarbon and consequently the observed dependency of the overall OH - aromatic + O₂ reaction rate constant on the substituents is expected to predominately affect the pathways leading to ring-retaining products. On the basis of the above observations dihydroxybenzene would be expected to be formed in significantly higher yields in the OH

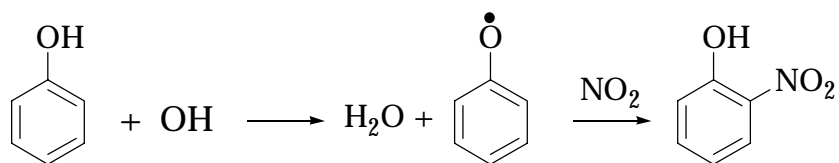
initiated oxidation of phenol compared to the yields of phenols from benzene + OH. Another effect of the very fast OH - phenol + O₂ reaction is that the OH - phenol + NO₂ reaction will be only of negligible importance, even at the comparably high concentrations of NO_x prevalent in the present study. In the experiments performed in the present work the final NO₂ concentrations were between 0.83 – 1.41 ppm (see Table 4.1). Even at the highest NO₂ concentration employed in these experiments, reactions of the OH - phenol adduct with O₂ will dominate by factors of more than 100 (1.6 x 10⁵ against 1.2 x 10³) over reaction with NO₂. This means that the major reaction of the OH - phenol adduct will be with O₂. The results support that this reaction results mainly in the formation of the 1,2-dihydroxybenzene.



However, from the present study it is not possible to say whether the reaction proceeds via a direct H-atom abstraction mechanism or over addition of O₂ followed by elimination of HO₂.

4.1.2.2 Discussion of the formation mechanism of benzoquinone and nitrophenol

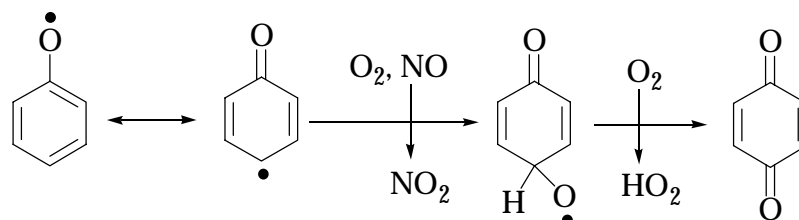
In the present work the formation of 1,4-benzoquinone and 2-nitrophenol has been observed with molar formation yields of about 3.7% and 5.8%, respectively. The calculated formation yield of 2-nitrophenol in the present study is similar to that from the work of Atkinson *et al.* (1992a). The formation of 2-nitrophenol can be described by the following general reaction sequence:



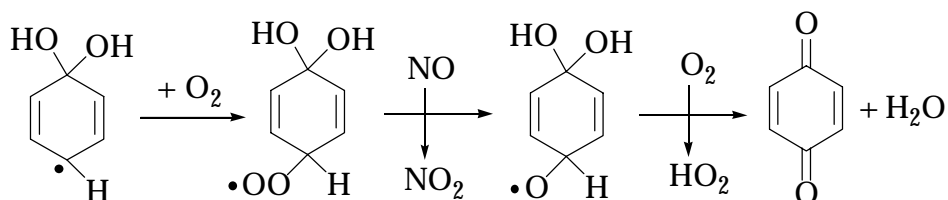
As observed previously by Atkinson *et al.* (1992a), the measured yield of 2-nitrophenol in the OH radical induced oxidation of phenol is similar to the calculated fraction of the reaction proceeding by H-atom abstraction from the OH group of ~ 9% at 298 K (uncertain to ± 50%). Considering the uncertainty of this estimation, as was indicated by Atkinson *et al.* (1992a), we can assume that in the system investigated in this work, formation of 2-nitrophenol results from the H-atom abstraction channel.

Both addition and abstraction pathways can be postulated for the formation of 1,4-benzoquinone.

The formation of 1,4-benzoquinone from the abstraction channel from phenol oxidation could occur through reactions such as:



The formation of 1,4-benzoquinone via an addition channel could involve the following reaction sequence:



In a recent FT-IR smog chamber product study of the atmospheric chemistry of the phenoxy radical (Platz *et al.*, 1998), 1,4-benzoquinone was not reported among the reaction products. In the work of Platz *et al.* (1998), the phenoxy radicals were produced by reactions of Cl atoms, produced via the photolysis of molecular chlorine, with phenol. Similarly, in this work reaction of Cl atoms with phenol was also used to produce phenoxy radicals. The reaction products stemming from phenoxy radical reactions with O₂, NO and NO₂ were examined. The product information obtained was analogous to that reported by Platz *et al.* (1998). No indication could be found for the formation of 1,4-benzoquinone. Hence, it is concluded from these observations that in the case of the OH + phenol reaction formation of 1,4-benzoquinone must occur mainly via the OH addition channel.

4.1.2.3 Summary of results

The OH radical initiated oxidation of phenol was investigated under conditions similar to the atmosphere (1000 mbar total pressure and a temperature of 298 ± 2 K). The formation of 1,2-dihydroxybenzene, 1,4-benzoquinone, 2-nitrophenol was observed. The major product identified in the present study was 1,2-dihydroxybenzene with a molar formation yield of 80.4%. 2-Nitrophenol formation in a yield similar to that reported by Atkinson *et al.* (1992a),

was observed. α -Dicarbonyl compounds such as glyoxal (CHOCHO) and glyoxalic acid (CHOCOOH), which have been observed in the OH initiated oxidation of phenol (Grosjean, 1991) in low yields, were not observed in the present work.

Based on the identified products and their formation yields, the results from the present study allow the reaction mechanism, shown in Figure 4.5, to be postulated for the reaction of OH radicals with phenol:

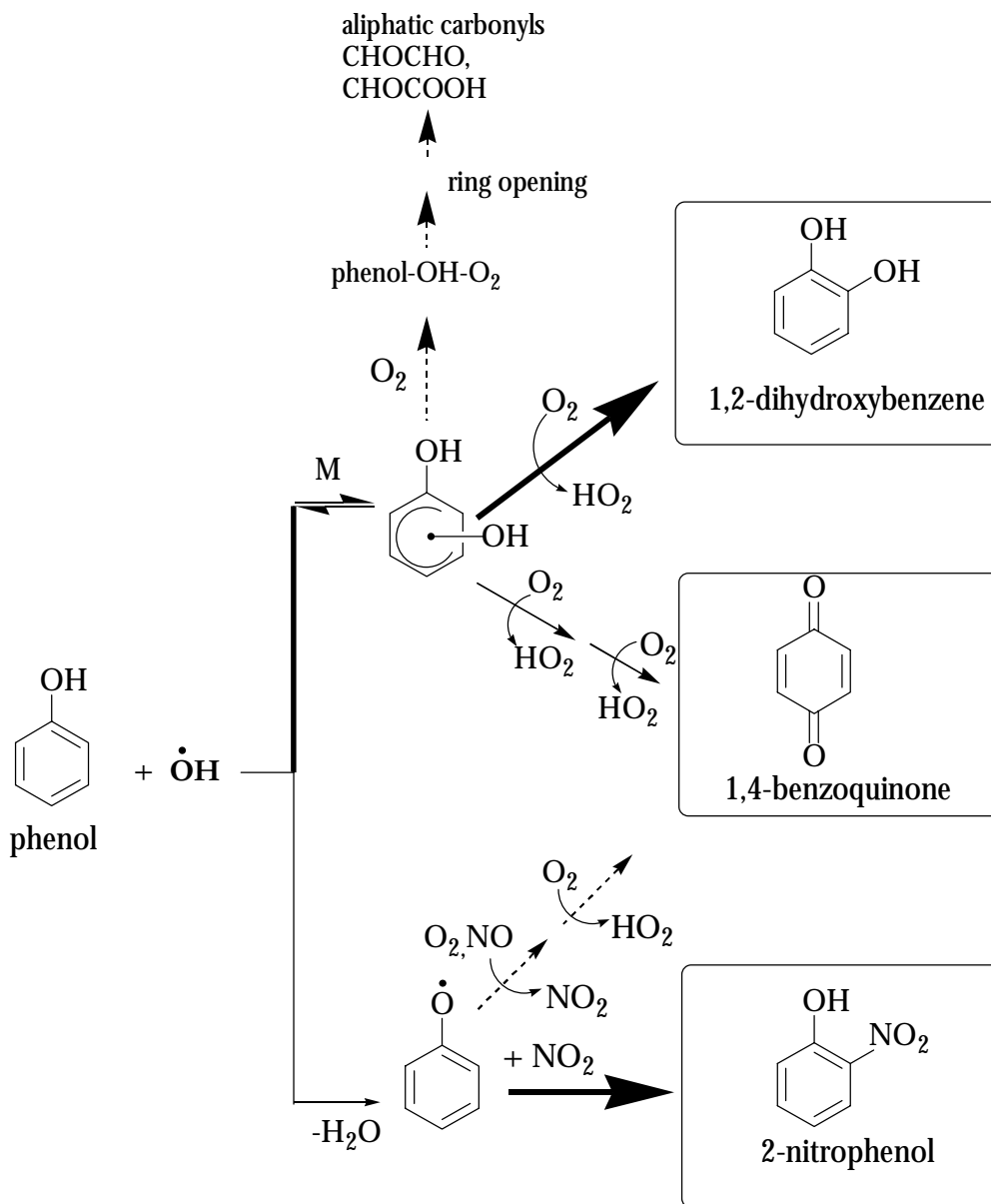


Figure 4.5 Simplified mechanism of the reaction of OH radicals with phenol. The bold arrow indicate the major reaction pathways.

4.2 Product study of the nitration of phenol by reaction with the NO₃ radical

A detailed product analysis of the NO₃ radical initiated oxidation of phenol has been performed. Products distributions were obtained for conditions corresponding to atmospheric pressure and temperature (1000 mbar and 298 ± 2 K). Experiments were made using the smog chamber systems at Wuppertal University and the European photoreactor EUPHORE.

4.2.1 Experimental results

4.2.1.1 1080 l quartz glass reactor

In the NO₃ radical initiated oxidation of phenol, using long path FT-IR absorption spectroscopy as analytical tool, the formation of 2-nitrophenol and 4-nitrophenol as the main products was observed.

Four dark experiments on phenol-NO₂-O₃-synthetic air reaction mixtures were performed. The initial and final reactant concentrations are given in Table 4.4.

Table 4.4 Initial and final concentrations of phenol-NO₂-O₃ mixtures in the 1080 l quartz glass reactor.

experiment	initial concentration (ppmv)			final concentration (ppmv)		
	phenol	O ₃ ^a	NO ₂	phenol	O ₃ ^a	NO ₂
PHE11	1.15	0.97	1.85	0.74	0.60	0.20
PHE12	3.30	1.04	1.90	2.47	0.71	0.13
PHE13	2.13	0.96	2.13	0.60	0.08	1.11
PHE14	1.01	1.17	1.70	0.60	0.74	0.03

^a maximum O₃ concentration measured.

Figure 4.6 shows an example of the FT-IR spectral data for an investigation on a phenol-NO₂-O₃-synthetic air mixture. In Figure 4.6 the spectrum A represents a typical product spectrum which was obtained after subtraction of the spectral features belonging to water, reactants (phenol, O₃ and NO₂) and HNO₃. Spectra B and C are the reference spectra of 2-nitrophenol and 4-nitrophenol, respectively. The residual spectrum D is a spectrum which was obtained after computer-aided subtraction of both 2-nitrophenol and 4-nitrophenol from spectrum A.

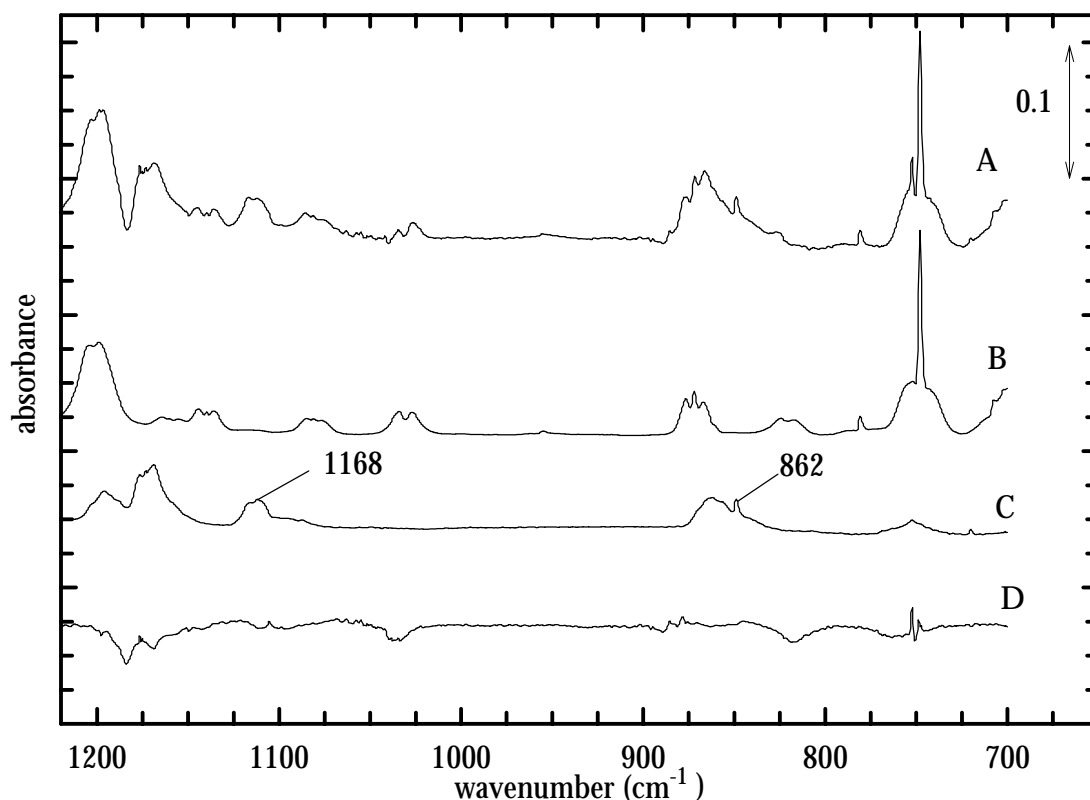


Figure 4.6 Infrared absorption spectra in the range 700-1220 cm^{-1} recorded in the 1080 l quartz glass reactor: A-product spectrum of a phenol- NO_2 - O_3 mixture after 15 min; B-reference spectrum for 2-nitrophenol; C-reference spectrum for 4-nitrophenol; D-residual spectrum obtained after subtraction of the absorption bands of all identified products.

As is shown in Figure 4.6 it is evident from simple visual comparison of the reference and product spectra that 2-nitrophenol and 4-nitrophenol are being both formed in the reaction system. HNO_3 , an important reaction co-product, was also identified. In the product spectra there were no indications for the formation of the 3-nitrophenol isomer. If this isomer is formed, its yield will be probably minor. As can be seen in Figure 4.6, the residual spectrum obtained after computer-aided subtraction of the 2-nitrophenol and 4-nitrophenol isomers, is practically devoid of spectral features.

The concentration-time profiles of the reactants and products for a typical experiment with phenol and NO_3 are presented in Figure 4.7.

The formation yields of the identified products were obtained from plots of their corrected concentration versus the consumed amount of phenol. Corrections were made for their loss to the wall surface since this was determined to be the most important sink process. The wall loss rates, which were obtained in the present work, are presented in Appendix II.

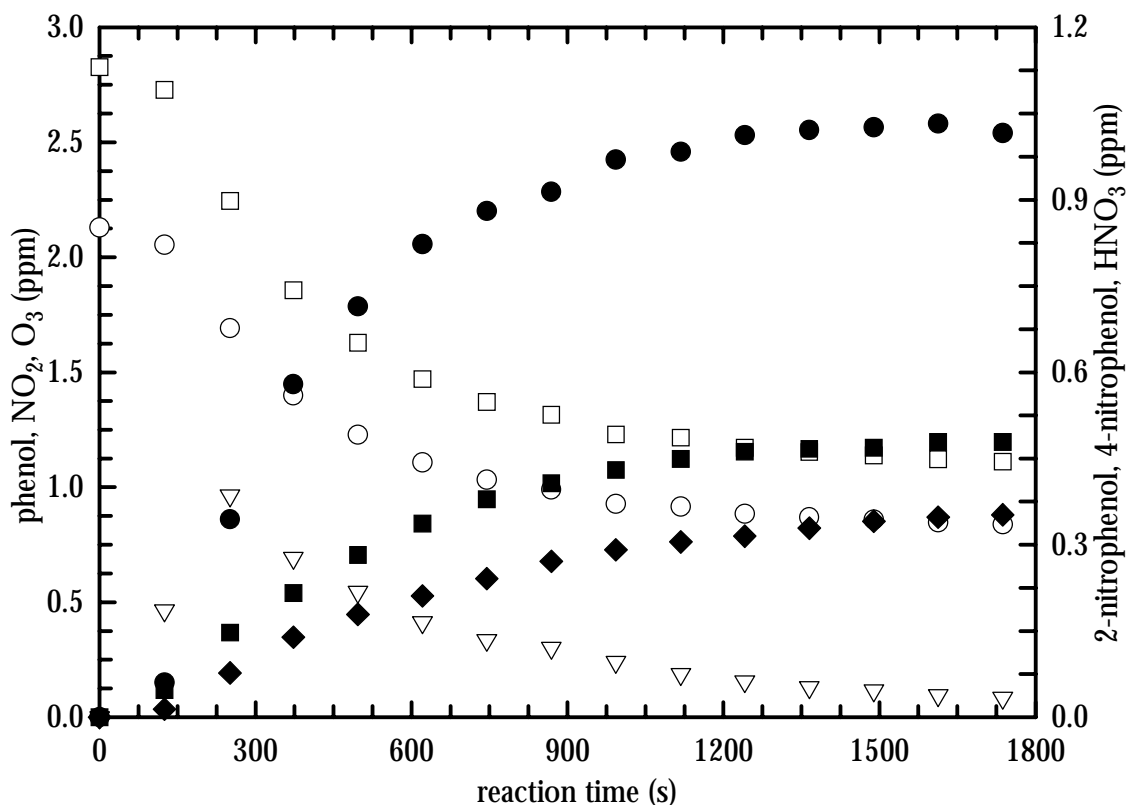


Figure 4.7 Concentration-time profile of the reactants and products identified in the NO_3 -initiated oxidation of the phenol: (○) -phenol; (□) - NO_2 ; (▽) - O_3 ; (●) - HNO_3 ; (◆) -2-nitrophenol (■) -4-nitrophenol.

Both 2-nitrophenol and 4-nitrophenol can also react with NO_3 radicals and, hence, secondary reactions must be taken into account in order to obtain their true formation yields. The rate constant for the reaction of the NO_3 radical with 2-nitrophenol is more than a factor of 80 lower than that for phenol + NO_3 (Atkinson *et al.*, 1992a). The 4-nitrophenol + NO_3 reaction rate constant has not been measured. Taking into account that the substituent effect of the nitro group does not appreciably change the NO_3 rate constant (Grosjean, 1985) it is expected that the reaction rate constant of the NO_3 radical with 4-nitrophenol is similar to that with 2-nitrophenol. Hence, secondary reactions of 2-nitrophenol and 4-nitrophenol during the NO_3 radical reaction with phenol can be considered negligible.

Figure 4.8 shows plots of the corrected concentrations of 2-nitrophenol, 4-nitrophenol and HNO_3 versus the amount of reacted phenol. All the plots show good linearity. The formation yields of the products were determined from linear regression analyses of the plots shown in Figure 4.8.

The corrected yields of the observed products, determined from four individual experiments on the NO_3 radical initiated oxidation of phenol, are listed in Table 4.5. The

errors quoted in Table 4.5 are a combination of the 2σ statistical errors from the linear regression analysis with the errors given by the subtraction procedure.

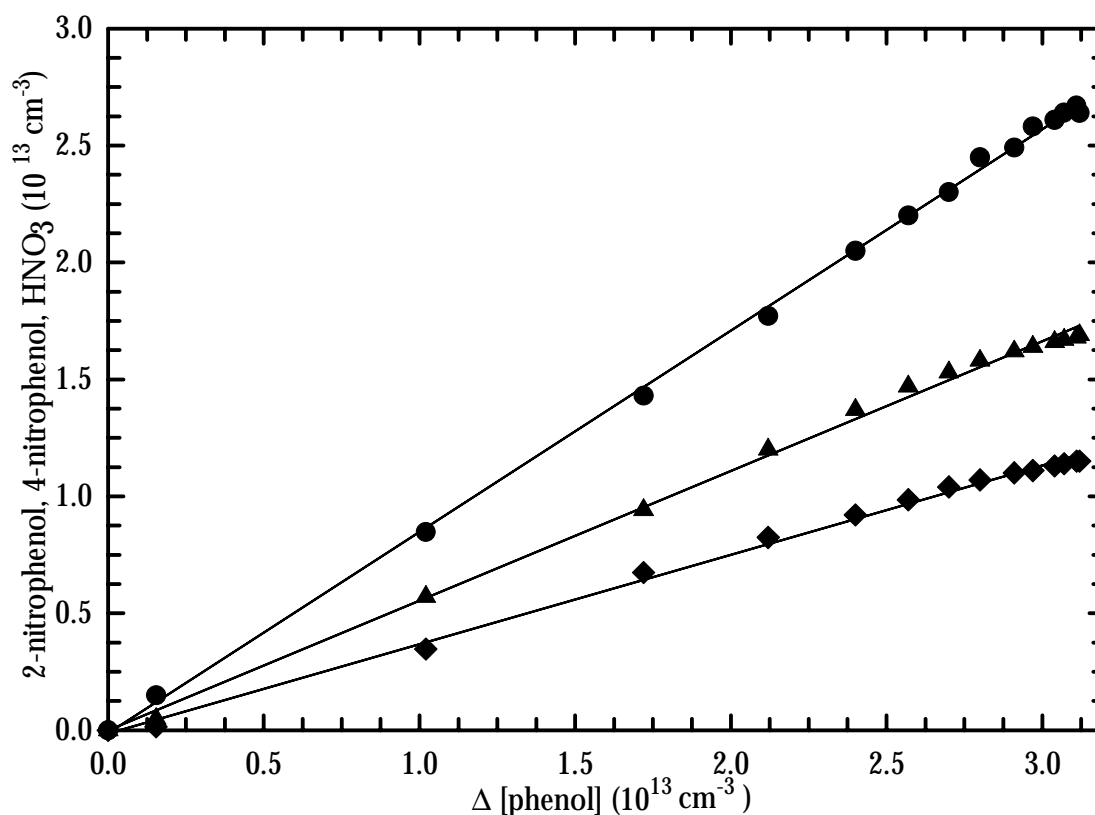


Figure 4.8 Plots of the corrected concentration of (◆)-2-nitrophenol, (▲)-4-nitrophenol and (●)-HNO₃ versus the amount of reacted phenol.

From the results presented in Table 4.5 it can be seen that 2-nitrophenol is formed in a yield of about 24.2% and 4-nitrophenol of about 50%. This clearly indicates that both nitrophenols are very important products in the NO₃ radical initiated oxidation of phenol (Olariu *et al.*, 2001).

Table 4.5 Formation yields of 2-nitrophenol, 4-nitrophenol and HNO₃ from the gas-phase reaction of the NO₃ radical with phenol.

experiment	product molar yields (%)		
	2-nitrophenol	4-nitrophenol	HNO ₃
PHE11	26.9 ± 1.2	56.6 ± 3.6	80.5 ± 4.6
PHE12	20.7 ± 1.1	50.4 ± 3.0	103.7 ± 5.1
PHE13	27.9 ± 1.5	40.5 ± 4.0	77.0 ± 4.5
PHE14	21.4 ± 1.2	52.6 ± 3.2	97.8 ± 4.9
average yield	24.2 ± 3.7	50.0 ± 6.8	89.7 ± 13.0

4.2.1.2 EUPHORE chamber

The aim of EUPHORE experiments was to establish the reaction products in the NO_3 radical initiated oxidation of phenol under conditions similar to the atmosphere at lower initial concentrations of the reactants. In order to determine the product distribution from the NO_3 + phenol reaction three mixtures of phenol- NO_2 - O_3 were investigated. The initial and final concentrations of reactants are summarized in Table 4.6.

Table 4.6 Initial and final experimental concentrations of reactants used for the nitration reaction of phenol with NO_3 radicals.

experiment	initial concentration (ppbv)			final concentration (ppbv)		
	phenol	O_3^a	NO_2	phenol	O_3^a	NO_2
PHE001	506	351	197 (388) ^b	229	72	95
PHE002	498	416	528	199	138	47
PHE003	389	363	404	91	131	78

^a maximum O_3 concentration measured;

^b second addition.

The formation of 2-nitrophenol, 4-nitrophenol and HNO_3 was observed in all three experiments performed in the EUPHORE chamber. This study confirms the formation of both nitrophenolic compounds in the NO_3 radical initiated oxidation of phenol as was observed in the studies performed in the Wuppertal laboratory (see Section 4.2.1).

Figure 4.9 shows an example of the FT-IR spectral data from one experiment. In Figure 4.9 it is evident that the product spectrum clearly shows spectral features characteristic for 2-nitrophenol. The residual spectrum, which was obtained after computer subtraction of the spectral features belonging to reactants and the identified products (2-nitrophenol, 4-nitrophenol and HNO_3) is practically absorption free (see Figure 4.9, D).

Figure 4.9 shows only the 2-nitrophenol reference spectrum. 4-Nitrophenol was identified using its characteristic absorption bands around 1196, 1168, 862 cm^{-1} . From the reference spectrum of 4-nitrophenol recorded in the 1080 l quartz glass reactor it is known that this nitrophenol has also an important absorption bands around 1610 and 1356 cm^{-1} for which FT-IR absorption cross section have been measured (see Appendix III).

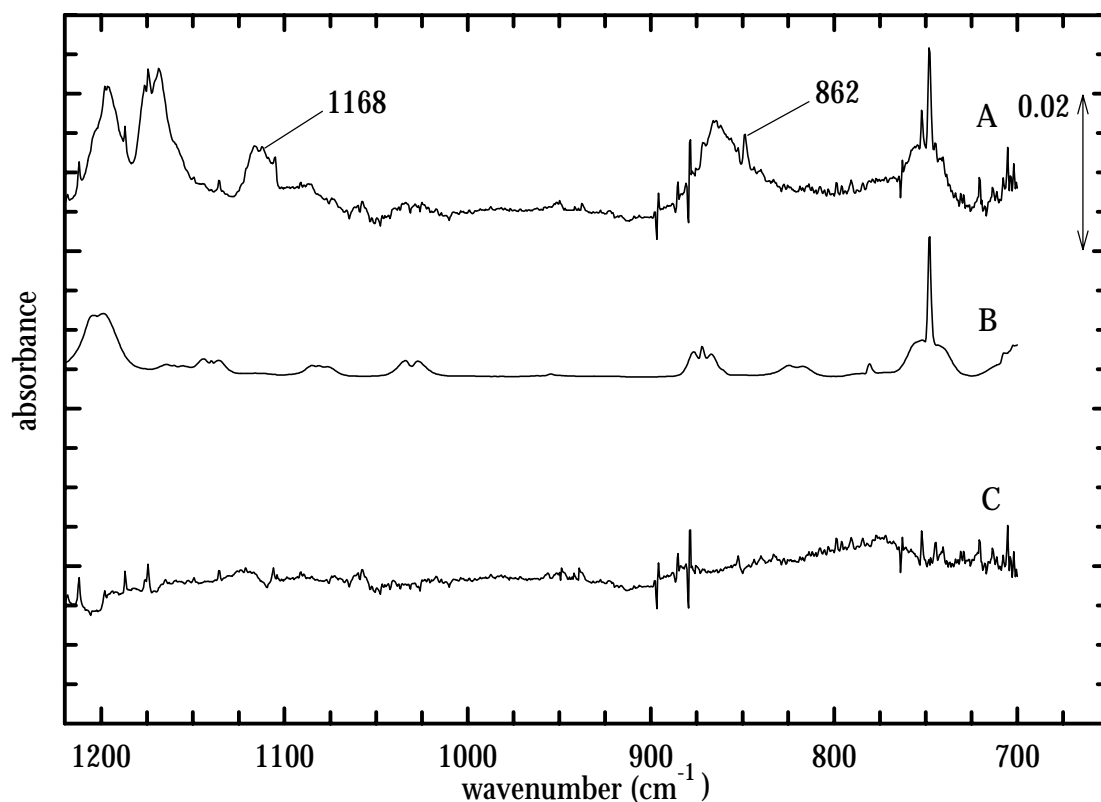


Figure 4.9 Infrared absorption spectra in the range 700-1220 cm^{-1} recorded in the EUPHORE chamber: A-Product spectrum of phenol- NO_2 - O_3 reaction mixture after 60 min; B-reference spectrum for 2-nitrophenol; C-residual spectrum after subtraction of the absorptions of all identified products.

Because of the overlap with the spectral features of H_2O between 2098-1249 cm^{-1} these bands could not be observed. For that reason quantitative results for the formation of 4-nitrophenol have not been obtained for the EUPHORE study.

The concentration-time profiles of the reactants and products identified in the NO_3 initiated oxidation of phenol for a typical experiment performed in EUPHORE are shown in Figure 4.10.

In deriving the nitrophenol formation yields, secondary reactions of the 2-nitrophenol by reaction with NO_3 radicals were neglected (see Section 4.2.1.1). Wall deposition was found to be the major loss process for 2-nitrophenol and HNO_3 (see Table II.2, Appendix II). Figure 4.11 shows plots of the corrected concentrations of 2-nitrophenol and HNO_3 (walls deposition and leak rate) versus the amount of consumed phenol. From the slope of the straight lines the real formation yield of the compounds was derived. The formation yields of the identified products are listed in Table 4.7.

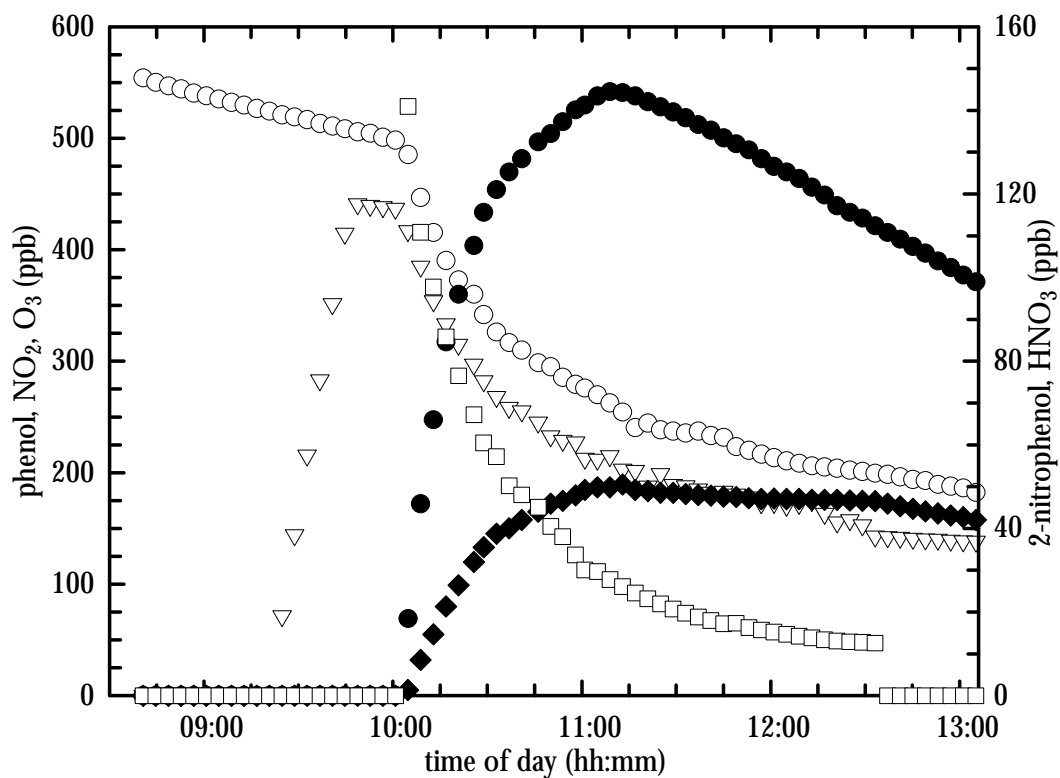


Figure 4.10 Concentration-time profiles of the reactants and products in the NO_3 radical initiated oxidation of phenol in EUPHORE (exp. 19.09.1998): (\circ)-phenol; (\square)- NO_2 ; (∇)- O_3 ; (\bullet)- HNO_3 ; (\blacklozenge)-2-nitrophenol.

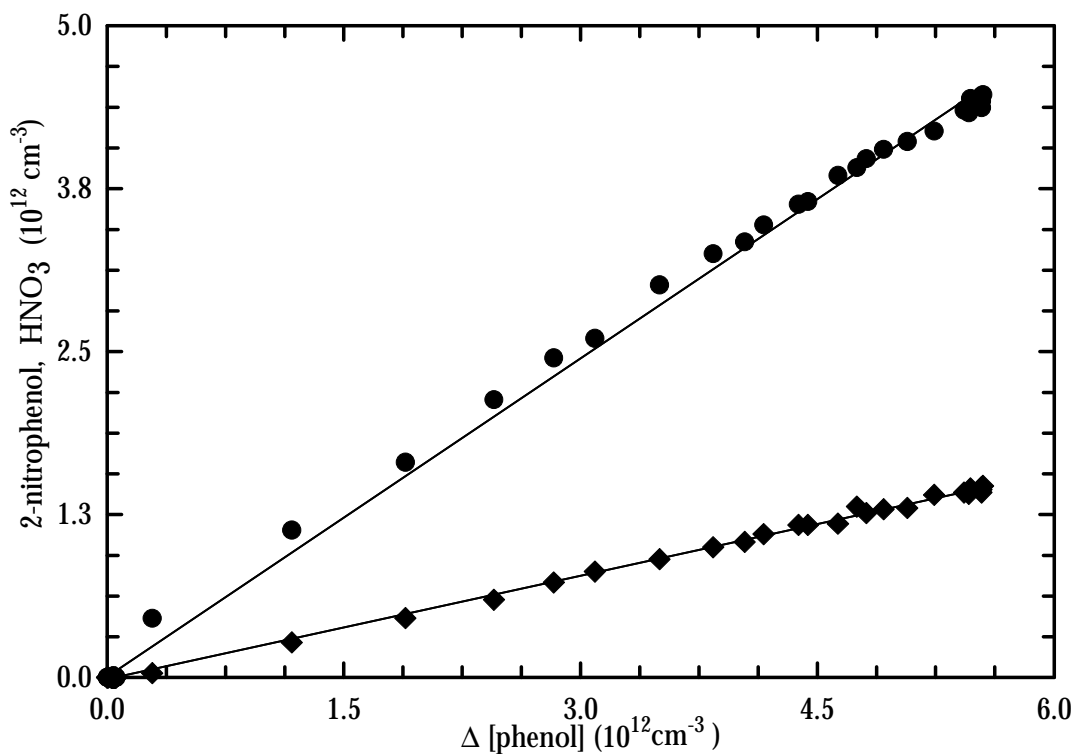


Figure 4.11 Plots of the corrected concentrations of (\blacklozenge)-2-nitrophenol and (\bullet)- HNO_3 versus the amount of consumed phenol.

Table 4.7 Formation yields of 2-nitrophenol and HNO₃ in the gas-phase reaction of the NO₃ radical with phenol in the EUPHORE chamber (Valencia/Spain).

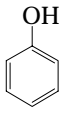
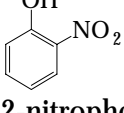
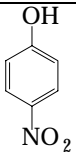
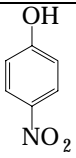
experiment	product molar yields (%)	
	2-nitrophenol	HNO ₃
PHE001	18.7 ± 2.0	64.8 ± 6.0
PHE002	25.1 ± 2.2	75.4 ± 7.0
PHE003	20.1 ± 1.9	81.2 ± 8.0
average yield	21.3 ± 3.3	73.8 ± 8.3

4.2.3 Discussion of the results

4.2.3.1 Comparison of results

An overview of the results concerning the measured formation yields of the identified products in the NO₃ initiated oxidation of phenol is presented in Table 4.8. The table also includes values found in the literature for the formation yields of the observed products (Atkinson *et al.*, 1992a; Bolzacchini *et al.*, 2001).

Table 4.8 Formation yields of the products observed in the gas-phase nitration reaction of phenol with NO₃ under different conditions.

reactant	product	conditions	yield (%)	reference
 phenol	 2-nitrophenol	NO ₂ /O ₃	24.2 ± 3.7	this work (1080 l reactor)
		NO ₂ /O ₃	21.3 ± 3.3	this work (EUPHORE)
		N ₂ O ₅	25.1 ± 5.1	Atkinson <i>et al.</i> , (1992a)
		N ₂ O ₅	38 ± 7	Bolzacchini <i>et al.</i> , (2001)
		NO ₂ /O ₃	51 ± 10	Bolzacchini <i>et al.</i> , (2001)
 4-nitrophenol	 4-nitrophenol	NO ₂ /O ₃	50.0 ± 6.8	this work (1080 l reactor)
		NO ₂ /O ₃	50.0 ± 10.0 ^a	this work (EUPHORE)
		N ₂ O ₅	-	Atkinson <i>et al.</i> , (1992a)
		N ₂ O ₅	-	Bolzacchini <i>et al.</i> , (2001)
		NO ₂ /O ₃	27.6 ± 7.9	Bolzacchini <i>et al.</i> , (2001)
HNO ₃	HNO ₃	NO ₂ /O ₃	89.7 ± 13.0	this work (1080 l reactor)
		NO ₂ /O ₃	73.8 ± 8.3	this work (EUPHORE)

^a estimated yield.

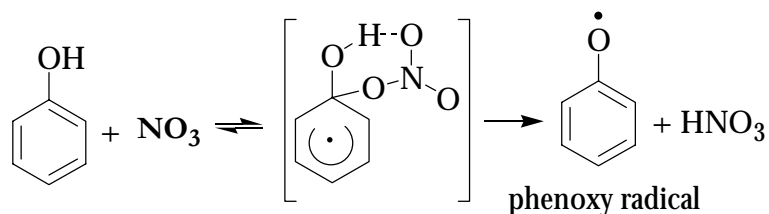
As can be seen in Table 4.8, where a direct comparison is possible, there are significant differences between the results of the three studies. The experimental approach used in the three studies was similar, although not identical.

In a recent study on the reaction of NO_3 with phenols, in different solvents, using Kyodai nitration, nitrophenols were also found to be the major reaction products (Barletta *et al.*, 2000). In the liquid phase 4-nitrophenol was found to be the major product, with a yield which varied in the range of 21 - 58%. In this study they also identified formation of 1,4-benzoquinone and two dinitrophenols as reaction products with formation yields in the range 1 - 7%.

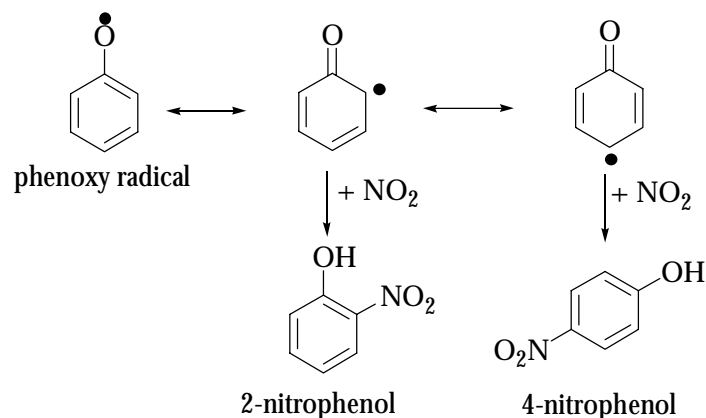
In the present work identification of 2-nitrophenol and 4-nitrophenol in the studied system agrees with the results from work of Bolzacchini *et al.* (2001), but there are discrepancies concerning the measured formation yields. The yield of 2-nitrophenol, as it was measured in the present work, is similar to that previously reported by Atkinson *et al.* (1992a). The only plausible explanation for the discrepancies concerning the formation yields of the identified products is that their production is highly affected by the experimental conditions (mostly by the amount of O_3 present in the reaction mixture).

4.2.3.2 Discussion of the formation of 2-nitrophenol and 4-nitrophenol

The results from the present work on the NO_3 radical initiated oxidation of phenol show that 2-nitrophenol and 4-nitrophenol are the most important products. The observed behaviour of the nitrophenolic compounds is in agreement with their formation through a mechanism involving phenoxy radicals, which are being formed by H-atom abstraction. The overall H-atom abstraction by NO_3 radicals is postulated to occur through the intermediacy of a six-membered transition state (Atkinson, 1991) via the following scheme:

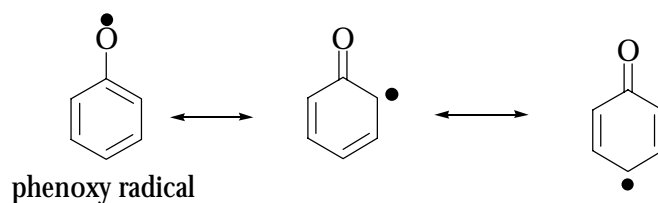


The formation of nitrophenolic compounds through the reaction of the phenoxy radical with NO_2 can be described by the following general mechanism as proposed by Carter (1990):



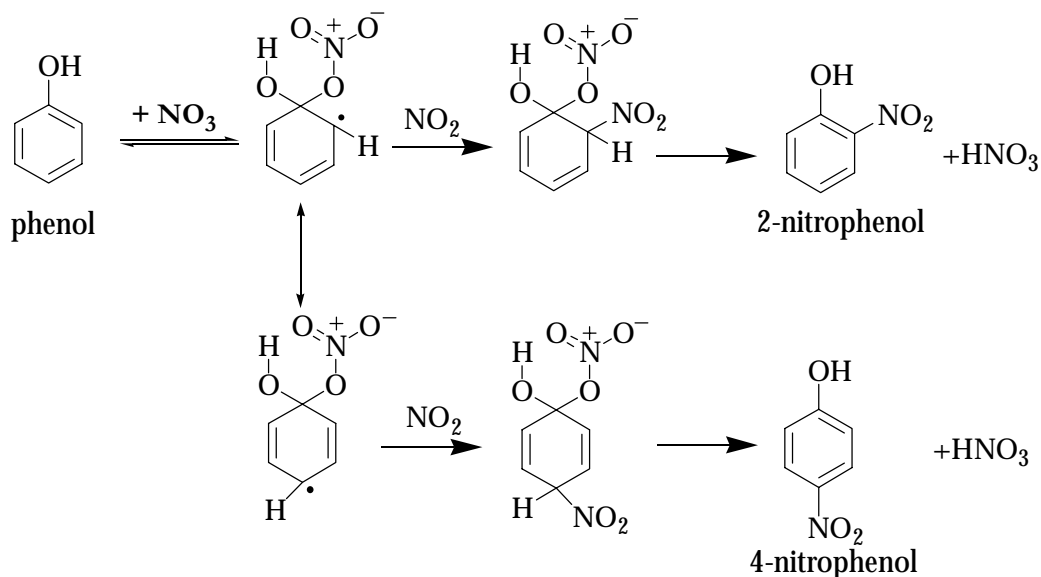
In the above general reaction mechanism it is expected that the initial NO₃ radical addition to the aromatic ring is reversible because of the short lifetime of the NO₃ - aromatic adduct with respect to its thermal decomposition back to reactants (Atkinson *et al.*, 1990; Atkinson, 1991). A decomposition rate of the NO₃ - monocyclic aromatic adduct of about $5 \times 10^8 \text{ s}^{-1}$ at 298 K has been estimated from a study of the reactions of naphthalene in N₂O₅-NO₃-NO-air mixtures (Atkinson *et al.*, 1990). As discussed by Atkinson *et al.* (1992a), it would be expected that reactions of phenoxy radicals with NO₂ will lead to a unity, or nearly unity, yield of nitrophenols.

The reaction mechanism proposed by Atkinson *et al.* (1992a), can be supported from a consideration of the electronic structure of the C₆H₅O radical, which can be represented as an admixture of three principle resonance structures:



Platz *et al.* (1998) using the Amsterdam Density Functional (ADF) code have calculated the electronic structure for the phenoxy radical. While intuitively the first resonance structure might be expected to dominate, in fact density functional calculations predict Mulliken spin densities of 0.40, 0.27 and 0.36 electrons at the phenoxy oxygen, *ortho* and *para* carbon positions, respectively. The *meta* position has a Mulliken density of only -0.10 electrons (Platz *et al.*, 1998). Hence, one would expect to observe formation of phenyl nitrate, *ortho*-nitrophenol and *para*-nitrophenol. The C₆H₅O-NO bond dissociation energy in phenyl nitrite is only 21 kcal mol⁻¹ (Berho *et al.*, 1998), and it seems reasonable to expect that phenyl nitrate will also be thermally unstable.

A hypothetical reaction mechanism, leading to the formation of 2-nitrophenol and 4-nitrophenol, was proposed by Bolzacchini *et al.* (2001). The reaction is initiated by the ipso-addition of the NO_3 radical to phenol as is shown in the following reaction scheme:



In the proposed mechanism it is assumed that the reaction in the gas-phase occurs via equilibrium addition of NO_3 to the *ipso* carbon with formation of an adduct. The adduct is stabilised by an intramolecular hydrogen bond. Further recombination reactions of this cyclohexadienyl adduct with NO_2 , then can lead to formation of two cyclohexadiene intermediates which subsequently can form the nitro-derivatives by elimination of HNO_3 .

Taking into account the above observation it is not surprising that only *ortho*- and *para*-nitrophenol were observed as significant products in the NO_3 radical initiated oxidation of phenol and, hence, the results of the present work support both reaction mechanisms as proposed by Atkinson *et al.* (1992a) and by Bolzacchini *et al.* (2001).

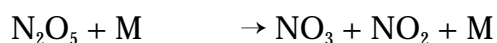
4.2.3.3 Discussion of the formation of HNO_3

HNO_3 was found to be an important co-product in the nitration of phenol with NO_3 radicals. In the present work, using the cross section from Mentel *et al.* (1996), the formation yield of HNO_3 was determined. Atkinson *et al.* (1992a) and Bolzacchini *et al.* (2001) have not reported the formation yield of HNO_3 in their studies.

HNO_3 can be formed in the gas-phase through the following reactions:



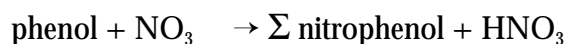
with $k_{298\text{K}} = 1.4 \times 10^{-12}$ (Atkinson *et al.*, 1992b);



with $k_{298\text{ K}} = 5.19 \times 10^{-2}$ (Atkinson *et al.*, 1992b);



with $k_{298\text{ K}} < 2.0 \times 10^{-21}$ (Atkinson *et al.*, 1992b);



with $k_{298\text{ K}} = 3.8 \times 10^{-12}$ (Calvert *et al.*, 2001).

HNO₃ can be formed by reaction between N₂O₅ and traces of H₂O (even if the experiments are carried out in dry conditions) or through the gas-phase reactions of the NO₃ radical with phenol. Taking into account the rate constants for the reactions listed above, it can be concluded that under the conditions employed in the experiments performed in this work, the formation of HNO₃ is mainly due to the reaction between phenol and NO₃ radicals. Because of the fast reaction of NO₃ with phenol the concentration of N₂O₅ will be small and, hence, its contribution to nitric acid formation will be of minor importance. It is well known that at 298 K, in air and at atmospheric pressure, N₂O₅ has a lifetime of 14 s with respect to its thermal decomposition to NO₃ radicals and NO₂. In the present work during the subtraction procedure no spectral features characteristic for N₂O₅ were observed supporting that its concentration in the system is low.

Considering that HNO₃ is the main co-product in the nitration of phenol with NO₃ radical this should also be reflected in the distribution of nitrophenol isomers yields. The yield of HNO₃, in the product studies of phenol + NO₃ in both the 1080 l quartz glass reactor and EUPHORE chamber, was observed to be formed in a yield of about 80% (see Table 4.8). Based on the qualitative and quantitative observations from the present study it can be expected that the sum of the formation yields of identified nitrophenol isomers should approximately equal the HNO₃ formation yield in these reaction systems. Taking this into account it is probable that the formation yield of 4-nitrophenol in EUPHORE chamber system experiments is about 50%.

4.2.3.4 Summary of results

The product formation during the nitration of phenol by NO₃ radicals were investigated using two chamber systems (1080 l quartz glass reactor and EUPHORE chamber). Good agreement was found between the product distributions measured in each of the chambers.

The experimental results show that 2-nitrophenol and 4-nitrophenol are the most important products from the NO₃ initiated oxidation of phenol. 2-Nitrophenol was found in a similar yield of around 24% in both chambers. The yield of 2-nitrophenol, as it was measured

in the present work, was found to be similar to that previously reported by Atkinson *et al.* (1992a). 4-Nitrophenol, which was identified in both chamber systems, was observed to be formed in a yield of about 50%. HNO_3 , as important co-products was also identified in both cases, in a yield of 90% in the 1080 l quartz glass reactor and of 74% in the EUPHORE chamber.

The results support the following simplified reaction mechanism for the reaction of NO_3 radicals with phenol:

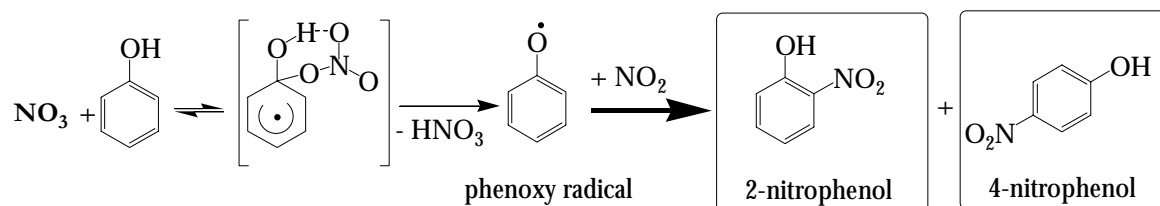


Figure 4.12 Simplified mechanism for the NO_3 radical initiated oxidation of phenol.

Mechanisms of the atmospheric oxidation of the cresol isomers

Studies relevant to the atmospheric chemistry of *ortho*-, *meta*- and *para*-cresol were performed under simulated atmospheric conditions using smog chamber systems at Wuppertal University (1080 l quartz glass reactor) and EUPHORE, Valencia/Spain.

5.1 Product analyses of the OH initiated oxidation of the cresol isomers

5.1.1 General results

The initial and final concentrations of the reactants employed during the experiments in the 1080 l quartz glass reactor are given in Table 5.1. Reactants and products were monitored using long path FT-IR spectroscopy. The main products observed in the OH radical initiated oxidation of cresols isomers include dihydroxybenzene, (methyl)benzoquinone and nitrocresol compounds.

Table 5.1 Initial and final reactant concentrations (ppmv) in experiments of the OH radical initiated oxidation of cresol isomers in the 1080 l quartz glass reactor.

experiment ^a	initial concentration (ppmv)				final concentration (ppmv)		
	cresol	CH ₃ ONO	NO	NO ₂	cresol	NO	NO ₂
OCR01	2.56	1.04	1.21	0.28	0.53	0.20	1.30
OCR02	1.16	0.99	1.20	0.21	0.15	0.30	1.20
OCR03	1.84	0.85	1.20	0.17	0.54	0.34	1.10
OCR04	1.86	1.15	0.50	1.20	1.00	0.23	1.40
OCR05	0.65	0.59	0.88	0.57	0.17	0.50	0.93
OCR06	1.16	0.60	1.07	0.35	0.34	0.57	0.72
OCR07	1.51	0.58	1.12	0.12	0.51	0.51	0.90
OCR08	2.03	0.52	1.00	0.36	0.79	0.40	0.91
MCR01	1.66	0.97	1.06	0.63	0.72	0.24	1.50
MCR02	1.17	0.74	1.23	0.35	0.23	0.26	1.14
MCR03	0.91	0.87	1.10	0.56	0.06	0.24	1.30
MCR04	1.31	0.69	0.95	0.70	0.40	0.20	1.20
MCR05	1.52	0.76	1.05	0.61	0.50	0.21	1.33
MCR06	2.46	0.77	1.00	0.51	1.26	0.23	1.30
PCR01	2.12	0.93	1.20	0.20	0.33	0.22	1.40
PCR02	2.72	0.82	1.22	0.30	0.96	0.42	1.26
PCR03	1.60	0.90	1.16	0.19	0.53	0.23	1.30
PCR04	0.54	0.68	0.53	1.00	0.10	0.21	1.14
PCR05	0.98	0.88	0.99	0.54	0.16	0.23	1.14
PCR06	1.53	0.96	0.83	0.74	0.31	0.17	1.20
PCR07	0.51	0.81	0.83	0.53	0.05	0.25	1.06

^a experimental designations: OCR=*ortho*-cresol, MCR=*meta*-cresol, PCR=*para*-cresol.

5.1.1.1 FT-IR spectral data from the reaction of OH with *ortho*-cresol

FT-IR spectral analyses showed the formation of the ring-retaining products 1,2-dihydroxy-3-methyl-benzene, methyl-1,4-benzoquinone and 6-methyl-2-nitrophenol from the gas-phase reaction of OH radicals with *ortho*-cresol in the presence of NO_x. Typical FT-IR data in the range of 1800–700 cm⁻¹ are presented in Figure 5.1.

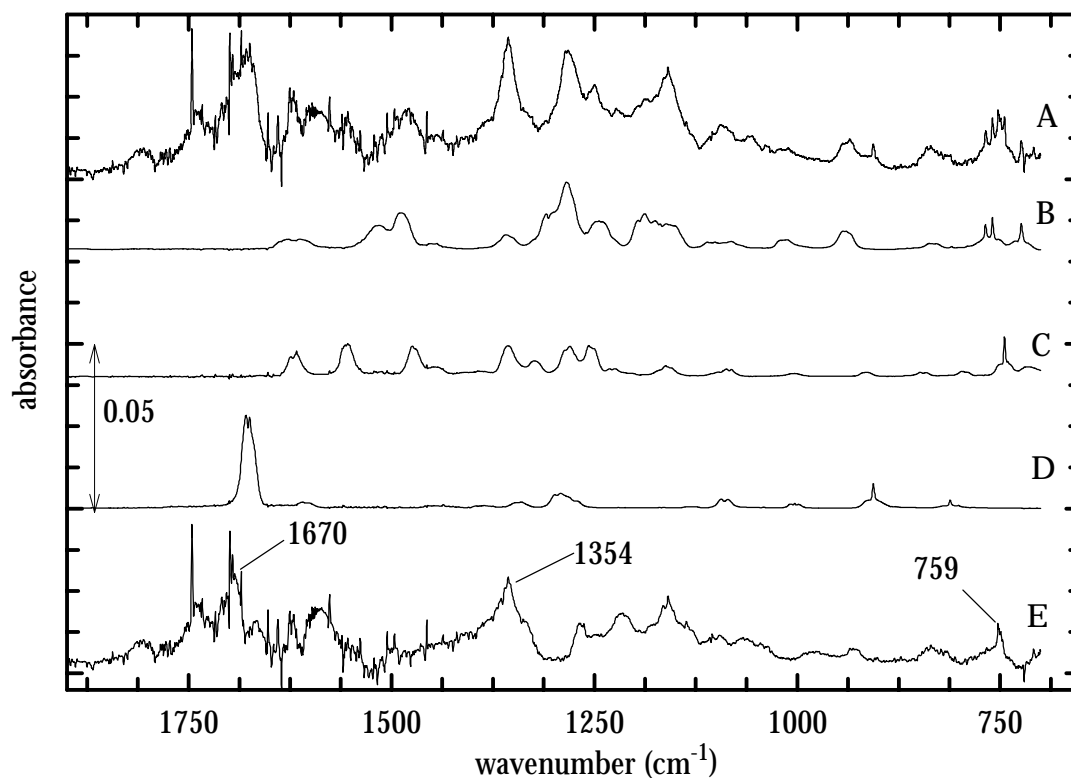


Figure 5.1 Infrared absorption spectra from the photo-oxidation of *ortho*-cresol in the range 1800–700 cm^{-1} : A-product spectrum; B-reference spectrum of 1,2-dihydroxy-3-methylbenzene; C-reference spectrum of 6-methyl-2-nitrophenol; D-reference spectrum of methyl-1,4-benzoquinone; E-residual spectrum after subtraction of all identified products.

In Figure 5.1, spectrum A shows a product spectrum obtained after subtraction of the spectral features belonging to water, reactants and some of the other small organic and inorganic co-products, e.g. H_2CO , HCOOH , CH_3OH , HNO_3 , CH_3NO_3 and HONO , from a spectrum which was recorded after approximately 12 min of irradiation. Spectrum B is the reference spectrum for 1,2-dihydroxy-3-methylbenzene, spectrum C that for 6-methyl-2-nitrophenol and spectrum D that the reference spectrum for methyl-1,4-benzoquinone. Trace E (Figure 5.1) is the residual spectrum obtained after subtraction of absorptions due to 1,2-dihydroxy-3-methylbenzene, 6-methyl-2-nitrophenol and methyl-1,4-benzoquinone from spectrum A.

The residual spectrum E, shows that some minor products have not been identified. The concentration-time profiles of *ortho*-cresol and its oxidation products are presented in Figure 5.2.

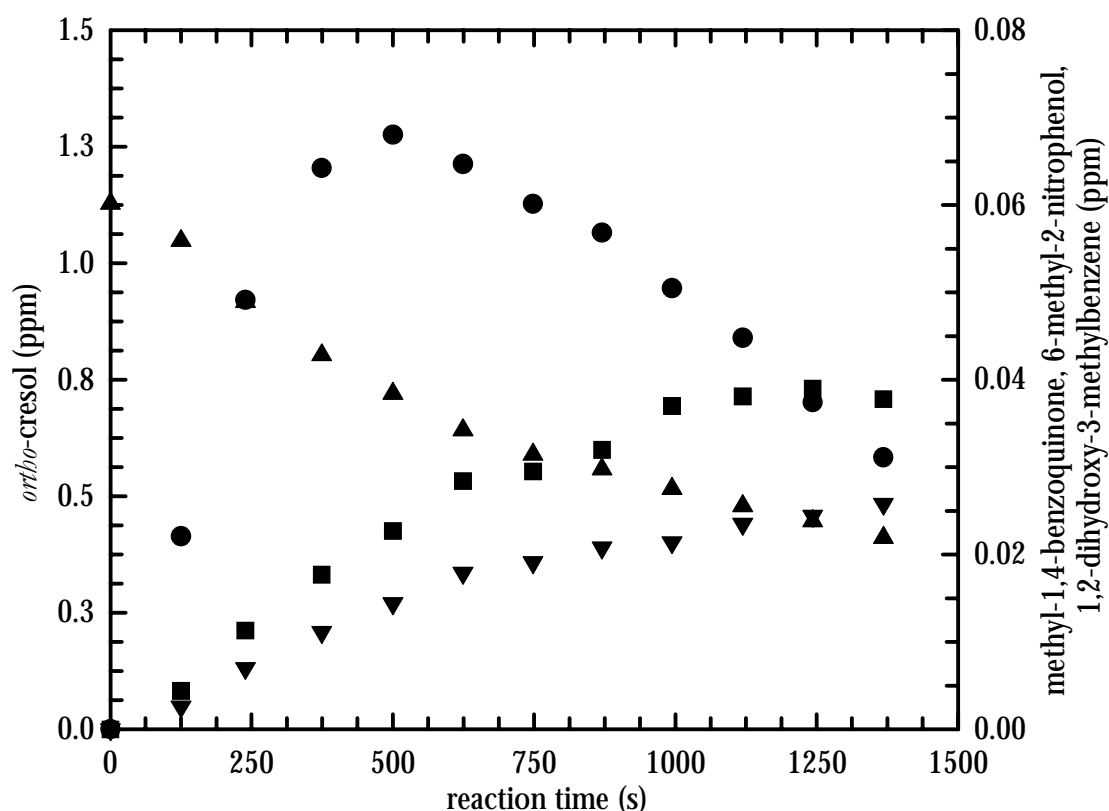


Figure 5.2 Concentration-time profiles of *ortho*-cresol and products identified in the OH initiated oxidation of *ortho*-cresol in the presence of NO_x : (▲)-*ortho*-cresol; (●)-1,2-dihydroxy-3-methylbenzene, (▼)-6-methyl-2-nitrophenol, (■)-methyl-1,4-benzoquinone.

5.1.1.2 FT-IR spectral data from the reaction of OH with *meta*-cresol

A wide range of ring-retaining products were identified during the reaction of OH radical with *meta*-cresol in the presence of NO_x .

Figure 5.3 exhibits infrared spectral information in the range $1800\text{-}700\text{ cm}^{-1}$ for the experiments performed on the OH-radical initiated oxidation of *meta*-cresol. Spectrum A from this figure shows the product spectrum after subtraction of all reactants and some of the other small organic and inorganic co-products. The other spectra (B, C, D, E and F) in this figure show the reference spectra of the all compounds which were identified in this reaction system, 1,2-dihydroxy-3-methylbenzene, 1,2-dihydroxy-4-methylbenzene, methyl-1,4-benzoquinone, 3-methyl-4-nitrophenol and 5-methyl-2-nitrophenol, respectively. Spectrum G is the residual spectrum obtained after subtraction of absorptions due to all the identified compounds.

The concentration-time profile of the reactant and products observed from the OH initiated oxidation of *meta*-cresol in the presence of the NO_x are presented in Figure 5.4.

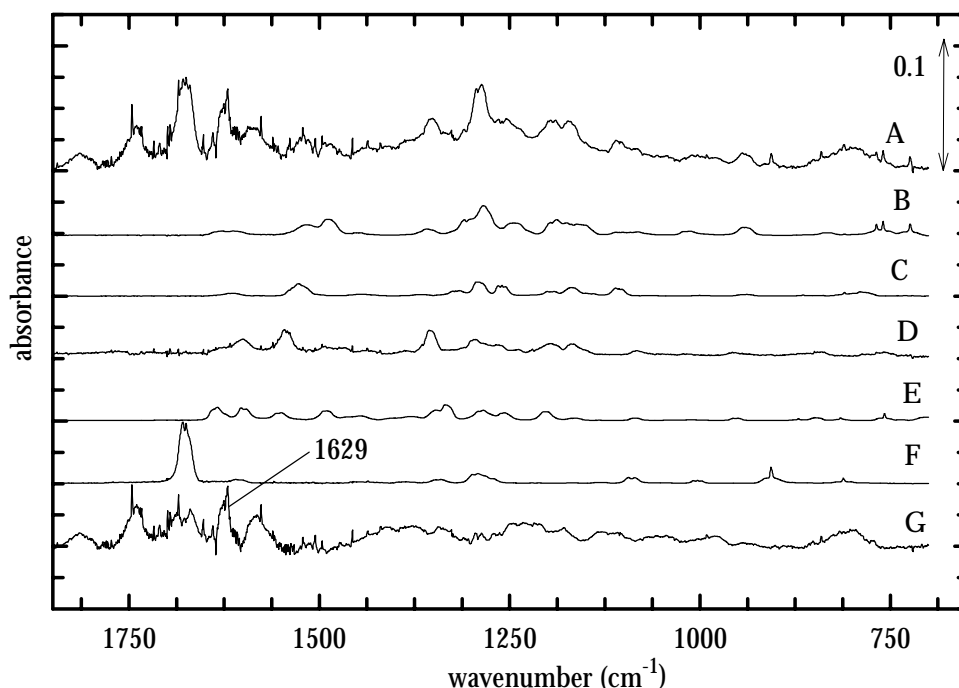


Figure 5.3 Infrared absorption spectra from the photo-oxidation of *meta*-cresol in the range 1800-700 cm^{-1} : A-product spectrum; B-reference spectrum of 1,2-dihydroxy-3-methylbenzene; C-reference spectrum of 1,2-dihydroxy-4-methylbenzene; D-reference spectrum of 3-methyl-4-nitrophenol; E-reference spectrum of 5-methyl-2-nitrophenol; F-reference spectrum of methyl-1,4-benzoquinone; G-residual spectrum after subtraction of all identified products.

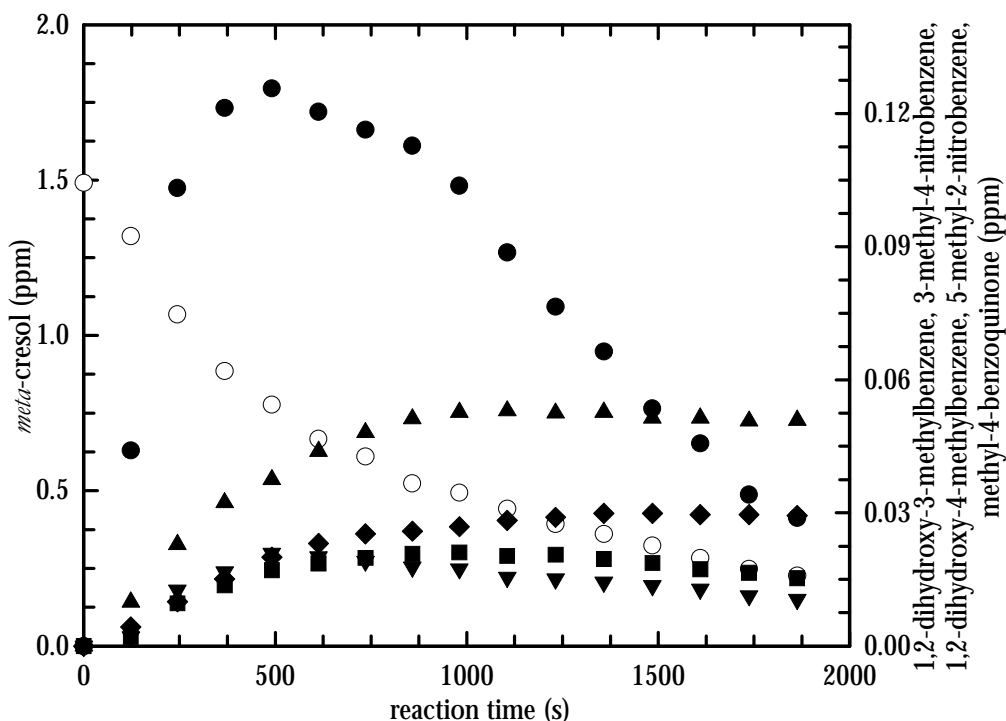


Figure 5.4 Concentration-time profiles of *meta*-cresol and the products identified in the OH initiated oxidation of *meta*-cresol in the presence of NO_x : (○)-*meta*-cresol; (●)-1,2-dihydroxy-3-methylbenzene; (▼)-1,2-dihydroxy-4-methylbenzene; (▲)-methyl-1,4-benzoquinone; (◆)-3-methyl-4-nitrophenol; (■)-5-methyl-2-nitrophenol.

5.1.1.3 FT-IR spectral data from the reaction of OH with *para*-cresol

Formation of the ring-retaining products 1,2-dihydroxy-4-methylbenzene and 4-methyl-2-nitrophenol was observed in the OH-initiated oxidation of *para*-cresol in the presence of NO_x . Figure 5.7 shows infrared spectral information in the range $1750\text{--}750\text{ cm}^{-1}$. Spectrum A is the product spectrum obtained after subtraction of all reactants and some of the well known organic and inorganic co-products (e.g. H_2CO , HCOOH , CH_3OH , HNO_3 , CH_3ONO_2 , HONO). Spectrum B is the reference spectrum for 4-methyl-1,2-dihydroxybenzene, spectrum C is the reference spectrum for 4-methyl-2-nitrophenol and spectrum D is the residual spectrum obtained after subtraction of absorptions due to 4-methyl-1,2-dihydroxybenzene and 4-methyl-2-nitrophenol.

The concentration-time profiles of the reactant and products observed for a typical experiment on *para*-cresol are presented in Figure 5.8.

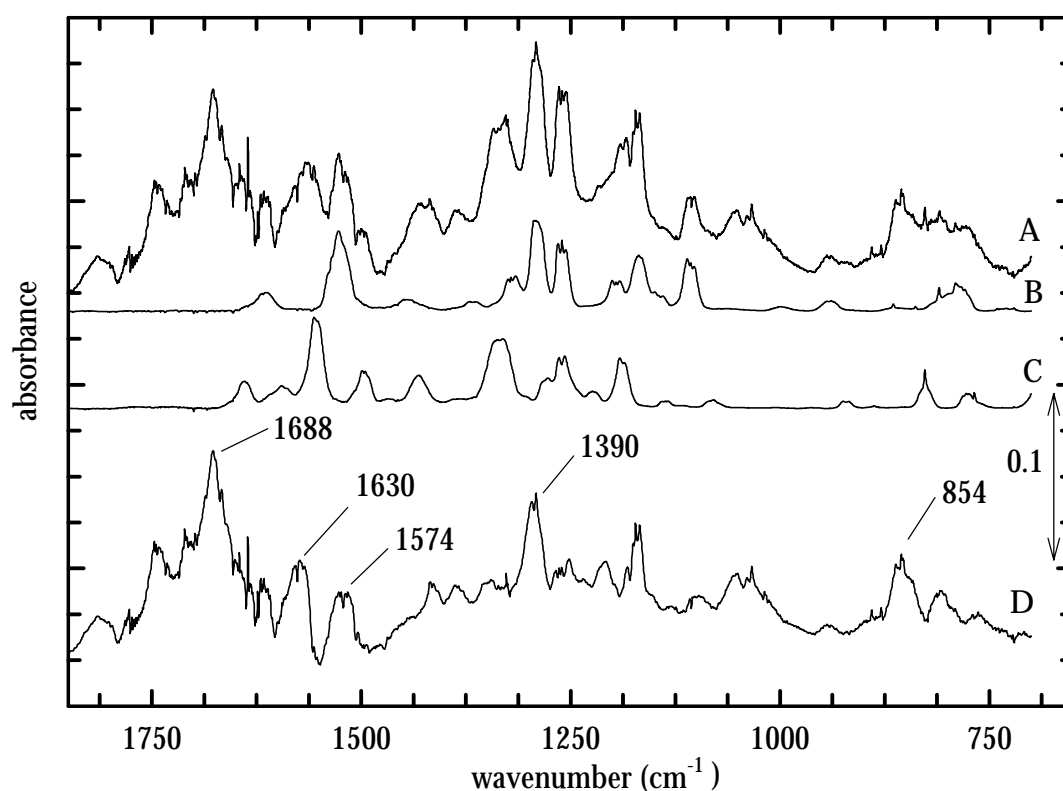


Figure 5.5 Infrared absorption spectra from the photo-oxidation of *para*-cresol in the range $1800\text{--}700\text{ cm}^{-1}$: A-product spectrum; B-reference spectrum of 1,2-dihydroxy-4-methylbenzene; C-reference spectrum of 4-methyl-2-nitrophenol; D-residual spectra after subtraction of all identified products.

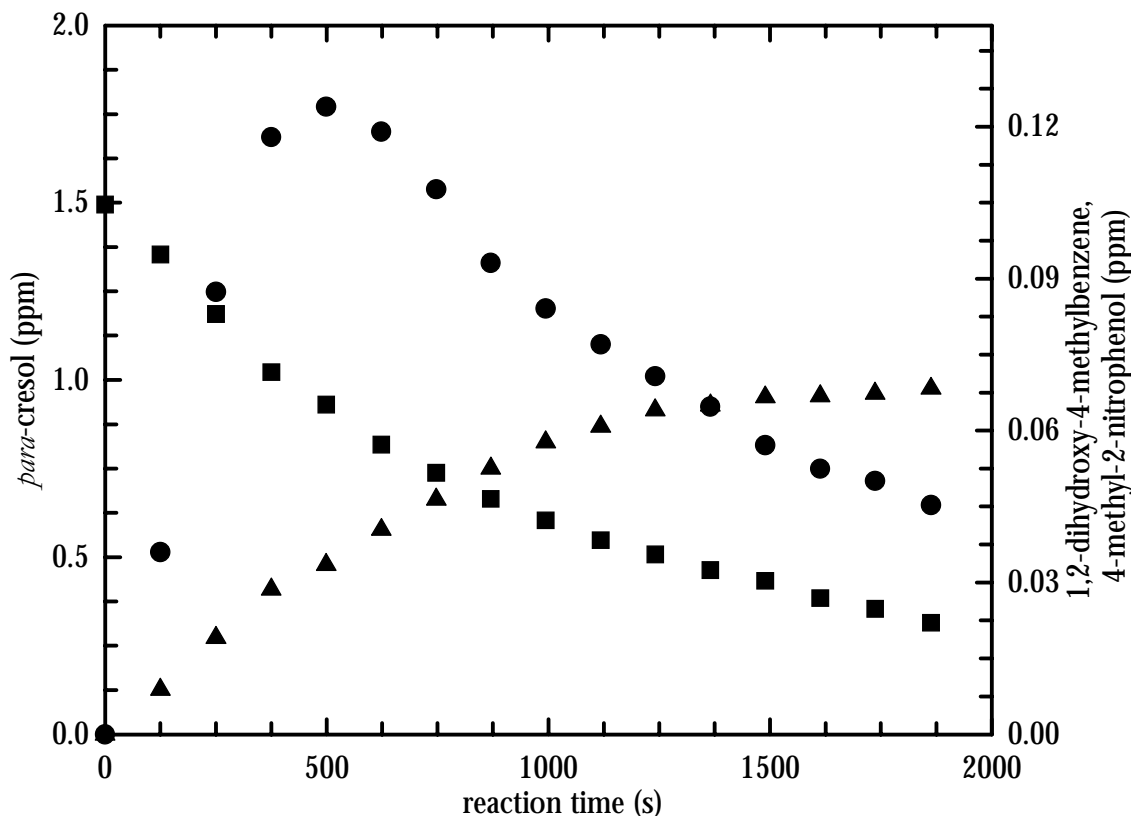


Figure 5.6 Concentration-time profiles of *para*-cresol and the products identified in the OH initiated oxidation of *para*-cresol in the presence of NO_x : (■)-*para*-cresol; (●)-1,2-dihydroxy-4-methylbenzene, (▲)-4-methyl-2-nitrophenol.

5.1.1.4 Data evaluation

Apart from the 1,2-dihydroxybenzene, reference spectra were available for the other possible dihydroxybenzene isomers that can be formed from the photo-oxidations of *ortho*-cresol (1,3- and 1,4-dihydroxy-3-methylbenzene), *meta*-cresol (1,5-dihydroxy-3-methylbenzene) and *para*-cresol (1,3-dihydroxy-4-methylbenzene). There were no indications in the product spectra for the formation of these other dihydroxybenzene isomers. If other isomers are formed, their yields will be minor.

Not all of the possible isomers of (methyl)benzoquinone and nitrocresol are commercially available. In the case of the nitrocresol isomers checks were made for those which were available or could be synthesised (see Appendix I.2). In the product spectra no other nitrocresols were identified apart from those which have been previously indicated in Sections 5.1.1.1 to 5.1.1.3.

In the OH initiated oxidation of cresols formation of (methyl)-1,2-benzoquinones may occur. These products are not commercially available and are expected to be thermally unstable. From the literature data (Patai, 1974), it is known that *ortho*-benzoquinones generally

absorb at higher wave number than the corresponding *para*-benzoquinones, if the substituents are the same. On the basis of the infrared data available in the literature concerning the spectral features of (methyl)-1,2-benzoquinones (Thomson, 1971), an analysis of the residual product spectra suggests that (methyl)-1,2-benzoquinone is formed under the experimental conditions (see for example *para*-cresol residual FT-IR spectra, Figure 5.5, D) The stretching vibrations of the carbonyl group in 1,2-benzoquinone (in solution) are at 1680 and 1658 cm^{-1} (Thomson, 1971).

Formation of hydroxybenzaldehyde isomers from the OH initiated oxidation of cresols at the CH_3 substituent is a possibility. However, no evidence was found for the formation of these compounds in the residual product spectra.

After spectral stripping of the identified products from the product spectra unidentified absorptions remained. In these residual spectra absorptions due to carbonyls and nitrates were evident.

The plots of the concentration of the all identified products versus time show that secondary reactions occurred for some products during the experiment (see Figures 5.2, 5.4 and 5.6). The product yields obtained from the analyses of the product spectra need to be corrected for reaction with OH radicals, wall loss and photolysis in order to derive their formation yields.

It was determined that wall deposition of the identified compounds is an important loss processes (see Appendix II). The photolysis rate constants of some identified compounds were determined to be negligible compared with wall deposition processes. For methyl-1,4-benzoquinone and nitrophenol concentration profiles versus time, no strong curvature was observed, therefore it would appear that these compounds are not strongly influenced by loss processes.

The identified compounds are also expected to react rapidly with the NO_3 radicals (Atkinson, 1994; Calvert *et al.*, 2001). However, the experimental conditions were such that the NO concentrations were sufficiently high to suppress the formation of O_3 and hence of NO_3 (see Table 5.1) and the dominant removal processes throughout the irradiation period were by reaction with OH radical and walls loss.

The measured concentrations of the products were corrected by taking into account the loss processes due to reaction with OH radicals and wall loss. Corrections were performed using the mathematical formalism proposed by Tuazon *et al.* (1986) which is presented in Appendix IV.

Values of 4.1×10^{-11} for $k(\text{OH}+\textit{ortho}\text{-cresol})$, 6.8×10^{-11} for $k(\text{OH}+\textit{meta}\text{-cresol})$ and $5.0 \times 10^{-11} \text{ cm}^3 \text{ molecule}^{-1} \text{ s}^{-1}$ for $k(\text{OH}+\textit{para}\text{-cresol})$ from Calvert *et al.* (2001) were used in the correction procedure. For the dihydroxy(methyl)benzenes and (methyl)benzoquinones the OH radical rate constants were taken from the relative kinetic performed within this study (Olariu *et al.*, 2000a) with: $k(\text{OH}+1,2\text{-dihydroxy-3-methylbenzene}) = (2.05 \pm 0.43) \times 10^{-10} \text{ cm}^3$

molecule⁻¹ s⁻¹, $k(\text{OH}+1,2\text{-dihydroxy-4-methylbenzene}) = (1.56 \pm 0.33) \times 10^{-10} \text{ cm}^3 \text{ molecule}^{-1} \text{ s}^{-1}$ and $k(\text{OH}+\text{methyl-1,4-benzoquinone}) = (2.35 \pm 0.47) \times 10^{-11} \text{ cm}^3 \text{ molecule}^{-1} \text{ s}^{-1}$.

The nitrocresol + OH rate constant has not been measured. Using the relationship between the ionization potential and the reactivity towards OH radicals, Grosjean (1990) estimated that the rate constants of nitrocresols with OH radicals are about $3.4 \times 10^{-13} \text{ cm}^3 \text{ molecule}^{-1} \text{ s}^{-1}$. This rate constant together with an average experimental OH concentration of $1 \times 10^7 \text{ molecule cm}^{-3}$ corresponds to a contribution of less than 5% to the overall loss processes in the chamber. Thus, secondary reactions of the nitrocresols with OH were neglected in deriving their formation yields.

Examples of the corrected ring-retaining product concentrations versus the amount of consumed *ortho*-, *meta*- and *para*-cresol are presented in Figures 5.7, 5.8 and 5.9, respectively. The corrected yields are listed in Tables 5.2, 5.3 and 5.4. The maximum values of the correction factors were: ~ 18 for 1,2-dihydroxy-3-methylbenzene, ~ 15 for 1,2-dihydroxy-4-methylbenzene, ~ 1.4 for methyl-1,4-benzoquinone and ~ 1.5 for the nitrocresols.

The errors quoted in Tables 5.2, 5.3 and 5.4 are a combination of the 2σ statistical errors from the linear regression analysis of the plots in Figure 5.7, 5.8 and 5.9 and the errors from the spectral subtraction procedure and the error introduced by the correction procedure from the rate constants of the products with OH radicals.

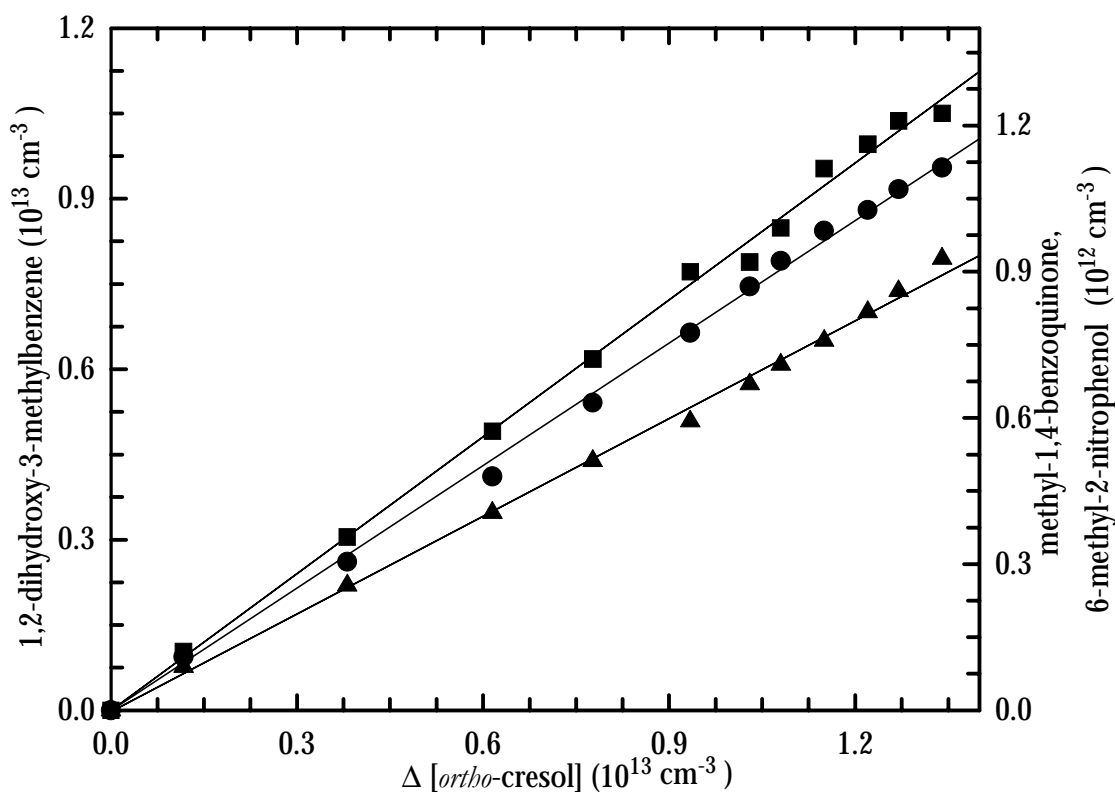


Figure 5.7 Plots of the corrected concentrations of (●)-1,2-dihydroxy-3-methylbenzene, (■)-methyl-1,4-benzoquinone and (▲)-6-methyl-2-nitrophenol versus the amount of reacted *ortho*-cresol.

Table 5.2 Yields of the ring-retaining products formed in the reaction of OH radicals with *ortho*-cresol at 1000 mbar total pressure of air and 298 ± 2 K.

experiment	product molar yields (%)		
	1,2-dihydroxy-3-methylbenzene	methyl-1,4-benzoquinone	6-methyl-2-nitrophenol
OCR01	64.8 ± 12.6	7.2 ± 1.0	6.1 ± 1.3
OCR02	65.0 ± 12.6	7.1 ± 1.0	6.1 ± 1.2
OCR03	71.0 ± 13.8	6.5 ± 0.9	5.8 ± 1.2
OCR04	73.5 ± 14.3	7.7 ± 1.1	5.6 ± 1.3
OCR05	78.3 ± 15.2	7.6 ± 1.1	10.1 ± 2.3
OCR06	75.0 ± 14.6	6.2 ± 0.8	7.5 ± 1.3
OCR07	85.0 ± 16.5	6.3 ± 0.9	6.2 ± 1.2
OCR08	74.6 ± 14.5	6.1 ± 0.8	6.9 ± 1.3
average yield	73.4 ± 14.6	6.8 ± 1.0	6.8 ± 1.5

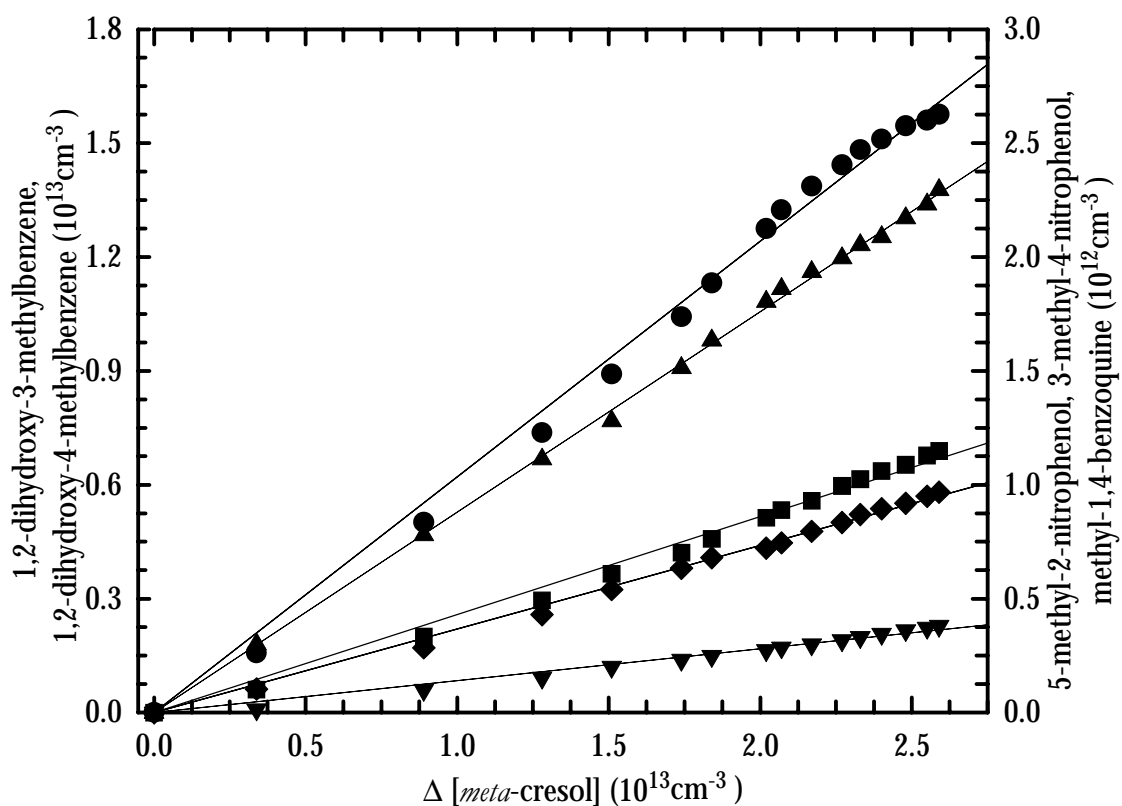


Figure 5.8 Plots of the corrected concentrations of (●)-1,2-dihydroxy-3-methylbenzene, (▼)-1,2-dihydroxy-4-methylbenzene, (▲)-methyl-1,4-benzoquinone, (◆)-3-methyl-4-nitrophenol and (■)-5-methyl-2-nitrophenol versus the amounts of reacted *meta*-cresol.

Table 5.3 Yields of the ring-retaining products from the reaction of OH radicals with *meta*-cresol at 1000 mbar total pressure of air and 298 ± 2 K.

experiment	product molar yields (%)				
	1,2-dihydroxy-3-methylbenzene	1,2-dihydroxy-4-methylbenzene	methyl-1,4-benzoquinone	3-methyl-4-nitrophenol	5-methyl-2-nitrophenol
MCR01	71.7 ± 14.3	7.4 ± 1.5	10.9 ± 1.5	4.1 ± 0.9	4.0 ± 0.8
MCR02	68.0 ± 13.6	10.6 ± 2.1	9.5 ± 1.3	5.6 ± 1.1	5.9 ± 1.2
MCR03	68.4 ± 13.6	10.6 ± 2.0	11.0 ± 1.5	4.6 ± 1.0	4.4 ± 0.9
MCR04	68.3 ± 13.6	10.4 ± 2.0	10.8 ± 1.5	4.7 ± 1.0	4.4 ± 0.9
MCR05	67.0 ± 13.4	8.4 ± 1.7	12.8 ± 1.8	3.6 ± 0.7	4.4 ± 0.9
MCR06	68.3 ± 13.6	8.0 ± 1.6	12.8 ± 1.8	3.4 ± 0.7	3.7 ± 0.7
average yield	68.6 ± 13.4	9.7 ± 2.7	11.3 ± 2.5	4.3 ± 1.6	4.4 ± 1.5

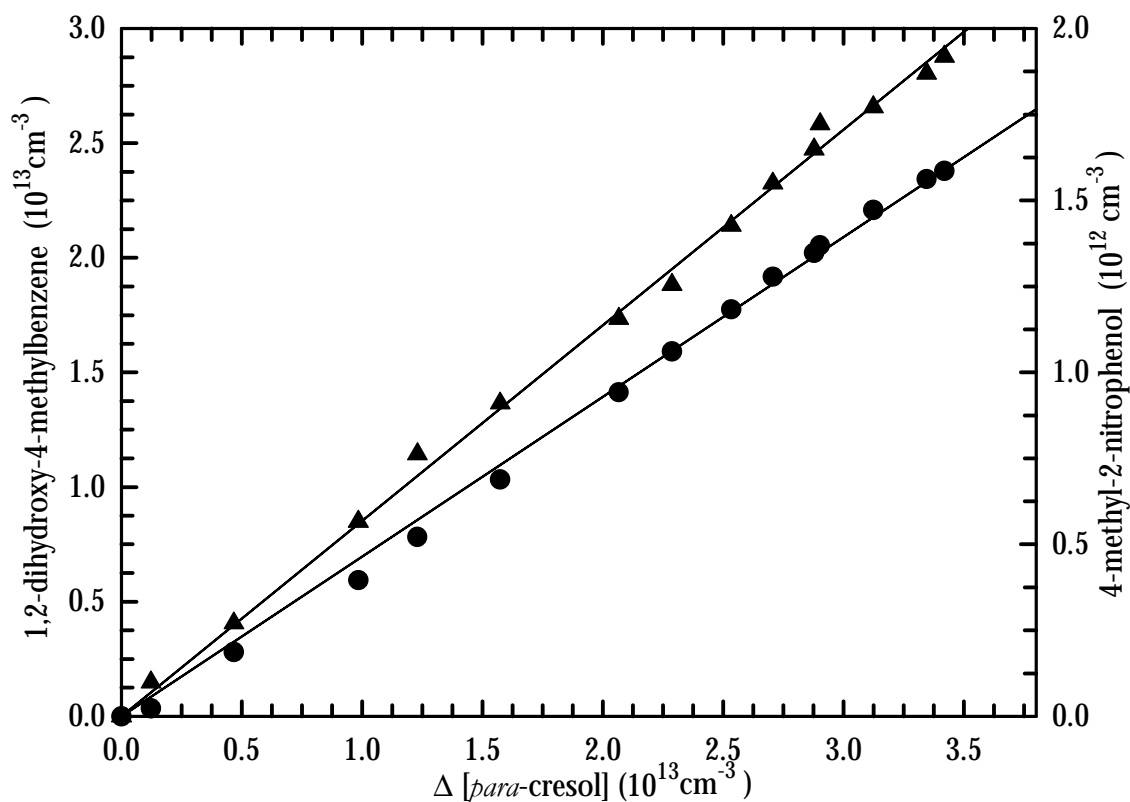


Figure 5.9 Plots of the corrected concentrations of (●)-1,2-dihydroxy-4-methylbenzene and (▲)-4-methyl-2-nitrophenol versus the amount of reacted *para*-cresol.

Table 5.4 Yields of the ring-retaining products yields from the reaction of OH radicals with *para*-cresol at 1000 mbar total pressure of air and 298 ± 2 K.

experiment	product molar yields (%)	
	1,2-dihydroxy-4-methylbenzene	4-methyl-2-nitrophenol
PCR01	67.7 ± 11.9	6.8 ± 1.4
PCR02	57.4 ± 10.1	5.6 ± 1.1
PCR03	69.4 ± 11.5	7.4 ± 1.5
PCR04	75.7 ± 13.4	10.1 ± 2.0
PCR05	53.9 ± 9.5	7.5 ± 1.5
PCR06	51.8 ± 9.2	7.4 ± 1.5
PCR07	72.4 ± 12.8	8.1 ± 1.6
average yield	64.1 ± 11.3	7.6 ± 2.2

5.1.2 Discussion of the results

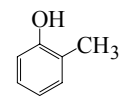
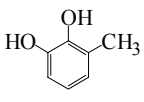
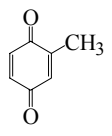
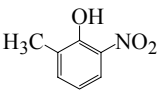
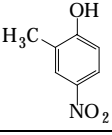
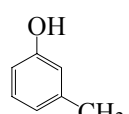
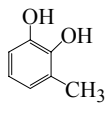
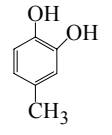
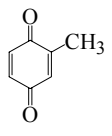
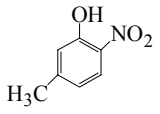
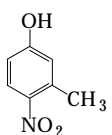
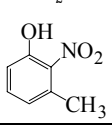
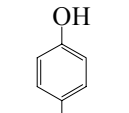
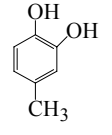
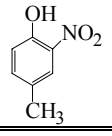
Table 5.5 gives an overview of the formation yields of the products identified in the photo-oxidation of cresol isomers in the presence of NO_x . In this table yields from the literature are also included.

Formation of 1,2-dihydroxy(methyl)benzene and methyl-1,4-benzoquinone from the gas-phase OH radical initiated oxidation of cresol isomers has not previously been reported, therefore, no literature data exists for comparison.

For the cresol isomers only formation of 1,2-dihydroxybenzene isomers was observed, i.e. compounds where the HO groups are vicinal to each other. In the case of *meta*-cresol formation of both of the possible 1,2-dihydroxy isomers, 1,2-dihydroxy-3-methylbenzene and 1,2-dihydroxy-4-methylbenzene was observed. In these compounds the new HO group is in *ortho* to the HO group and *para* to the CH_3 group.

From the results of the present study it can be concluded that 1,2-dihydroxy(methyl)benzenes isomers are without doubt the major gas-phase reaction products of the OH radical initiated oxidation of all the cresol isomers (Olariu *et al.*, 2000b). A recent finding from a pulse radiolysis study of the reaction of OH radicals with cresols in deoxygenated and oxygenated solutions (Choure *et al.*, 1997) also indicated dihydroxy(methyl)benzenes as the major reaction products. In this study, the yields of the dihydroxy products were higher in the deoxygenated than in the oxygenated solutions. In the study of Choure *et al.* (1997) in the oxygenated solutions of the cresols mainly the dihydroxy(methyl)benzenes with OH groups *ortho* to each other were formed. In the case of *meta*-cresol the formation of 1,5-dihydroxy-3-methylbenzene was also observed.

Table 5.5 Summary of the formation yields of the products identified in the OH-radical initiated photo-oxidation of cresol isomers at 1000 mbar total pressure of air and 298 ± 2 K.

reactant	product	yield (this work)	yield (literature)	
 <i>ortho</i> -cresol		1,2-dihydroxy-3-methylbenzene	73.4 ± 14.6	-
		methyl-1,4-benzoquinone	6.8 ± 1.0	-
		6-methyl-2-nitrophenol	6.8 ± 1.5	5.1 ± 1.5^a $4.9 \div 11^b$
		6-methyl-4-nitrophenol	n.d. ^c	$4.9 \div 11^b$
 <i>meta</i> -cresol		1,2-dihydroxy-3-methylbenzene	68.6 ± 13.4	-
		1,2-dihydroxy-4-methylbenzene	9.7 ± 2.7	-
		methyl-1,4-benzoquinone	11.3 ± 2.5	-
		5-methyl-2-nitrophenol	4.4 ± 1.5	1.6 ± 0.1^a
		3-methyl-4-nitrophenol	4.3 ± 1.6	-
		3-methyl-2-nitrophenol	n.d. ^c	1.6 ± 0.1^a
 <i>para</i> -cresol		1,2-dihydroxy-4-methylbenzene	64.1 ± 11.3	-
		4-methyl-2-nitrophenol	7.5 ± 2.2	10 ± 4^a

^a Atkinson *et al.* (1992a); ^b Grosjean (1985), sum: 6-methyl-2-nitrophenol and 6-methyl-4-nitrophenol; ^c not detected.

Therefore, the behavior of dihydroxy(methyl)benzene formation from OH + cresols in solution is very similar to that observed for the same reactions in the gas-phase in this work.

In the present study of the OH initiated oxidation of *ortho*- and *meta*-cresol formation of 1,4-benzoquinones was observed. The formation of a 1,4-benzoquinone is not possible for *para*-cresol. The yields of the 1,4-benzoquinones take the order OH + *ortho*-cresol (6.8) < OH + *meta*-cresol (11.3).

Nitrocresol formation has been reported previously for the reaction of OH with the cresol isomers (Grosjean, 1985; Atkinson *et al.*, 1992a). As seen in Table 5.5, the yield of 6-methyl-2-nitrophenol determined in the present work for OH + *ortho*-cresol, is in reasonable agreement with that reported by Atkinson *et al.* (1992a). Grosjean (1985) observed 6-methyl-2-nitrophenol and 6-methyl-4-nitrophenol as products in a combined yield that varied over the range 4.9 - 11%. In this study Grosjean (1985) did not provide any information concerning the relative yields of the two methyl-nitrophenol isomers. No reference spectrum is available for 6-methyl-4-nitrophenol, however, the residual product infrared spectra (see Figures 5.1, E) still retained spectral features characteristic for a nitrocresol compound even after subtraction of the absorptions of 6-methyl-2-nitrophenol. Therefore, it is quite possible that 6-methyl-4-nitrophenol is also being formed in the OH + *ortho*-cresol reaction, however, due to the non-availability of a reference spectrum a positive was not possible.

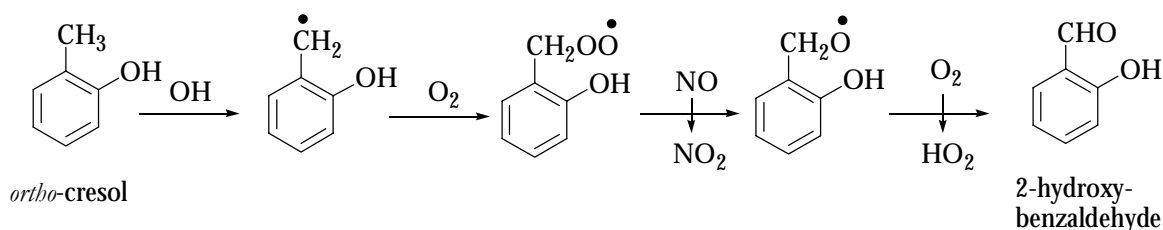
Apart from *meta*-cresol the yields of methyl-2-nitrophenol are in reasonable agreement with those reported by Atkinson *et al.* (1992a). In the case of *meta*-cresol the yield of 5-methyl-2-nitrophenol measured by Atkinson *et al.* (1992a) is more than a factor of 2 lower than that measured in this work. In addition, Atkinson *et al.* (1992a) observed the formation of 3-methyl-2-nitrophenol in the same yield as 5-methyl-2-nitrophenol. In the present work no evidence could be found for the formation of 3-methyl-2-nitrophenol but formation of 3-methyl-4-nitrophenol was observed in a yield equivalent to that of 5-methyl-2-nitrophenol. Other nitrocresol isomers which may be formed might difficult to observe in the residual FT-IR product spectra (see Figure 5.3) because of overlapping spectral features of the other unidentified compounds.

The observed ring-retaining products account for approximately 87, 98 and 72% carbon in the OH radical initiated oxidation of *ortho*-, *meta*- and *para*-cresol, respectively. Presently, it can only be speculated as to the nature of the missing carbon. As noted in the results section the yields of other dihydroxybenzene and nitrophenol isomers must be very minor, therefore, it suspected that the missing carbon is probably in the form of carbonyl ring-fragmentation products (e.g. maleic anhydride, ketoacid), carbonyl ring-retaining products (e.g. *ortho*-benzoquinone) and aromatic nitrates.

As in the phenol case, it is interesting to note that the yields of the dihydroxy(methyl)benzenes from the reaction of OH with the monohydroxybenzenes are much higher than the yields of monohydroxybenzenes formed from the reaction of OH with

the parent alkylbenzene, i.e. toluene for the cresols. In the case of OH + toluene, ~12% *ortho*-cresol, ~3% *meta*-cresol and ~3% *para*-cresol (Klotz *et al.*, 1998) are formed compared to ~73% 1,2-dihydroxy-3-methylbenzene, ~68% 1,2-dihydroxy-3-methylbenzene and ~64% 1,2-dihydroxy-4-methylbenzene from OH + *ortho*-, *meta*- and *para*-cresol. These differences obviously reflect a major difference in the oxidation pathways of the cresol isomers compared to toluene. Whereas in the OH radical initiated photo-oxidation of toluene ~30% of the reaction leads to ring-retaining products and ~70% to ring-fragmentation products, for the cresol isomers from this study the yield of ring-retaining products is certainly more than 70% in all cases. For *meta*-cresol the yield of the ring-retaining compounds is, within the experimental error limits, close to unity.

The reaction of OH with the cresol isomers can proceed by H-atom abstraction from the O-H bonds of the HO substituent and the C-H bonds of the CH₃ substituents and by OH radical addition to the aromatic ring (Calvert *et al.*, 2001). At 298 K approximately 7% of the overall reaction of OH with *ortho*-cresol proceeds via H-atom abstraction (Atkinson, 1989) the remaining 93% being addition. From kinetic data it is known that the abstraction rate constant for *ortho*-cresol is considerably higher than for toluene (Atkinson, 1989). Based on this observation it is expected that H-atom abstraction from the CH₃ substituents of the cresols is of negligible importance. This is confirmed by the product analysis where no evidence was found for the formation of hydroxybenzaldehyde isomers which could be produced via the reaction sequence:

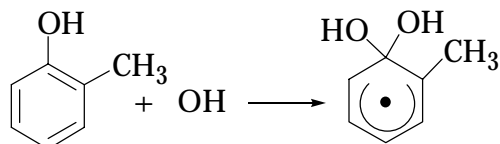


For the mechanistic discussions presented in the following section it has been assumed that H-atom abstraction for the cresols only occurs from the OH group and that the fraction of H-atom abstraction for *meta*- and *para*-cresol is similar to that for *ortho*-cresol.

5.1.2.1 Discussion of the formation mechanism of dihydroxy(methyl)benzene in the OH-initiated oxidation of the cresol isomers

In the reaction of OH with the cresol isomers, dihydroxybenzene can only be formed via an OH radical addition reaction pathway. There are several distinct addition points for the OH

radical to form OH-aromatic adducts (Grosjean, 1991). Thermochemical calculations have predicted that addition of OH at the existing OH substituent forms the most thermochemically favorable adduct (Benson, 1976):



In previous mechanistic considerations of the OH radical initiated oxidation of cresols (Grosjean, 1985; Atkinson *et al.*, 1992a) this has often been considered to be the sole addition pathway for subsequent mechanistic development. However, the large yields of 1,2-dihydroxybenzenes measured in the present gas-phase study and also the liquid phase study of Choure *et al.* (1997) support that addition at the position *ortho* to the OH substituent dominates.

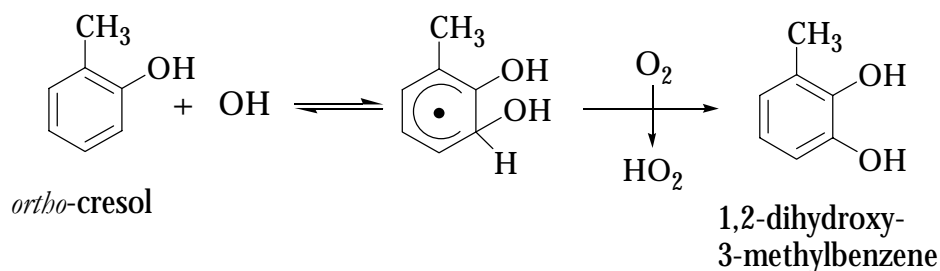
The OH - adducts can react with O₂ or NO₂ in the system. Presently, only rate constants for the reaction of OH - *meta*-cresol adducts at 330 K are known (Zetzsch *et al.*, 1997): OH - *meta*-cresol + O₂ → products, $k = 8 \times 10^{-14} \text{ cm}^3 \text{ molecule}^{-1} \text{ s}^{-1}$; OH - *meta*-cresol + NO₂ → products, $k = 4 \times 10^{-11} \text{ cm}^3 \text{ molecule}^{-1} \text{ s}^{-1}$. For the toluene - OH adducts, rate constants of $k_{(\text{OH-toluene} + \text{O}_2)} = 6.0 \times 10^{-16} \text{ cm}^3 \text{ molecule}^{-1} \text{ s}^{-1}$; $k_{(\text{OH-toluene} + \text{NO}_2)} = 3.6 \times 10^{-11} \text{ cm}^3 \text{ molecule}^{-1} \text{ s}^{-1}$ were determined for 298 K (Knispel *et al.*, 1990; Bohn, 2001). It becomes clear that while the reaction rate constants with NO₂ are not significantly higher for the OH - *meta*-cresol adduct than for the OH - toluene adduct, the rate constant for the O₂ reaction is more than 2 orders of magnitude faster for OH - *meta*-cresol compared to OH - toluene. As discussed in Section 4.1.2.1 and on the basis of the above kinetic data dihydroxy(methyl)benzenes would be expected to be formed in significantly higher yields in the OH initiated oxidation of cresol isomers compared to the yields of cresols from toluene + OH.

Another effect of the very fast OH - *meta*-cresol + O₂ reaction is that the OH-*meta*-cresol + NO₂ reaction will be only of negligible importance, even at the comparably high concentrations of NO_x prevalent in the present study. In the experiments performed in synthetic air at relatively low NO_x conditions listed in Table 5.1 the final NO₂ concentrations were between 0.7 – 1.5 ppm. Even at the highest NO₂ concentration employed in these experiments the reaction of the OH - *meta*-cresol adduct with O₂ will dominate by a factor of more than 300 (4.3×10^5 against 1.32×10^3) over reaction with NO₂. It can be expected that the situation will be analogous for *ortho*- and *para*-cresol.

As shown in the present study the major reaction of the OH - aromatic adducts with O₂ leads to formation of 1,2-dihydroxybenzenes. From studies on OH with alkylbenzenes the

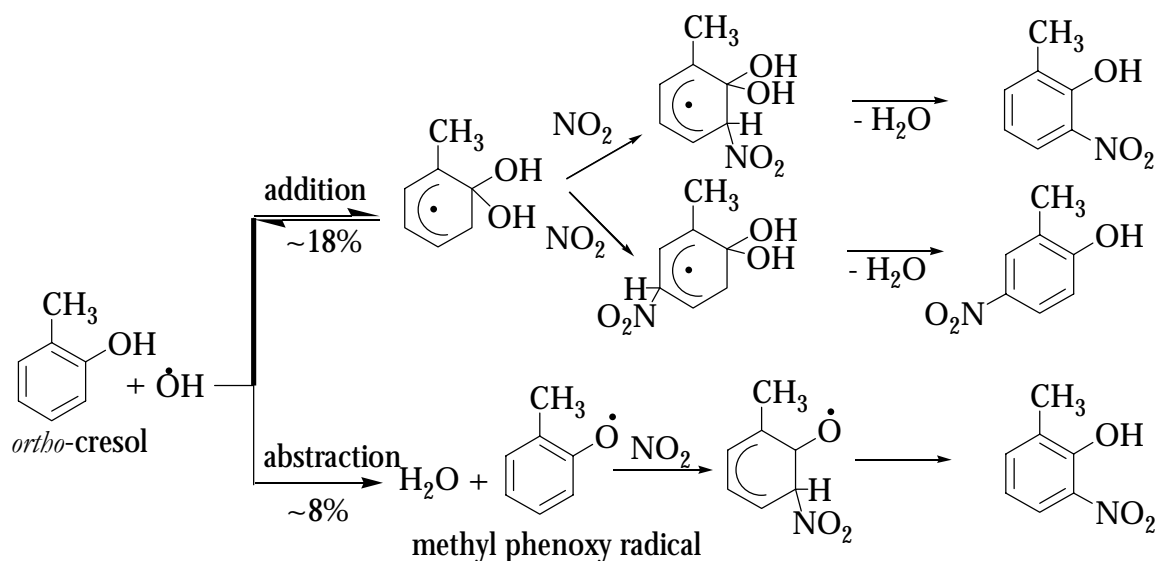
evidence supports that once O₂ adds to the OH - adduct cyclisation rapidly occurs. Since no evidence is found in the present work for products from cyclisation this would suggest that direct H-atom abstraction probably occurs. In the solution studies (Choure *et al.*, 1997) it was concluded that the addition mechanism occurs, however, no evidence was presented to support this.

The formation 1,2-dihydroxy-3-methylbenzene probably proceeds via the following reaction mechanism:

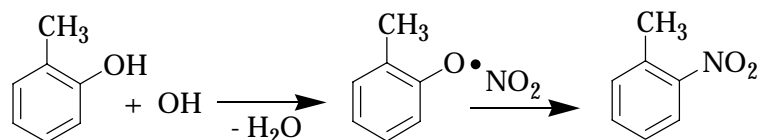


5.1.2.2 Discussion of the formation mechanism of nitrocresols

As observed previously by Atkinson *et al.* (1992a) the yield of nitrophenols measured in the OH radical induced oxidation of phenol are similar to the calculated fraction of the reaction proceeding by H-atom abstraction from the OH group of ~ 9% at 298 K (uncertain to \pm 50%). The situation is similar for the reaction of OH with the cresol isomers, where ~ 7% is estimated for the abstraction channel and the nitrocresols yields are of approximately the same magnitude. Grosjean (1985), however, from his study on OH + *ortho*-cresol concluded that nitrocresols are formed in both the addition and abstraction channels. The theoretical upper limit of nitrocresol formation was determined to be about 26% (Grosjean, 1985) with 8% from the abstraction channel and 18% from the adduct reaction with NO₂:

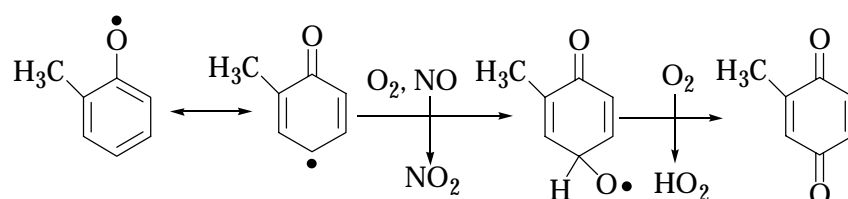


The yields of the nitrocresols derived from the present work on the OH + cresol reaction are roughly similar to what is calculated from the H-atom abstraction channel by Atkinson (1989) and support that these compounds are only formed via the H-atom abstraction pathway from the OH group and further reaction of the methylphenoxy radicals thus formed with NO₂, e.g. for *ortho*-cresol:



5.1.2.3 Discussion of the formation mechanism of methyl-1,4-benzoquinone

In principal further reactions of the methylphenoxy radicals formed via the H-atom abstraction channel from the OH substituent could give rise to the (methyl)benzoquinone formation observed for *ortho*-cresol and *meta*-cresol, e.g. 1,4-benzoquinone, through reactions such as:

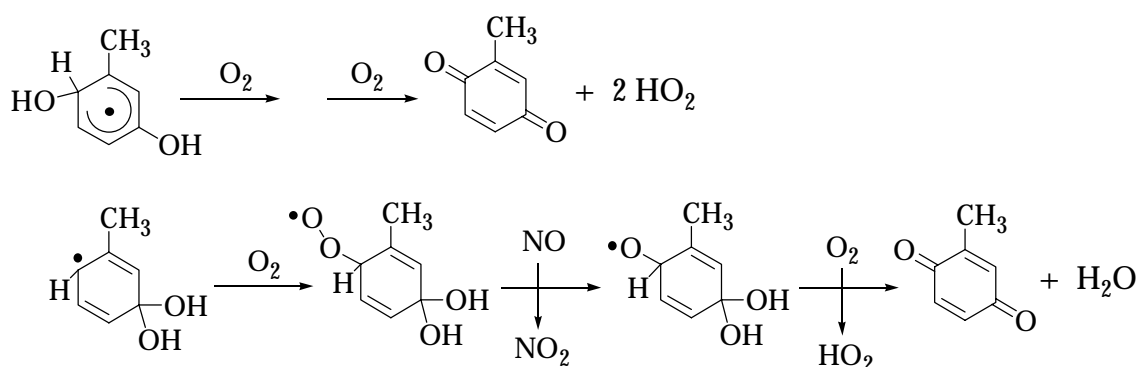


In order to provide evidence for or against such a scheme, reaction of Cl atoms with *ortho*-cresol in the presence and absence of NO_x was examined. Interestingly, in the absence of NO_x formation of methyl-1,4-benzoquinone was observed with a yield of approximately 5%. With NO_x in the system formation of methyl-1,4-benzoquinone was not observed. Obviously, the presence of the CH₃ group with its positive inductive effect is changing the reaction pathways of the 2-methyl-phenoxy radical compared to the phenoxy radical (see Chapter 4, Section 4.1.2.2). In the absence of NO₂, methyl-1,4-benzoquinone is thought to be formed via a reaction of the 2-methyl-phenoxy radical as outlined above.

In the reactions of OH with *ortho*- and *meta*-cresol in the presence of NO_x, the combined yields of the (methyl)benzoquinones and (methyl)nitrophenols are much higher than the fraction of the reaction estimated to be proceeding by H-atom abstraction from the OH group of ~ 7%. As indicated the yields of (methyl)nitrophenols formed from OH with the cresols are roughly similar to what is expected from the H-atom abstraction channel; this

suggests that the observed (methyl)benzoquinone formation must stem mainly from the OH addition channel.

The reaction mechanism for methyl-1,4-benzoquinone formation via addition of the OH radical to the cresols is not clear from the present study. Since there is no discernible curvature in the plots of the amounts of methyl-1,4-benzoquinone formed against the amount of cresol consumed (see Figures 5.7 and 5.8) it would appear that they are primary products in OH + cresol reactions. Possible mechanisms could involve OH radical addition at positions either *para* or *ipso* to the OH substituent, e.g. for *meta*-cresol + OH:



5.1.2.4 Reaction mechanisms

Based on the identified products and on their formation yields from the present study reaction mechanisms for the OH radical initiated oxidation of *ortho*-, *meta*- and *para*-cresol in the presence of NO_x has been developed.

Figure 5.10 shows the mechanism for the reaction of *ortho*-cresol and OH.

It is considered that addition is the major pathway ($\sim 92\%$ of the total OH reaction), with OH radical addition preferentially at the position *ortho* to the OH substituent. The methyl phenoxy radicals thus formed react with O_2 to form ring-retaining products such as 1,2-dihydroxy-3-methylbenzene and methyl-1,4-benzoquinone. The cresol-OH adducts may also react with O_2 resulting in aromatic ring-opening and in the formation of aliphatic carbonyl products including ketoacids such as pyruvic acid ($\text{CH}_3\text{C}(\text{O})\text{COOH}$), however, the present work suggests that this is a minor process.

The close correspondence of the nitrocresol formation yield from *ortho*-cresol with the fraction of the overall OH radical reaction estimated to proceed by H-atom abstraction from the OH group implies that the nitrophenols from phenolic compounds arise mainly from the abstraction channel.

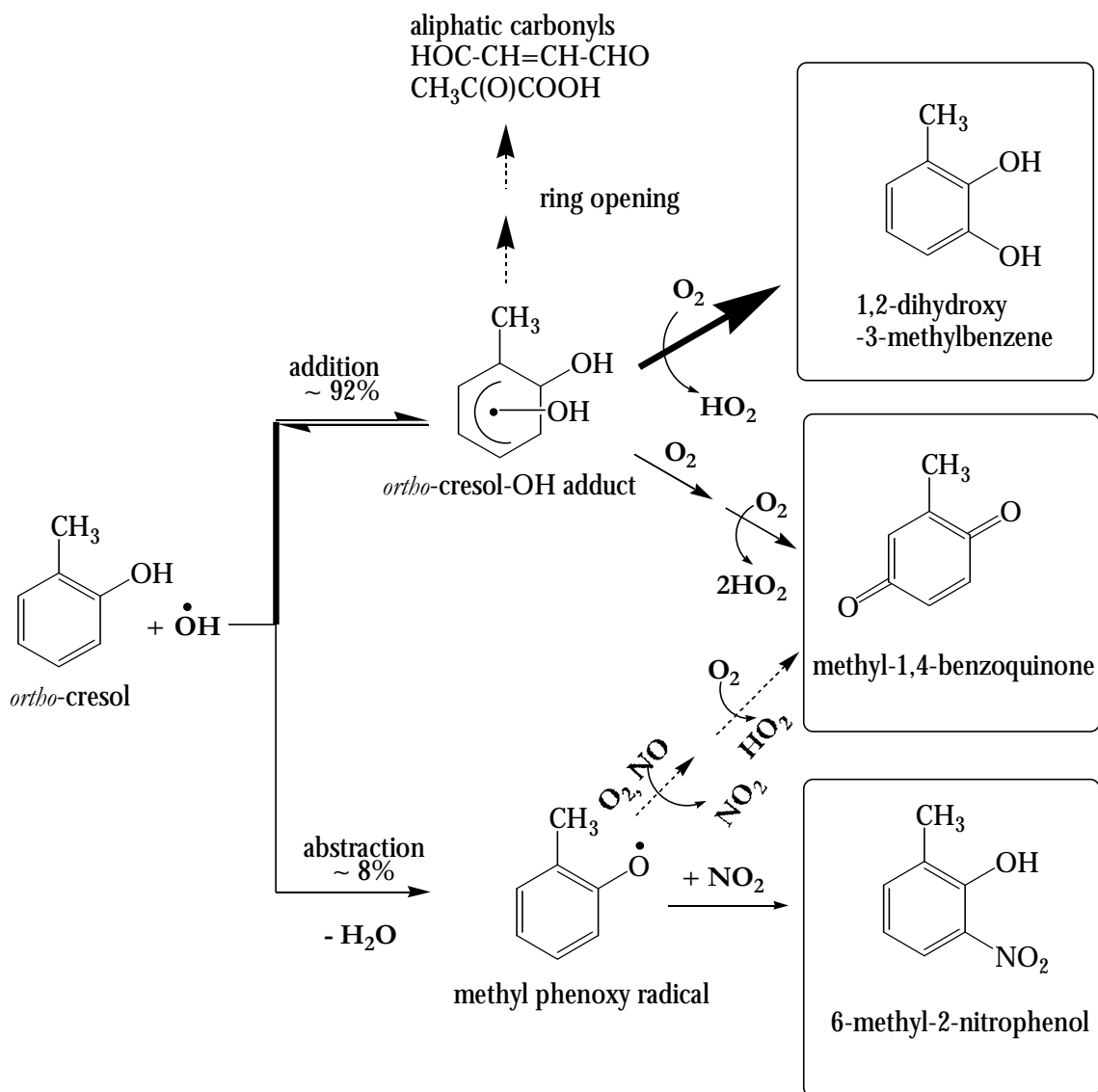


Figure 5.10 Simplified mechanism showing pathways to the observed products from the reaction of OH radicals with the *ortho*-cresol isomer. The bold arrows indicate suspected major reaction pathways.

The OH radical initiated oxidation of *meta*-cresol has been found to yield several ring retaining-compounds. A general mechanism for the OH initiated oxidation of *meta*-cresol is presented in Figure 5.11.

In the OH initiated oxidation of *meta*-cresol, OH may add on the C_2 and C_4 carbon as well as on the OH-bearing C_3 carbon. Addition on the C_2 and C_4 carbon, will probably lead to two competitive pathways. These are reaction with O_2 by addition and by abstraction. Reaction with O_2 by H-atom abstraction, which dominates, will lead to a diphenol, namely 1,2-dihydroxy-3-methylbenzene for C_2 and 1,2-dihydroxy-4-methylbenzene for C_4 . Reaction with O_2 by addition, if not entirely negligible, will lead to ring cleavage products such as dicarbonyls and ketoacids. The results of the present work support that the reaction of the

meta-cresol OH - adduct (C₃) with O₂ probably leads to benzoquinone formation. Nitrocresols are formed by reaction of NO₂ with the methyl phenoxy radical resulting from the H-atom abstraction from the HO group.

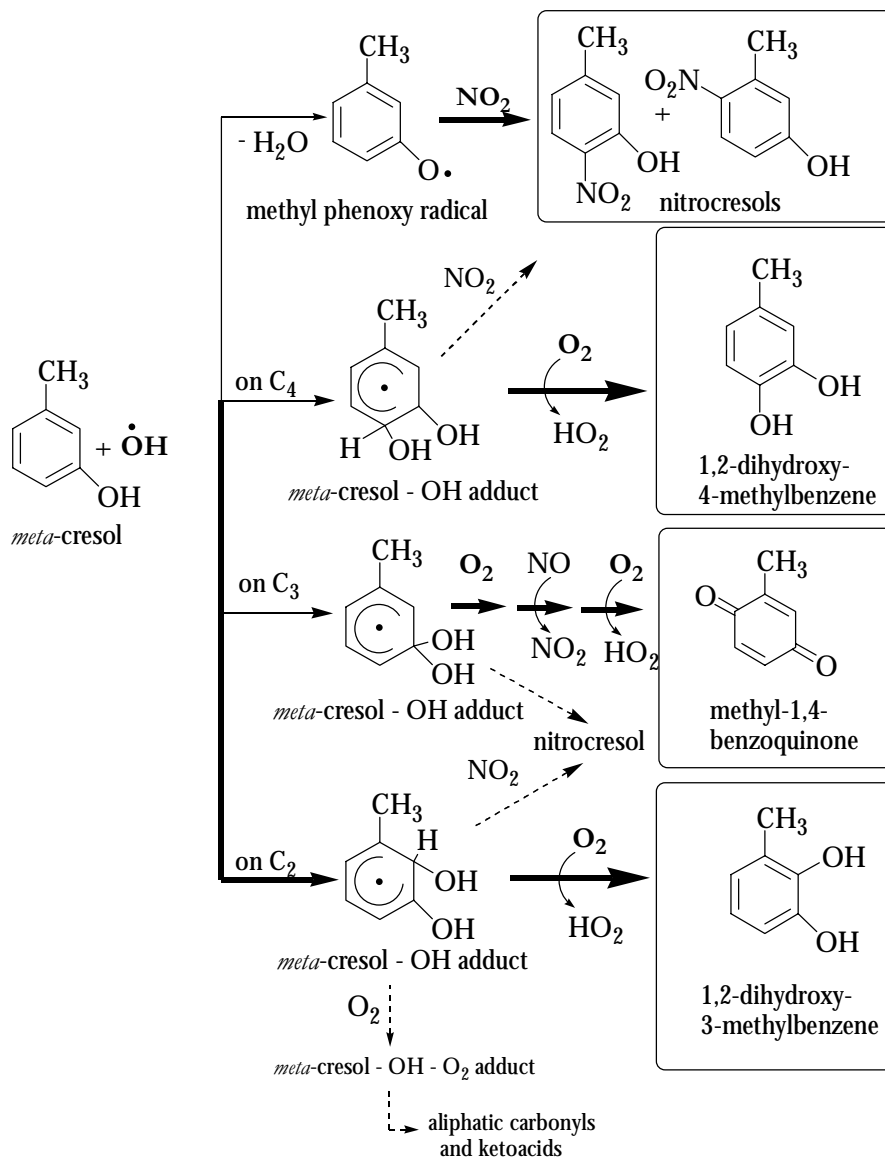


Figure 5.11 Simplified mechanism showing pathways to the observed products from the reaction of OH radicals with the *meta*-cresol isomer. The bold arrows indicate suspected major reaction pathways.

In the photo-oxidation of *para*-cresol formation of two ring-retaining compounds: 1,2-dihydroxy-4-methylbenzene and 4-methyl-2-nitrophenol, has been observed. The general mechanism of *para*-cresol is shown in Figure 5.12.

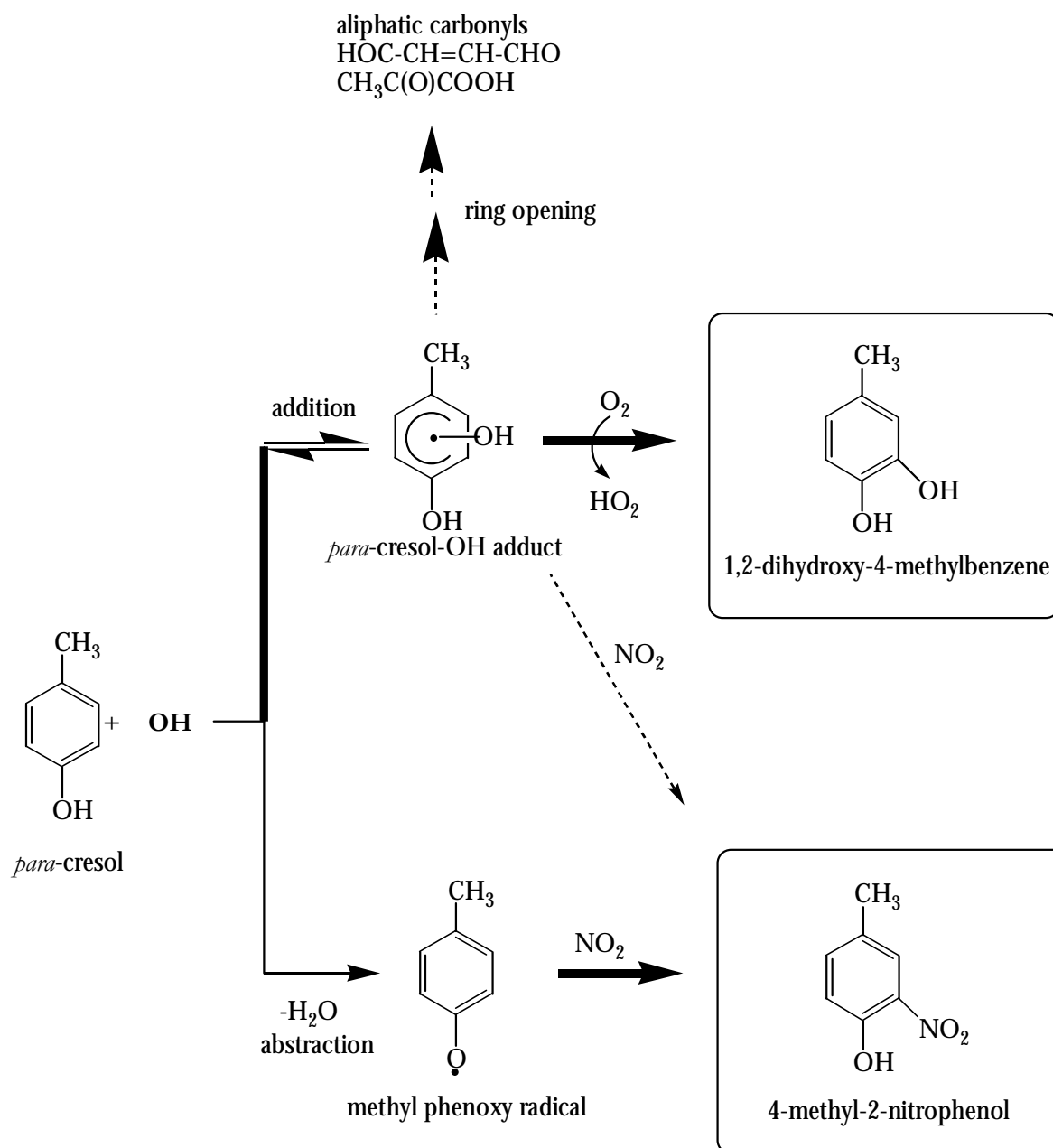


Figure 5.12 Simplified mechanism showing pathways to the observed products from the reaction of OH radicals with the *para*-cresol isomer. The bold arrows indicate suspected major reaction pathways.

5.2 Product study of the nitration of cresol isomers by reaction with the NO₃ radical

Product analyses of the NO₃ radical initiated oxidation of cresol isomers have been performed in the smog chamber system at Wuppertal University and EUPHORE, Valencia/Spain. Reaction of O₃ with NO₂ was used for in situ generation of NO₃ radicals in both the 1080 l quartz glass reactor and the EUPHORE chamber.

5.2.1 Experimental data

5.2.1.1 1080 l quartz glass reactor

A series of cresol-NO₂-O₃-synthetic air dark experiments were carried out for each isomer of cresol; the initial and final reactant concentrations are summarised in Table 5.6.

In the NO₃ radical initiated oxidation of cresol isomers using long path FT-IR spectroscopy, formation of nitrocresols and benzoquinone as the main products was observed.

Table 5.6 Initial and final reactant concentrations (ppmv) employed in experiments of the NO₃ radical initiated oxidation of cresols in the 1080 l quartz glass reactor.

experiment ^a	initial concentration (ppmv)			final concentration (ppmv)		
	cresol	O ₃ ^b	NO ₂	cresol	O ₃ ^b	NO ₂
OCR11	0.67	1.16	2.50	0.056	0.53	0.080
OCR12	1.03	1.10	2.40	0.360	0.56	0.130
OCR13	1.51	1.04	2.60	0.650	0.46	0.090
OCR14	2.11	1.00	2.70	1.240	0.43	0.280
MCR11	0.40	1.40	0.98	0.120	1.13	0.180
MCR12	0.61	1.49	2.14	0.040	1.00	0.057
MCR13	0.84	1.27	2.29	0.190	0.76	0.000
MCR14	1.24	1.00	2.26	0.620	0.60	0.187
PCR11	0.62	1.60	2.40	0.100	1.10	0.000
PCR12	0.88	1.30	2.80	0.260	0.70	0.100
PCR13	1.42	1.50	2.70	0.670	1.00	0.160
PCR14	2.50	1.40	3.05	1.500	0.80	0.160

^a experimental designations: OCR=*ortho*-cresol, MCR=*meta*-cresol, PCR=*para*-cresol;

^b maximum O₃ concentration measured.

5.2.1.1.1 FT-IR spectral data from the reaction of NO_3 with *ortho*-cresol

In the NO_3 radical initiated oxidation of *ortho*-cresol, the FT-IR analysis indicated formation of 6-methyl-2-nitrophenol, methyl-1,4-benzoquinone and the important co-product HNO_3 .

Figure 5.13 shows an example of the FT-IR spectral data for one typical experiment on *ortho*-cresol- $\text{NO}_2\text{-O}_3$ performed in the 1080 l quartz glass reactor. In Figure 5.13 spectrum A shows a typical product spectrum obtained after subtraction of the spectral features belonging to water, reactants (*ortho*-cresol, O_3 and NO_2) and HNO_3 . Spectra B and C show reference spectra of methyl-1,4-benzoquinone and 6-methyl-2-nitrophenol, respectively.

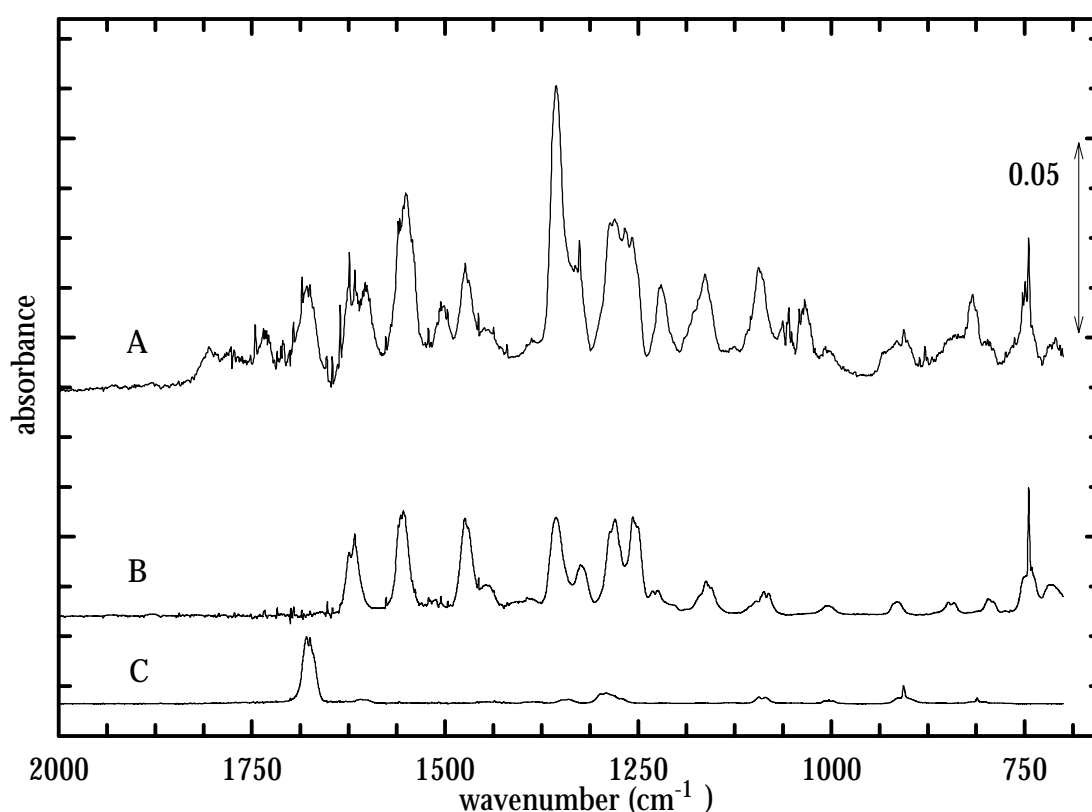


Figure 5.13 Infrared absorption spectra from the NO_3 radical initiated oxidation of *ortho*-cresol in the 1080 l quartz glass reactor: A-product spectrum; B-reference spectrum of 6-methyl-2-nitrophenol; C-reference spectrum of methyl-1,4-benzoquinone.

6-Methyl-2-nitrophenol was not commercially available and was synthesised using the method of Winzor (1935) (see Appendix I.2). From a simple visual comparison of the reference and product spectra presented in Figure 5.13 it is obvious that both 6-methyl-2-nitrophenol and methyl-1,4-benzoquinone are being formed.

The residual product spectrum was checked for the formation of other nitrocresol isomers, i.e. 2-methyl-3-nitrophenol and 2-methyl-5-nitrophenol (see Figure 5.14). None of these isomers could be detected suggesting that, if formed, their yields are minor.

Another possible nitrocresol isomer which can be formed from the nitration reaction is 2-methyl-4-nitrophenol. Unfortunately no reference spectrum was available to check for formation of this compound.

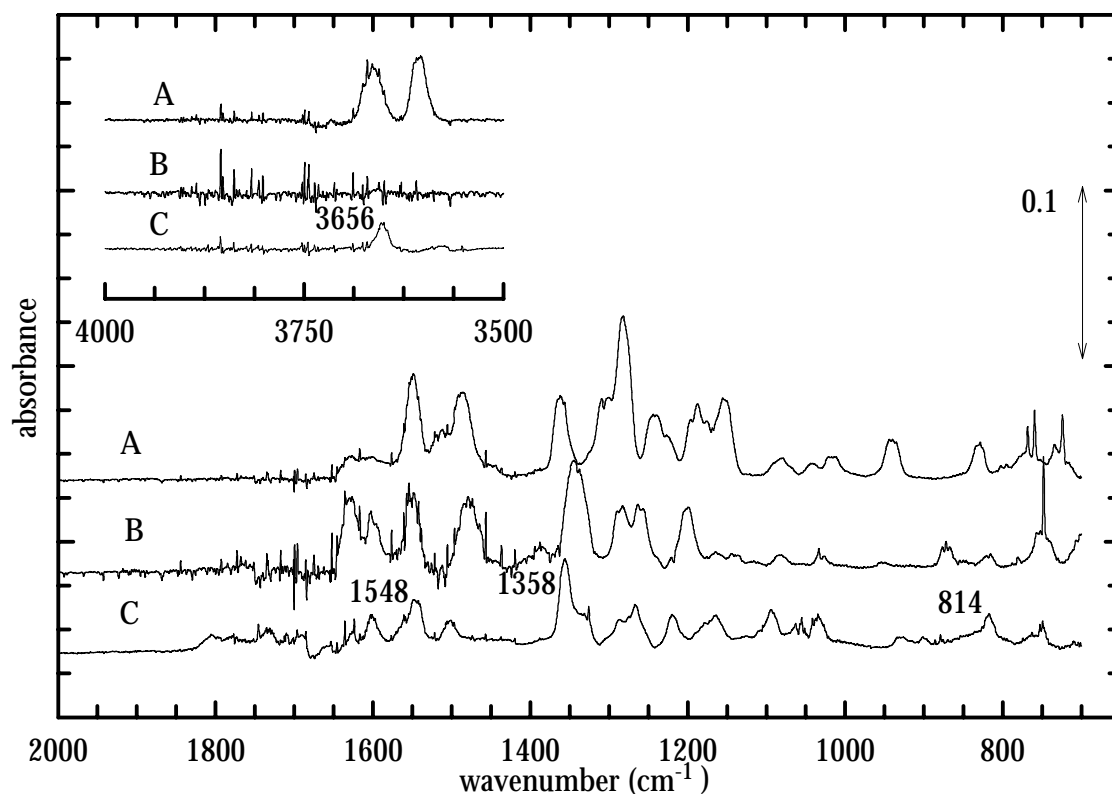


Figure 5.14 Infrared absorption spectra in the range of 2000-700 and 4000-3500 cm^{-1} : A-reference spectrum for 2-methyl-3-nitrophenol; B-reference spectrum for 2-methyl-5-nitrophenol; C-residual product spectrum resulting after subtraction of methyl-1,4-benzoquinone and 6-methyl-2-nitrophenol from spectrum A in Figure 5.13.

However, the remaining residual product spectrum (Figure 5.14, C) shows several intense absorptions around 3656, 1601, 1548, 1358, 1266, 1219, 1166, 1095, 817 and 749 cm^{-1} , which are characteristic for nitrophenol compounds (see Figure 5.13, C and Figure 5.14, A and B). Therefore, since all of the other possible nitrocresol compounds have been either detected or eliminated it is quite probable that 6-methyl-4-nitrophenol is being formed in the *ortho*-cresol- NO_3 system.

The concentration-time profile of the reactants and products identified in the NO_3 -initiated oxidation of the *ortho*-cresol for a typical experiment are shown in Figure 5.15.

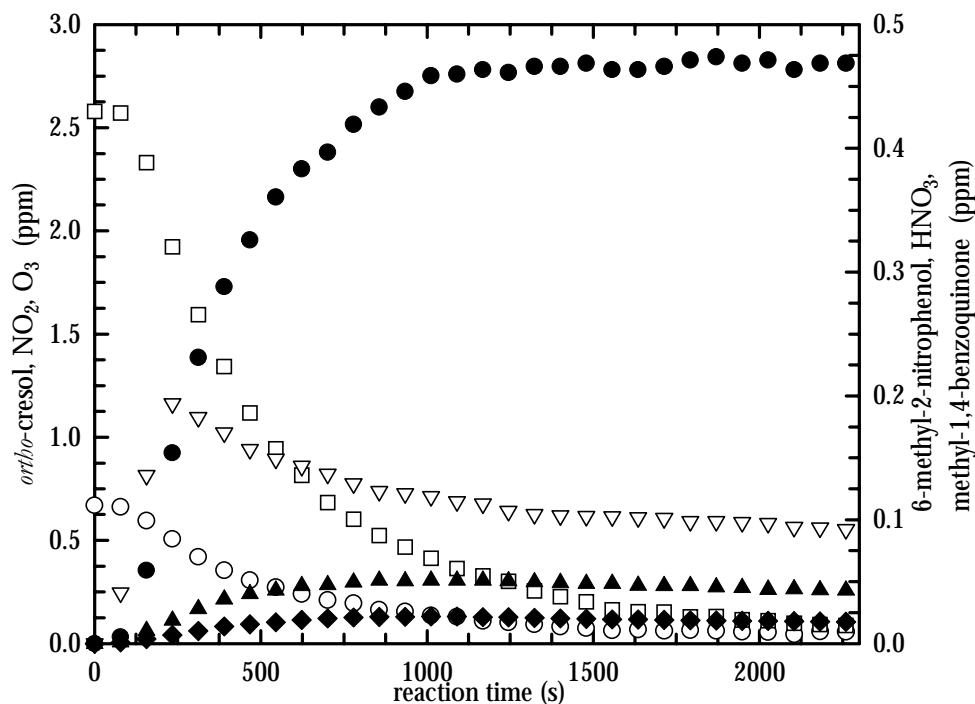


Figure 5.15 Concentration-time profiles of the reactants and products identified in the NO_3 -initiated oxidation of *ortho*-cresol in the 1080 l quartz glass reactor: (\circ) -*ortho*-cresol; (\square) - NO_2 (∇) - O_3 ; (\blacktriangle) -6-methyl-2-nitrophenol; (\blacklozenge) -methyl-1,4-benzoquinone; (\bullet) - HNO_3 .

5.2.1.1.2 FT-IR spectral data from the reaction of NO_3 with *meta*-cresol

An analysis of the FT-IR spectra showed the formation of 3-methyl-4-nitrophenol, 5-methyl-2-nitrophenol, 3-methyl-2-nitrophenol, methyl-1,4-benzoquinone and HNO_3 (as co-product) from the gas-phase reaction of NO_3 radicals with *meta*-cresol. Typical FT-IR data in the range of $1800 - 700 \text{ cm}^{-1}$ obtained from experiments performed in the 1080 l quartz glass reactor are presented in Figure 5.16.

In Figure 5.16 spectrum A shows the product spectrum obtained after subtraction of the spectral features belonging to water, reactants (*meta*-cresol, O_3 , NO_2) and HNO_3 . Spectra B, C and D show the reference spectra for the identified nitrocresols 5-methyl-2-nitrophenol, 3-methyl-2-nitrophenol and 3-methyl-4-nitrophenol, respectively. Spectrum E shows the reference spectrum of methyl-1,4-benzoquinone. From some of the products it is evident from a simple visual comparison of Figure 5.16 that they are being formed. For others this only becomes apparent in the spectral analysis. The residual spectrum (Figure 5.16, F) obtained after computer subtraction of the spectral features belonging to reactants and the identified products shows that some, probably minor, products were not identified.

Concentration-time profiles of the reactants and products identified in the NO_3 radical initiated oxidation of *meta*-cresol for a typical experiment are shown in Figure 5.17.

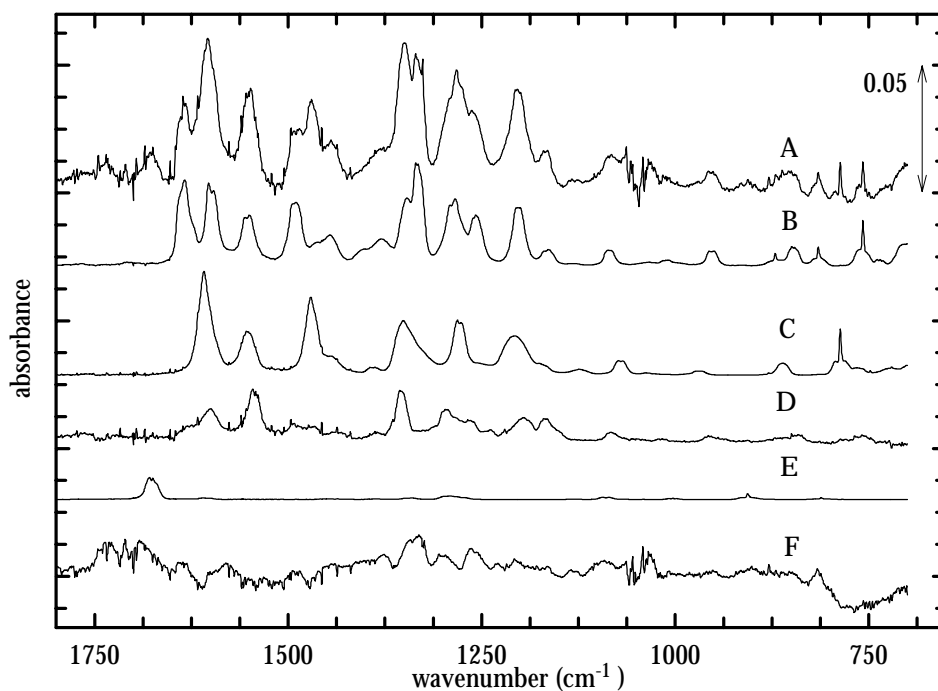


Figure 5.16 Infrared absorption spectra from the NO_3 radical initiated oxidation of *meta*-cresol in the 1080 l quartz glass reactor: A-product spectrum; B-reference spectrum of 5-methyl-2-nitrophenol; C-reference spectrum of 3-methyl-2-nitrophenol; D-reference spectrum of 3-methyl-4-nitrophenol; E-reference spectrum of methyl-1,4-benzoquinone; F-residual spectrum after subtraction of all identified products.

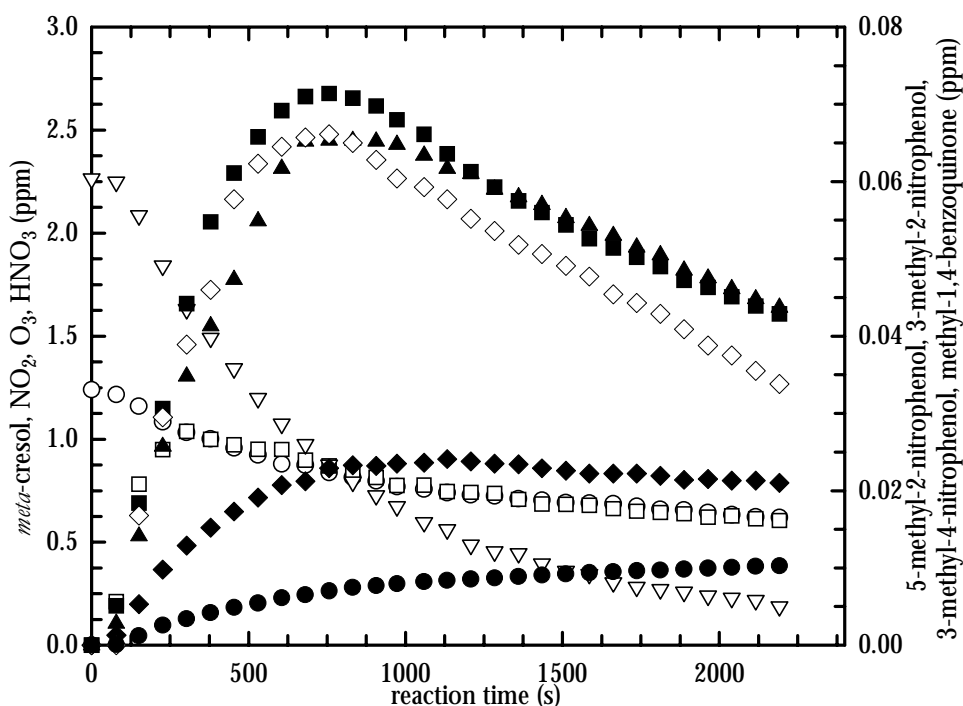


Figure 5.17 Concentration-time profiles of the reactants and products identified in the NO_3 -initiated oxidation of *meta*-cresol in the 1080 l quartz glass reactor: (\square) -*meta*-cresol; (∇) - NO_2 ; (\square) - O_3 ; (\bullet) - HNO_3 , (\blacksquare) -5-methyl-2-nitrophenol; (\diamond) -3-methyl-4-nitrophenol; (\blacktriangle) -3-methyl-2-nitrophenol; (\blacklozenge) -methyl-1,4-benzoquinone.

5.2.1.1.3 FT-IR spectral data from the reaction of NO_3 with *para*-cresol

The FT-IR analysis of the spectral data showed that the NO_3 radical reaction with *para*-cresol led to the formation of 4-methyl-2-nitrophenol and HNO_3 .

Figure 5.18 shows an example of the FT-IR spectral data for a typical experiment. In Figure 5.18 it can be seen that the product spectrum, resulting from the subtraction of all reactants (*para*-cresol, NO_2 , O_3) and other inorganic compounds (as HNO_3), clearly shows spectral features characteristic for 4-methyl-2-nitrophenol.

After spectral stripping of the identified products from the product spectrum, some intense absorptions remained in the residual spectrum. The residual product spectrum (see Figure 5.14, C) showed intense absorptions around 1700, 1573, 1395, 1336 and 874 cm^{-1} , which are characteristic for nitrophenol compounds (see Figure 5.16, B, C, D; Figure 5.18, B).

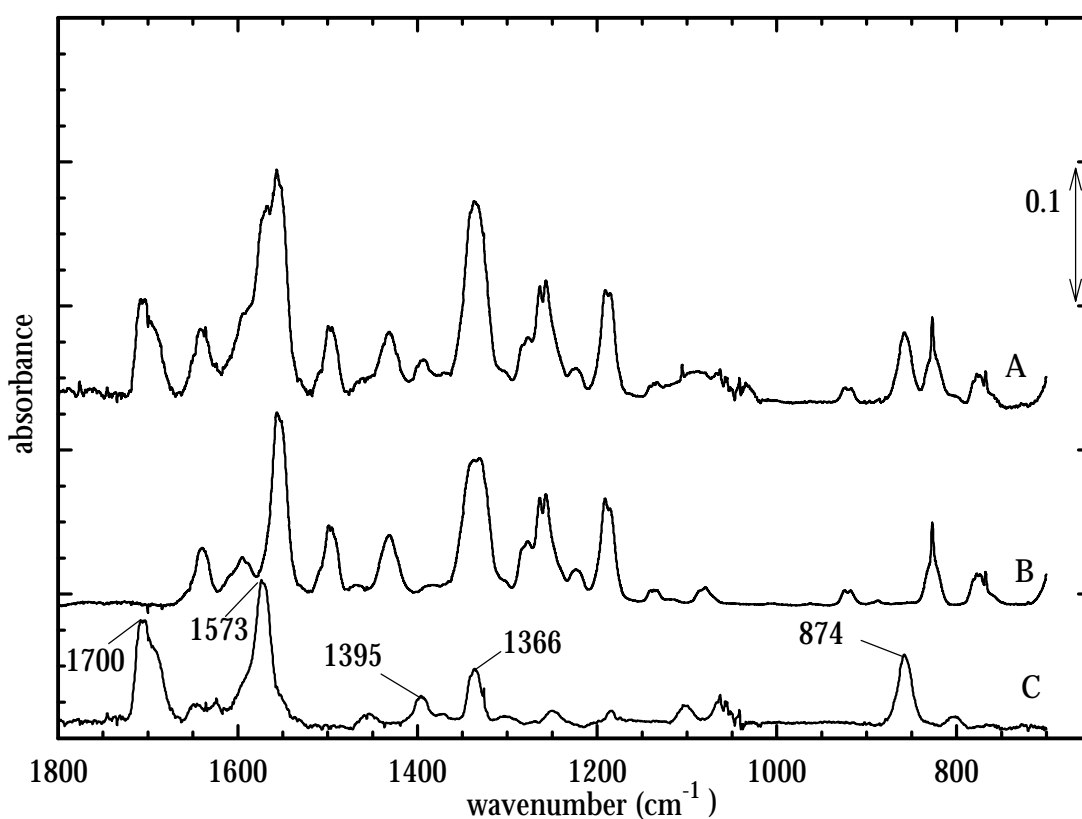


Figure 5.18 Infrared absorption spectra from the NO_3 radical initiated oxidation of *para*-cresol in the 1080 l quartz glass reactor: A-product spectrum; B-reference spectrum of 4-methyl-2-nitrophenol; C-residual product spectrum after subtraction of 4-methyl-2-nitrophenol.

Unfortunately not all of the possible isomers of nitrophenols from *para*-cresol are commercially available. The formation of 4-methyl-3-nitrophenol can occur in the reaction systems.

Concentration-time profiles of the reactants and products identified in the NO_3 initiated oxidation of *para*-cresol for a typical experiment are shown in Figure 5.19.

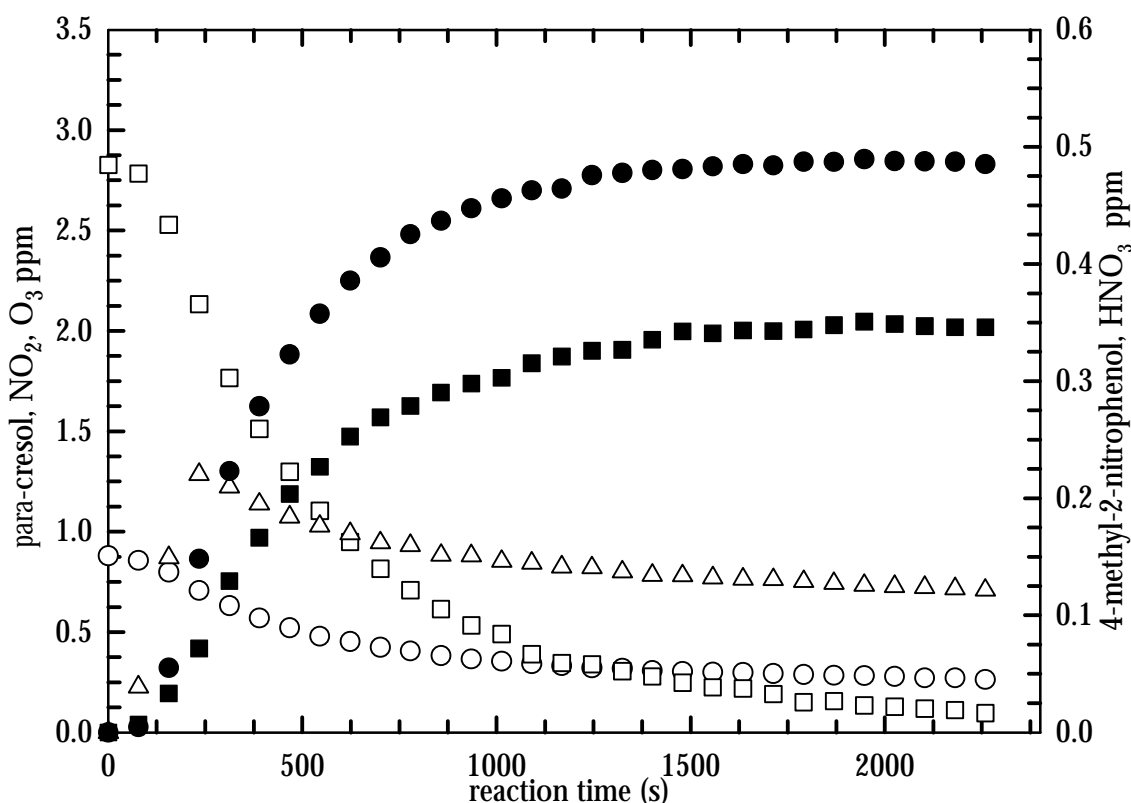


Figure 5.19 Concentration-time profiles of the reactants and products identified in the NO_3 -initiated oxidation of *para*-cresol in the 1080 l quartz glass reactor: (○)-*para*-cresol; (□)- NO_2 ; (▽)- O_3 ; (■)-4-methyl-2-nitrophenol; (●)- HNO_3 .

5.2.1.2 EUPHORE chamber

In September 1998 and May 1999 five dark experiments were performed on the NO_3 radical initiated oxidation of cresol isomers to identify the oxidation products: *ortho*-cresol (2 experiments), *meta*-cresol (one experiment) and *para*-cresol (2 experiments). The initial and final concentrations of reactants are summarised in Table 5.10.

The main products observed matched closely those identified in the experiments performed in the 1080 l quartz glass reactor (see Section 5.2.1.1). There was only one exception. In the *ortho*-cresol- NO_2 - O_3 reaction study from EUPHORE chamber formation of 2-methyl-nitrophenol was not observed. In fact, after subtraction of the all known compounds from the FT-IR spectra only weak absorptions remained. Methyl-1,4 benzoquinone was

identified as a trace product from this oxidation reaction. There was no indication in the product spectra for the formation of other compounds.

Table 5.10 Initial and final experimental concentrations of reactants used for the nitration reaction of cresol isomers with the NO_3 radical in the EUPHORE chamber.

experiment ^a	initial concentration (ppbv)			final concentration (ppbv)		
	cresol	O_3^b	NO_2	cresol	O_3^b	NO_2
OCR001	253	425	563	71	157	68
OCR002	405	379	518	187	265	18
MCR001	588	175	583	188	124	21
PCR001	200	293	389	30	173	103
PCR002	398	402	421	40	266	209

^a experimental designations: OCR=*ortho*-cresol, MCR=*meta*-cresol, PCR=*para*-cresol;

^b maximum O_3 concentration measured.

One reasonable explanation for the lack of absorption bands in the residual spectrum can be that the amounts of the products which were formed in these two experiments were under the FT-IR detection limits of the experimental set-up employed for the analysis. With an optical pathlength of 330 m in chamber A of EUPHORE, the minimum amounts of 6-methyl-2-nitrophenol and methyl-1,4-benzoquinone which can be detected are about 40 and 20 ppb, respectively.

5.2.2.1.1 FT-IR spectral data from the reaction of NO_3 with *meta*-cresol

The FT-IR product analysis of the dark experiment performed on a *meta*-cresol- NO_2 - O_3 mixture showed the formation of 3-methyl-4-nitrophenol, 5-methyl-2-nitrophenol, 3-methyl-4-nitrophenol and HNO_3 . The results partly confirm those obtained in the 1080 l quartz glass reactor. Figure 5.20 shows FT-IR spectral data from an experiment performed in the EUPHORE chamber. The residual spectrum obtained after computer subtraction of the spectral features belonging to reactants and the identified products is practically absorption free (see Figure 5.20, E). In the 1080 l quartz glass reactor experiments formation of methyl-1,4-benzoquinone was observed with a yield of about 4% (see Section 5.2.2, Table 5.7). It is possible that this compound is also being formed under the conditions in EUPHORE, however, its concentration was under the detection limit of the system.

Concentration-time profiles of the reactants and products identified in the NO_3 initiated oxidation of the *meta*-cresol for the experiment are shown in Figure 5.21.

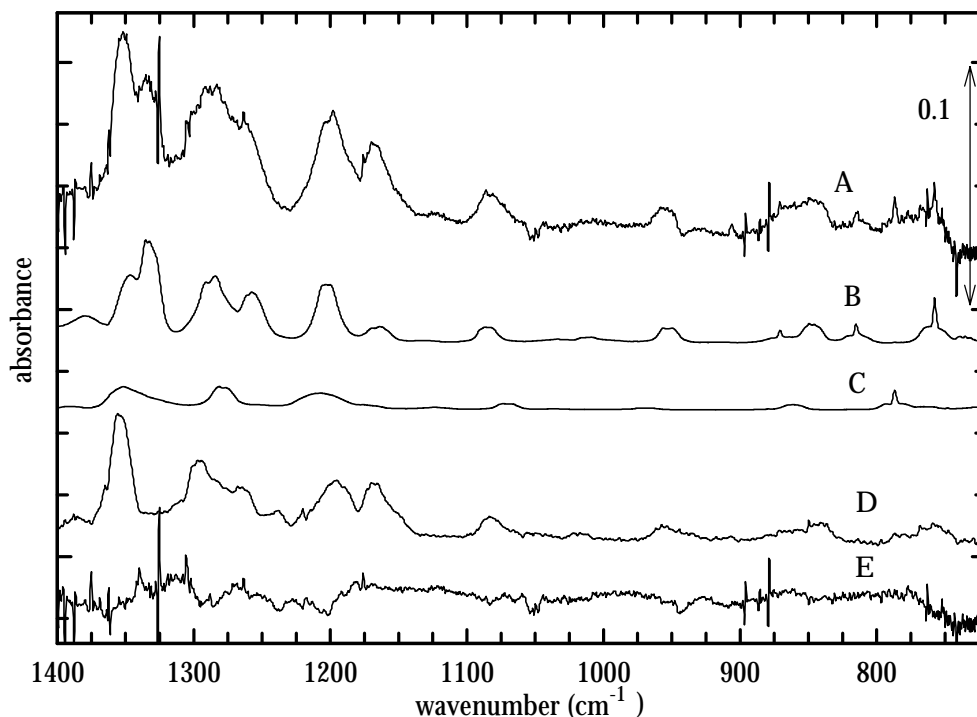


Figure 5.20 Infrared absorption spectra from the NO_3 radical initiated oxidation of *meta*-cresol in the EUPHORE chamber: A-product spectrum; B-reference spectrum of 3-methyl-2-nitrophenol; C-reference spectrum of 5-methyl-2-nitrophenol; D-reference spectrum of 3-methyl-4-nitrophenol; E-residual spectrum after subtraction of all identified products.

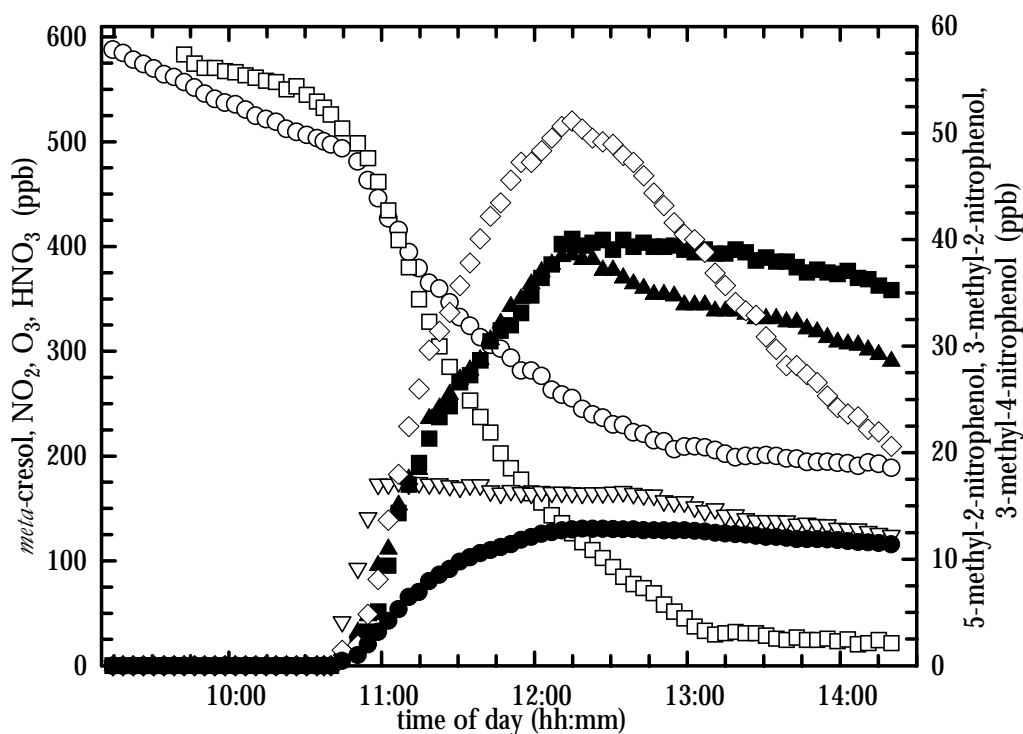


Figure 5.21 Concentration-time profiles of reactants and identified products in a *meta*-cresol- NO_2 - O_3 oxidation EUPHORE experiment: (○)-*meta*-cresol; (□)- O_3 ; (□)- NO_2 ; (▲)-3-methyl-2-nitrophenol; (■)-5-methyl-2-nitrophenol; (◇)-3-methyl-4-nitrophenol; (●)- HNO_3 .

5.2.2.1.2 FT-IR spectral data from the reaction of NO_3 with *para*-cresol

The formation of 4-methyl-2-nitrophenol and HNO_3 was observed in both experiments performed in the EUPHORE chamber on *para*-cresol- NO_2 - O_3 mixtures. Figure 5.22 shows an example of the FT-IR spectral data from one experiment. This study confirms the formation of 4-methyl-2-nitrophenol in the NO_3 radical initiated oxidation of *para*-cresol as was observed in the study in the 1080 l quartz glass reactor (see Section 5.2.1.1).

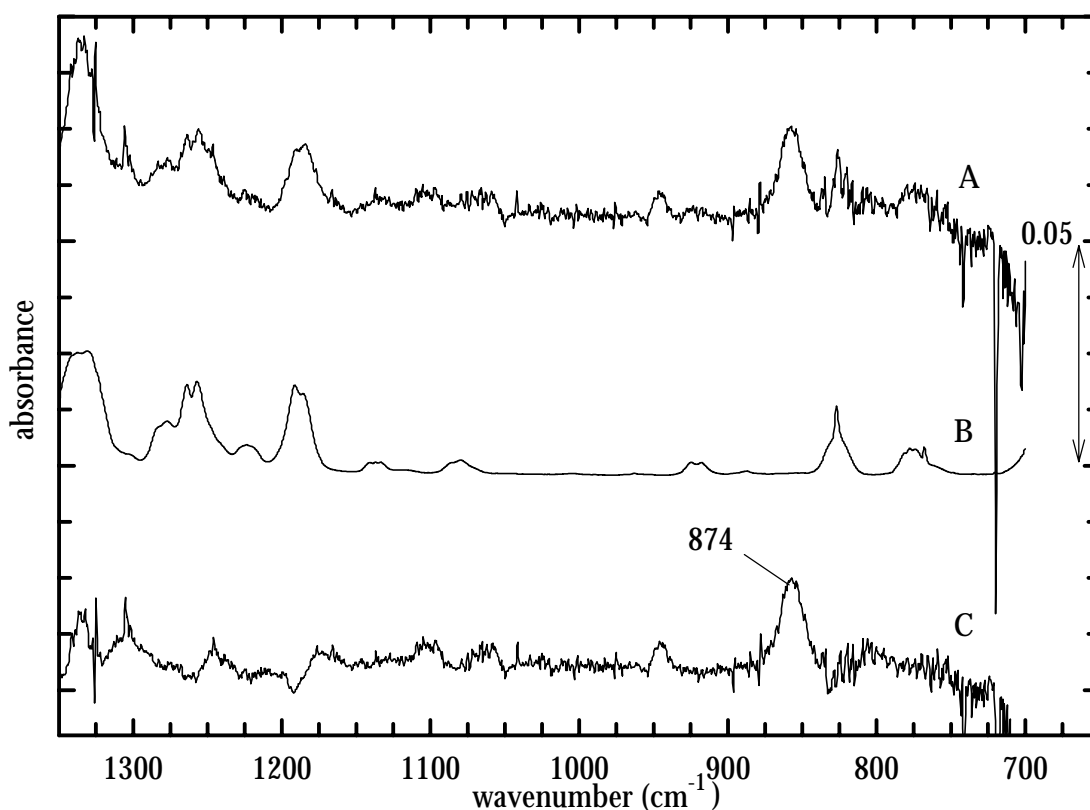


Figure 5.22 Infrared absorption spectra from the NO_3 radical initiated oxidation of *para*-cresol in the EUPHORE chamber: A-product spectrum; B-reference spectrum of 4-methyl-2-nitrophenol in the range 1350-700 cm^{-1} ; C-residual spectrum resulting from subtraction of all identified products.

Unfortunately in the EUPHORE chamber experiments the FT-IR analysis of the spectra cannot be made over the entire IR spectral range because of strong H_2O absorptions between 3980-3411 and 2098-1249 cm^{-1} . The relative humidity in the EUPHORE chamber, even under “dry” conditions, is much higher than in the 1080 l quartz glass reactor. Many of the absorption bands remaining in the residual product spectrum overlap with the spectral features of H_2O .

Therefore, it is difficult to say whether or not that if other products such as has been observed from 1080 l quartz glass reactor experiments (see Section 5.2.1.1.3) is being formed

in the EUPHORE experiments. The residual product spectrum shows one intense absorption around 874 cm^{-1} . This band was also observed in the residual spectrum from the study on *para*-cresol- NO_2 - O_3 reaction mixtures in the 1080 l quartz glass reactor.

Concentration-time profiles of the reactants and products identified in the NO_3 -initiated oxidation of the *para*-cresol for a typical experiment are shown in Figure 5.23.

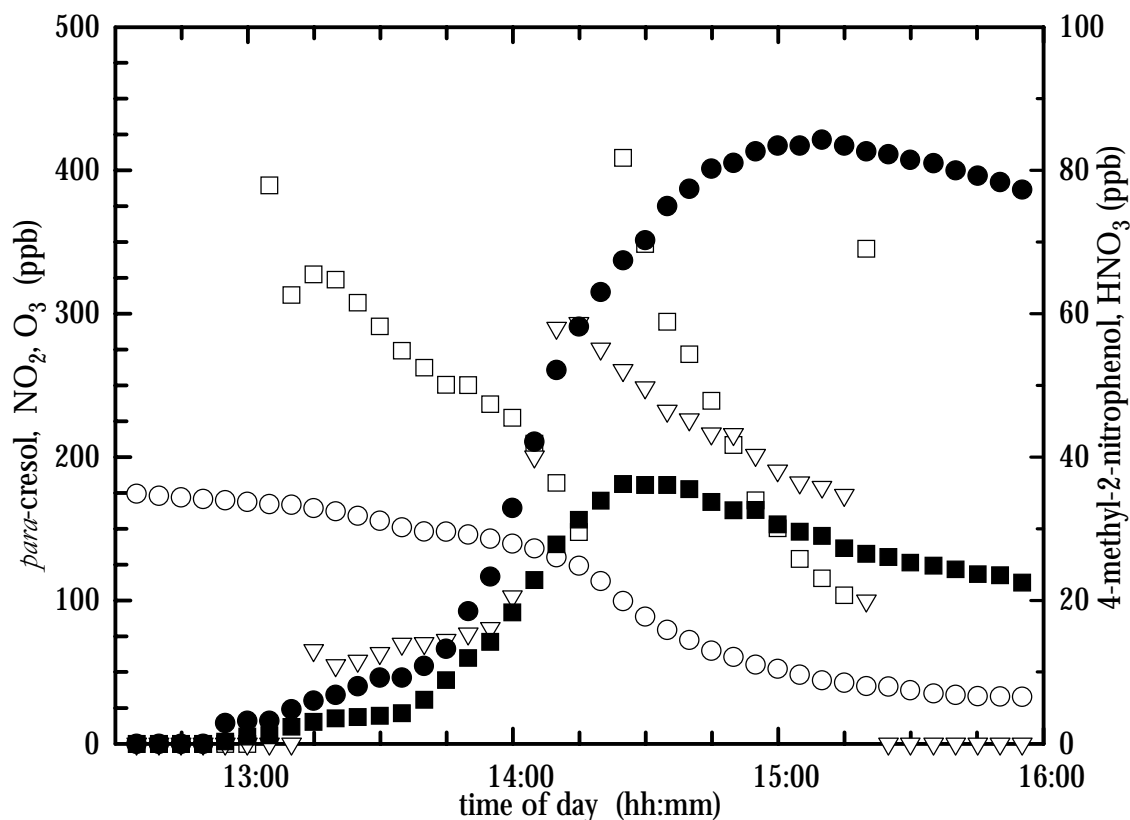


Figure 5.23 Concentration-time profiles of reactants and identified products for a *para*-cresol- NO_2 - O_3 oxidation EUPHORE experiment: (○)-*para*-cresol; (△)- O_3 ; (□)- NO_2 ; (■)-4-methyl-2-nitrophenol; (●)- HNO_3 .

5.2.2 Data evaluation

5.2.2.1 The 1080 l quartz glass reactor studies

The formation yields of the identified products were obtained from plots of their corrected concentration versus the consumed amount of cresol.

The nitrocresol compounds can also react with NO_3 radicals and, hence, these secondary reactions must be taken into account in order to obtain their true formation yields. The nitrocresol + NO_3 and methyl-1,4-benzoquinone + NO_3 reactions rate constants have not been measured. On the basis of relationships between the ionization potential, a measure of electronic density, and nitrocresol reactivity towards NO_3 radicals, Grosjean (1990)

estimated that the reaction of NO_3 radicals with nitrocresols is slow, i.e. $k = 1 \times 10^{-14} \text{ cm}^3 \text{ molecule}^{-1} \text{ s}^{-1}$. This rate constant together with an average NO_3 experimental concentration of about $(6 - 10) \times 10^6 \text{ molecule cm}^{-3}$ corresponds to a loss of about 2% of nitrocresols in the chamber. For methyl-1,4-benzoquinone it can be expected that the reaction rate constant with the NO_3 radical is even slower than the NO_3 radical reaction with the nitrocresol. Thus, secondary reactions of the nitrocresols and methyl-1,4-benzoquinone were neglected in deriving their formation yields. Consequently, corrections were only made for their loss to the wall surface since this was determined to be the most important sink process. The wall loss rates are presented in Appendix II.

The corrected amounts of nitrocresols, methylbenzoquinone and HNO_3 observed for *ortho*-, *meta*- and *para*-cresol are plotted versus the amounts of cresols reacted in Figures 5.24, 5.25 and 5.26, respectively. In agreement with expectations that secondary reactions of the nitrocresols with NO_3 radical are of no importance, these plots exhibit no obvious curvature. From least-squares analysis of the plots shown in Figures 5.24, 5.25 and 5.26, respectively, the product formation yields have been obtained (Olariu *et al.*, 2001). The corrected yields, determined from four individual experiments for each of the cresol isomers are listed in Tables 5.7, 5.8 and 5.9. The errors quoted in these tables are a combination of the 2 σ statistical errors from the linear regression analyses and the errors given by the subtraction procedure.

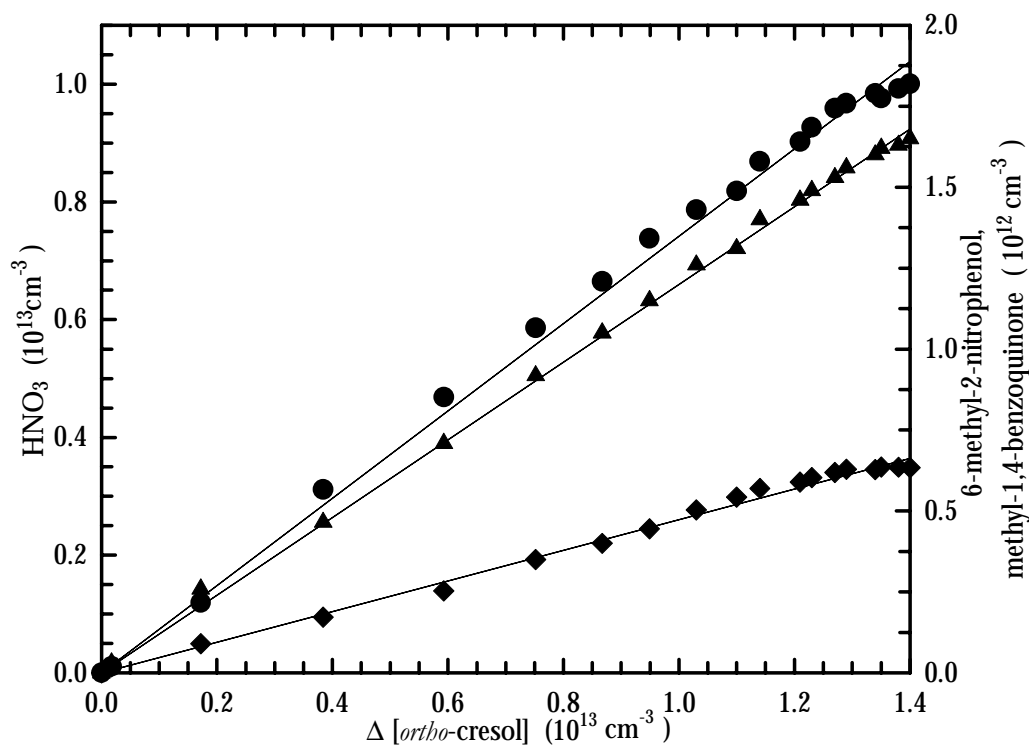


Figure 5.24 Plots of the corrected concentrations of (\blacktriangle)-6-methyl-2-nitrophenol, (\blacklozenge)-methyl-1,4-benzoquinone and (\bullet)- HNO_3 versus the amount of consumed *ortho*-cresol.

Table 5.7 Formation yields of 6-methyl-2-nitrophenol, methyl-1,4-benzoquinone and HNO₃ from the gas-phase reaction of the NO₃ radical with *ortho*-cresol in the 1080 l quartz glass reactor.

experiment	product molar yields (%)		
	6-methyl-2-nitrophenol	methyl-1,4-benzoquinone	HNO ₃
OCR11	11.9 ± 0.9	4.5 ± 0.3	85.6 ± 5.9
OCR12	11.4 ± 0.8	4.5 ± 0.3	77.9 ± 5.4
OCR13	11.4 ± 0.8	4.4 ± 0.3	74.9 ± 5.2
OCR14	11.3 ± 0.8	4.3 ± 0.3	70.5 ± 4.9
average yield	11.5 ± 0.8	4.4 ± 0.3	77.2 ± 6.3

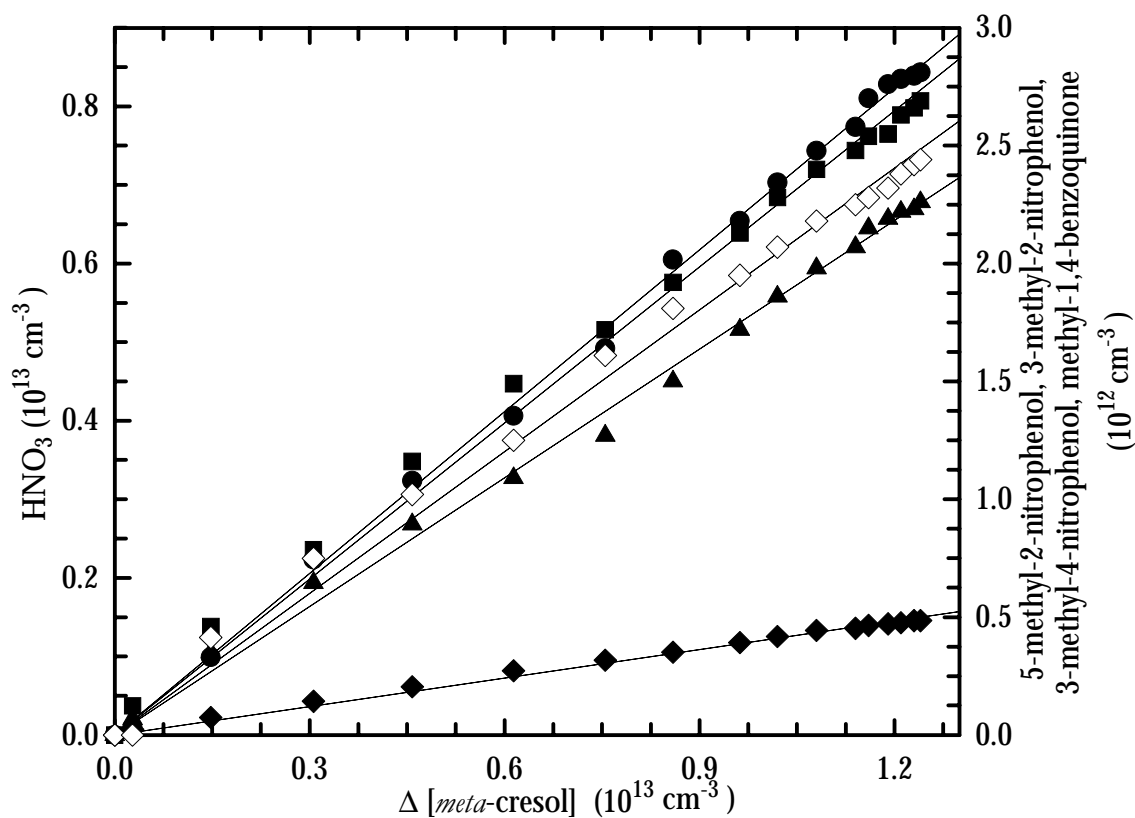


Figure 5.25 Plots of the corrected concentrations of (■)-5-methyl-2-nitrophenol, (▲)-3-methyl-2-nitrophenol, (◇)-3-methyl-4-nitrophenol, (◆)-methyl-1,4-benzoquinone and (●)-HNO₃ versus the amount of consumed *meta*-cresol.

Table 5.8 Formation yields of nitrocresols, methyl-1,4-benzoquinone and HNO₃ from the gas-phase reaction of the O₃ radical with *meta*-cresol in the 1080 l quartz glass reactor.

experiment	product molar yields (%)				
	3-methyl-2-nitrophenol	3-methyl-4-nitrophenol	5-methyl-2-nitrophenol	methyl-1,4-benzoquinone	HNO ₃
MCR11	22.6 ± 1.7	22.5 ± 1.5	23.0 ± 1.6	3.2 ± 0.22	75.3 ± 5.2
MCR12	18.2 ± 1.3	19.5 ± 1.4	21.3 ± 1.4	4.4 ± 0.30	65.6 ± 4.5
MCR13	23.7 ± 1.7	23.8 ± 1.6	24.5 ± 1.7	4.6 ± 0.32	68.7 ± 4.8
MCR14	20.5 ± 1.5	22.7 ± 1.6	25.4 ± 1.7	4.8 ± 0.33	79.7 ± 5.5
average yield	21.2 ± 2.4	22.8 ± 1.8	23.5 ± 1.8	4.2 ± 0.7	72.3 ± 6.4

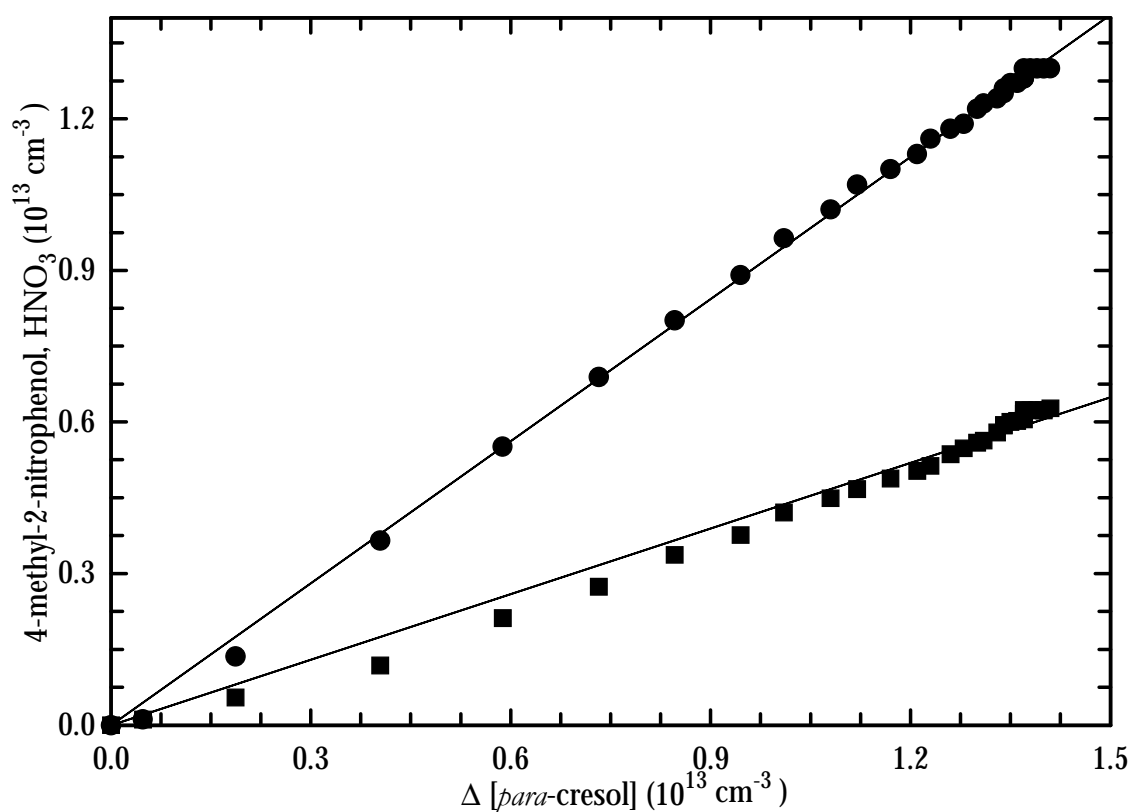
Figure 5.26 Plots of the corrected concentrations of (■)-4-methyl-2-nitrophenol and (●)-HNO₃ versus the amount of consumed *para*-cresol.

Table 5.9 Formation yields of 4-methyl-2-nitrophenol and HNO₃ from the gas-phase reaction of the NO₃ radical with *para*-cresol in the 1080 l quartz glass reactor.

experiment	product molar yields (%)	
	4-methyl-2-nitrophenol	HNO ₃
PCR11	41.7 ± 2.9	91.8 ± 6.4
PCR12	46.5 ± 3.2	94.8 ± 6.6
PCR13	39.0 ± 2.7	80.4 ± 5.6
PCR14	38.2 ± 2.6	72.7 ± 5.0
average yield	41.3 ± 3.7	85.0 ± 10.2

5.2.2.2 The EUPHORE chamber studies

The corrected formation yields of the identified products from the EUPHORE chamber experiments were obtained in the same way as previously discussed (see Section 5.2.2.1). Corrections were only made for wall loss of the identified products since this was determined to be the most important sink process (see Appendix II).

The amounts of nitrocresols and HNO₃ measured in the EUPHORE experiments study are plotted versus the amounts of cresols reacted in Figures 5.27 and 5.28. The corrected yields of the identified products, determined from individual experiments for each of the cresol isomers are listed in Table 5.11. The errors quoted in these tables are a combination of the 2σ statistical errors from the linear regression analysis and the errors given by the subtraction procedure.

Table 5.11 Corrected formation yields of the nitrocresols and HNO₃ from the gas-phase reaction of NO₃ radicals with *meta*- and *para*-cresol in EUPHORE chamber.

experiment	product molar yields (%)			
	3-methyl-2-nitrophenol	3-methyl-4-nitrophenol	5-methyl-2-nitrophenol	HNO ₃
MCR001	22.3 ± 1.6	25.4 ± 1.7	22.4 ± 1.5	91.1 ± 6.3

experiment	product molar yields (%)	
	4-methyl-2-nitrophenol	HNO ₃
PCR001	45.3 ± 3.4	88.7 ± 6.2
PCR002	43.4 ± 3.2	83.7 ± 5.8
average yield	44.3 ± 3.3	86.2 ± 6.0

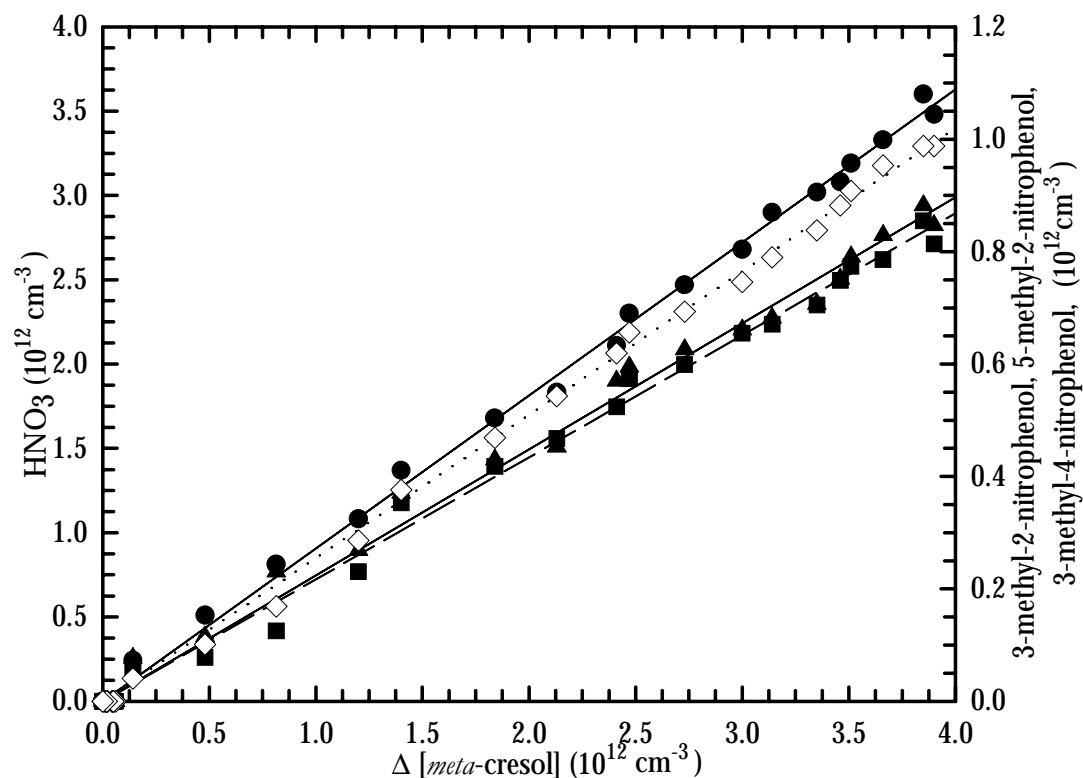


Figure 5.27 Plots of the corrected concentrations of (■)-5-methyl-2-nitrophenol, (▲)-3-methyl-2-nitrophenol, (◇)-3-methyl-4-nitrophenol and (●)- HNO_3 versus the amount of consumed *meta*-cresol.

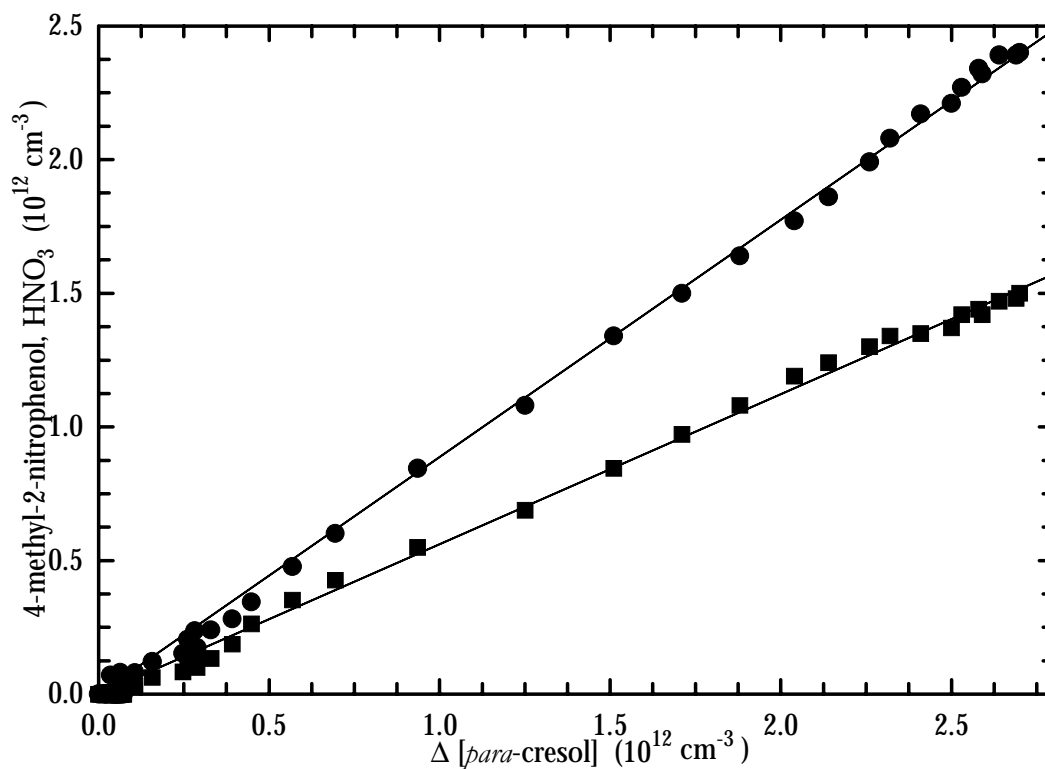


Figure 5.28 Plots of the corrected concentrations of (■)-4-methyl-2-nitrophenol and (●)- HNO_3 versus the amount of consumed *para*-cresol.

5.2.3 Discussion of the results

5.2.3.1 Comparison of results

An overview of the results from the present study concerning the formation yields of the identified products in the NO₃ initiated oxidation of cresol isomers is presented in Table 5.12.

The table also includes values found in the literature for the formation yields of the observed products (Grosjean, 1985; Atkinson *et al.*, 1992a). As can be seen in Table 5.12, in some cases there are significant differences in the yields of the products from the literature studies and the results from the present study.

The results from the present study on the reaction of NO₃ radicals with the cresol isomers have shown the formation of products not observed in previous studies (see Table 5.12) which provides new information with regard to the reaction pathways in NO₃ + cresol systems.

In the present study, apart for *ortho*-cresol, good agreement was found between the product distributions measured in the two chamber systems.

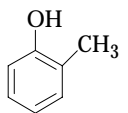
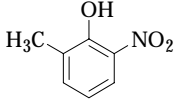
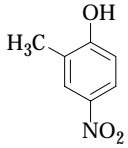
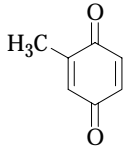
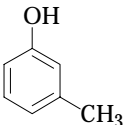
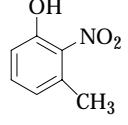
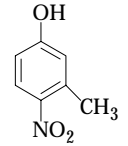
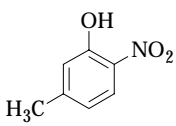
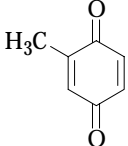
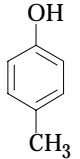
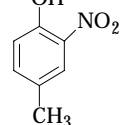
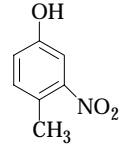
The formation of methyl-1,4-benzoquinone from the gas-phase NO₃ radical initiated oxidation of *ortho*-cresol and *meta*-cresol has been not previously reported.

The yields of nitrocresols, as measured in the present work, are in reasonable agreement with those reported by Atkinson *et al.* (1992a), apart for the *para*-cresol case (see Table 5.13) where the present results differ by nearly a factor of 2 from the literature value.

As discussed in Sections 5.2.1.2, usable information concerning the product distributions on *ortho*-cresol-NO₂-O₃ reaction systems have been obtained only from experiments carried out in the 1080 l quartz glass reactor. FT-IR analysis of the experimental data from 1080 l quartz glass reactor, indicated that 6-methyl-2-nitrophenol and methyl-1,4-benzoquinone are the oxidation products formed in NO₃ + *ortho*-cresol. The yield of 6-methyl-2-nitrophenol measured in the present work is similar to that previously reported by Atkinson *et al.* (1992a). The formation of 6-methyl-2-nitrophenol was also reported by Grosjean (1985), who also observed formation of 6-methyl-4-nitrophenol. However, he did not provide any information concerning the relative yields of the two methyl-nitrophenol isomers. From the present study it can be concluded that formation of 6-methyl-4-nitrophenol is quite likely with an estimated yield of about 10%.

In the *meta*-cresol-NO₂-O₃ reaction system, formation of 3-methyl-2-nitrophenol, 5-methyl-2-nitrophenol and 3-methyl-4-nitrophenol was observed in this work (see Sections 5.2.1.1.2 and 5.2.1.2.1). 3-Methyl-2-nitrophenol and 5-methyl-2-nitrophenol formation have been reported previously for this reaction by Atkinson *et al.* (1992a). Atkinson *et al.* (1992a) did not report the formation of 3-methyl-4-nitrophenol.

Table 5.12 Formation yields of the products observed in the gas-phase nitration reaction of cresol with NO₃.

reactant	products	yield (%) (this work)		yield (%) (literature)	
		1080 I	EUPHORE		
 <i>ortho</i> -cresol		6-methyl-2-nitrophenol	11.5 ± 0.8	n.d. ^a	12.8 ± 2.8 ^b 2.4 ÷ 23.0 ^c
		6-methyl-4-nitrophenol	probably	n.d. ^a	2.4 ÷ 23.0 ^c
		methyl-1,4-benzoquinone	4.4 ± 0.3	trace	-
	HNO ₃	nitric acid	77.2 ± 6.3	95.9 ± 4.8	-
 <i>meta</i> -cresol		3-methyl-2-nitrophenol	21.2 ± 1.4	22.3 ± 1.6	16.8 ± 2.9 ^b
		3-methyl-4-nitrophenol	22.8 ± 1.8	25.4 ± 1.7	-
		5-methyl-2-nitrophenol	23.5 ± 1.8	22.4 ± 1.5	19.6 ± 3.6 ^b
		methyl-1,4-benzoquinone	4.2 ± 0.7	n.d. ^a	-
	HNO ₃	nitric acid	72.3 ± 6.4	91.1 ± 6.3	-
 <i>para</i> -cresol		4-methyl-2-nitrophenol	41.3 ± 3.7	44.3 ± 3.3	74 ± 16 ^b
		4-methyl-3-nitrophenol	probably	n.d. ^a	-
	HNO ₃	nitric acid	85.0 ± 10.2	86.2 ± 7.0	-

^a n.d. - not determined; ^b Atkinson *et al.* (1992a); ^c Grosjean (1985), sum of 6-methyl-2-nitrophenol and 6-methyl-4-nitrophenol.

From the results of this study it can be concluded that the 3-methylnitrophenol isomers are the main gas-phase reaction products of the reaction of the NO₃ radical initiated oxidation of *meta*-cresol.

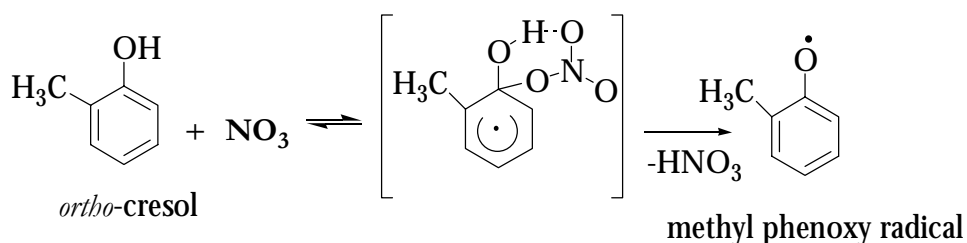
In the investigations on *para*-cresol formation of 4-methyl-2-nitrophenol was observed as the main product in both chambers. Atkinson *et al.* (1992a) have reported only formation of 4-methyl-2-nitrophenol from the reaction of NO₃ with *para*-cresol which is in fact, the main expected product. In a liquid phase study on the NO₃ radical mediated nitration of *para*-cresol (Barletta *et al.*, 2000) 4-methyl-2-nitrophenol was reported as the major reaction product in the Kyodai nitration of *para*-cresol with a yield formation ranging between 38 - 83%.

The observed products from the present study account for approximately 16, 72 and 44% carbon in the NO₃ radical initiated oxidation of *ortho*-, *meta*- and *para*-cresol, respectively. As noted in the results section not all the oxidation products have been identified. Therefore, it is suspected that the majority of missing carbon may well be in the form of unidentified nitrocresols and probably some ring-fragmentation products. This fact is supported by the residual product infrared spectra presented in the experimental sections (see Section 5.2.1.1 and 5.2.1.2).

The results from this study show that the main products from the NO₃-radical initiated reaction of cresols are nitrocresol isomers and methyl-1,4-benzoquinone. Also HNO₃, has been identified as an important co-product in all the experiments performed in the present work.

5.2.3.2 Discussion of the formation mechanism of nitrocresols

As was presented (see Chapter 1 and Chapter 4, Section 4.2) the gas-phase reactions of the NO₃ radical with phenolic compounds have been postulated to proceed via an overall H-atom abstraction mechanism which occurs through the intermediacy of a six-membered transition state (Atkinson *et al.*, 1992a). For example, for *ortho*-cresol:



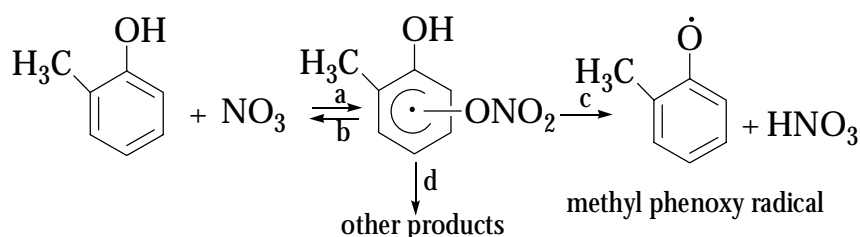
The methyl phenoxy radical thus formed reacts with NO₂ to form nitrocresols (Carter, 1990). However, such a reaction mechanism, as discussed by Atkinson *et al.* (1992a), from the simple mechanistic picture presented above would be expected to lead to a unit, or near unit,

yield of nitrophenols. As can be seen in Table 5.12, the yield of the identified product are below unity. Clearly the reaction mechanism of NO_3 with cresols are more complex than previously thought and other reaction pathways, possibly involving ring cleavage most occur.

As it was noted earlier (see Chapter 4, Section 4.2.3.2) the reaction mechanism proposed by Atkinson *et al.* (1992a) can be supported from a consideration of the electronic structure of the $\text{C}_6\text{H}_5\text{O}$ radical. In fact, Platz *et al.* (1998) using the Amsterdam Density Functional (ADF) code, has calculated the electronic structure for the phenoxy radical which support that phenoxy oxygen, *ortho*- and *para*-carbon positions, are dominate. Thus, formation of *ortho*-nitro and *para*-nitrocresols is to expected.

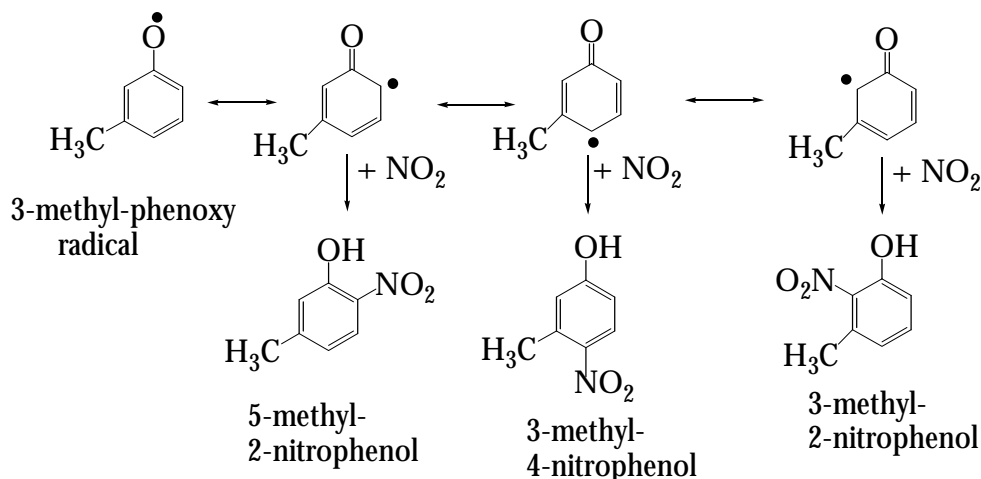
However, the initial addition of the NO_3 radical to aromatic ring may also be strongly dependent on the identity and position of substituent groups on the aromatic ring, as is the case for the corresponding OH radical reaction.

The results from the present work indicate that the degradation reactions of the cresol isomers very likely involve more than one pathway. Atkinson *et al.* (1992a) suggested that the following general mechanism should be used in order to explain the oxidation reaction of phenols initiated by NO_3 radicals:



In an extension of the previous mechanism, it is expected that the NO_3 -aromatic adduct which is formed in the first step of the reaction is further involved in three competitive reactions: first, decomposition back to reactants because of the short lifetime of the NO_3 -aromatic adduct with respect to its thermal decomposition (Atkinson *et al.*, 1990; Atkinson, 1991); second, elimination of HNO_3 with the formation of an methyl phenoxy radical and third, reaction to other products, possibly involving the formation of ring cleavage compounds. The total measured rate constants k are then given by $k = k_a(k_c + k_d)/(k_b + k_c + k_d)$, where k_a , k_b , k_c , k_d are the rate constant for reaction (a) through (d). The product data from the present work support that $k_c > k_d$ to a factor of ~ 10 , which has previously been predicted by Atkinson *et al.* (1992a).

From the present study, formation of nitrocresol isomers can only be explained by further reaction of the methyl phenoxy radical with NO_2 as has previously been proposed by Atkinson *et al.* (1992a), e.g. for *meta*-cresol:



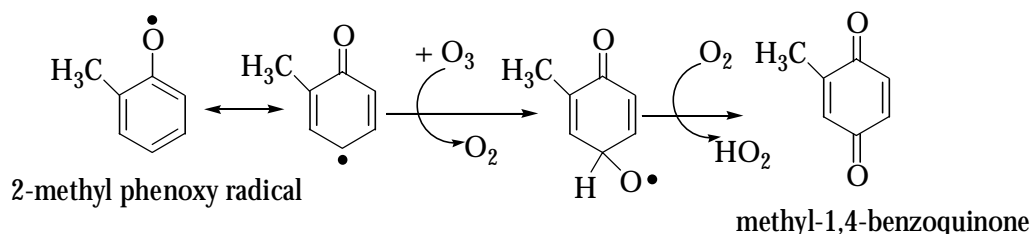
5.2.3.3 Discussion of the formation mechanism of methyl-1,4-benzoquinone

Formation of the methyl-1,4-benzoquinone products from the NO₃ radical initiated reaction of *ortho*-cresol and *meta*-cresol has not been reported previously. This work is the first to report a benzoquinone compound as product in the gas phase from the NO₃ radical initiated reaction of cresol isomers. In the present work, methyl-1,4-benzoquinone was determined to be formed in a yield of about 4% for each of the cresol isomers. The formation of methyl-1,4-benzoquinone is not possible for *para*-cresol.

From the FT-IR study of the reaction of O₂ with the phenoxy radical by Platz *et al.* (1998) it was concluded that reaction with O₂ is unimportant and an upper limit of this reaction rate constant of about $5.0 \times 10^{-21} \text{ cm}^3 \text{ molecule}^{-1} \text{ s}^{-1}$ at 296 K was estimated. As discussed in Chapter 4, Section 4.2.3, 1,4-benzoquinone was not identified among the products of the NO₃ radical initiated oxidation of phenol. This result was expected. In the cases of *ortho*- and *meta*-cresol the nitration reaction with NO₃ radicals led to the formation of methyl-1,4-benzoquinone. Obviously, the presence of the CH₃ group with its positive inductive effect is changing the reaction pathways of the 2-methyl-phenoxyl radical compared to the phenoxy radical. Earlier (see Section 5.1) it was indicated that in addition to studies on the reactions of the OH and NO₃ radicals with cresol isomers the reaction of Cl atoms with *ortho*-cresol in the presence and absence of NO_x was also examined. It was observed that the formation yield of methyl-1,4-benzoquinone from *ortho*-cresol-Cl₂ (in the absence of NO₂) irradiation mixtures was similar to that from *ortho*-cresol-NO₂-O₃ reaction mixtures. It was also observed that the formation of methyl-1,4-benzoquinone in the chlorine experiments is strongly dependent on the presence of NO₂ in the systems. In the presence of high NO₂ concentrations in the system formation of methyl-1,4-benzoquinone is completely suppressed.

As discussed in Section 5.1.2.3, the simplified mechanism of the formation of methyl-1,4-benzoquinone involves a methyl phenoxy radical which can further react with O_2 to form this compound. In the studied system the methyl phenoxy radical can react with NO_2 , other phenoxy radicals, O_2 or O_3 . Rate constants for the reaction of the phenoxy radical with O_2 , NO_2 and other phenoxy radicals are known for a temperature of 296 K (Platz *et al.*, 1998): $k_{(\text{phenoxy} + O_2)} < 5 \times 10^{-21} \text{ cm}^3 \text{ molecule}^{-1} \text{ s}^{-1}$; $k_{(\text{phenoxy} + NO_2)} = 2.08 \times 10^{-12} \text{ cm}^3 \text{ molecule}^{-1} \text{ s}^{-1}$; $k_{(\text{self-reaction})} = 1.2 \times 10^{-11} \text{ cm}^3 \text{ molecule}^{-1} \text{ s}^{-1}$. Kinetic data for the analogous reactions of the methyl phenoxy radical are not yet available in the literature. Because of the presence of a CH_3 group in the methyl phenoxy radical it can be expected that this increases its reactivity considerably. This is due to the strong positive inductive effect of this group.

Taking into account the experimental conditions employed in the experiments performed in the present work together with above kinetic data, it can be concluded that the reaction of the methyl phenoxy radical with NO_2 will dominate. Thus, the lack of formation of methyl-1,4-benzoquinone in the $Cl-NO_2$ experiments is not unexpected. Under the experimental conditions employed for *ortho*- and *meta*-cresols formation of methyl-1,4-benzoquinone can probably be explained by the presence of O_3 in the reaction mixture. No kinetic data for the reaction of the methyl phenoxy radical with O_3 are known. A possible mechanism that may explain the formation of methyl-1,4-benzoquinone under the experimental conditions for the work on cresol isomers are reactions such as (e.g. *ortho*-cresol):



5.2.3.4 Discussion of the formation of HNO_3

HNO_3 was found to be an important co-product in the nitration of cresol isomers and also phenol (see Chapter 4, Section 4.2) with NO_3 . Grosjean (1985) and Atkinson *et al.* (1992a) did not give information on the formation yield of HNO_3 in their studies.

It was noted earlier that HNO_3 can be formed in the gas-phase through several reactions which can occur in the system (see Chapter 4, Section 4.2.3.3). Because of the fast reaction of NO_3 radicals with cresol isomers, the formation of N_2O_5 is minimised under the experimental conditions employed in the present study. In the present work, the HNO_3 formation can be attributed mainly to reaction between cresols and NO_3 radicals. As is seen in

Table 5.12 the formation yield of HNO₃, accounts for between 72 - 96% of the cresols reacted.

Considering that HNO₃ is the main product in the nitration of cresol isomers with NO₃ radical this should also be reflected in the distribution of nitrophenol isomer yields. Based on the qualitative and quantitative observation from the present study it can be suggested that the yield of HNO₃ supports the reaction proceeding by H-atom abstraction from the OH substituent, and the sum of the formation yields of nitrocresol isomers should approximately equal the HNO₃ formation yield in these reaction systems.

5.2.4 Summary of results

The results from this study show that the important products from the NO₃-radical initiated reaction of cresols are nitrocresol isomers and methyl-1,4-benzoquinone. Also HNO₃ has been identified as an important co-product in all the experiments performed in the present work.

Based on the experimental data of the identified products from the NO₃ radical initiated oxidation of cresol isomers the following general reaction mechanism is proposed:

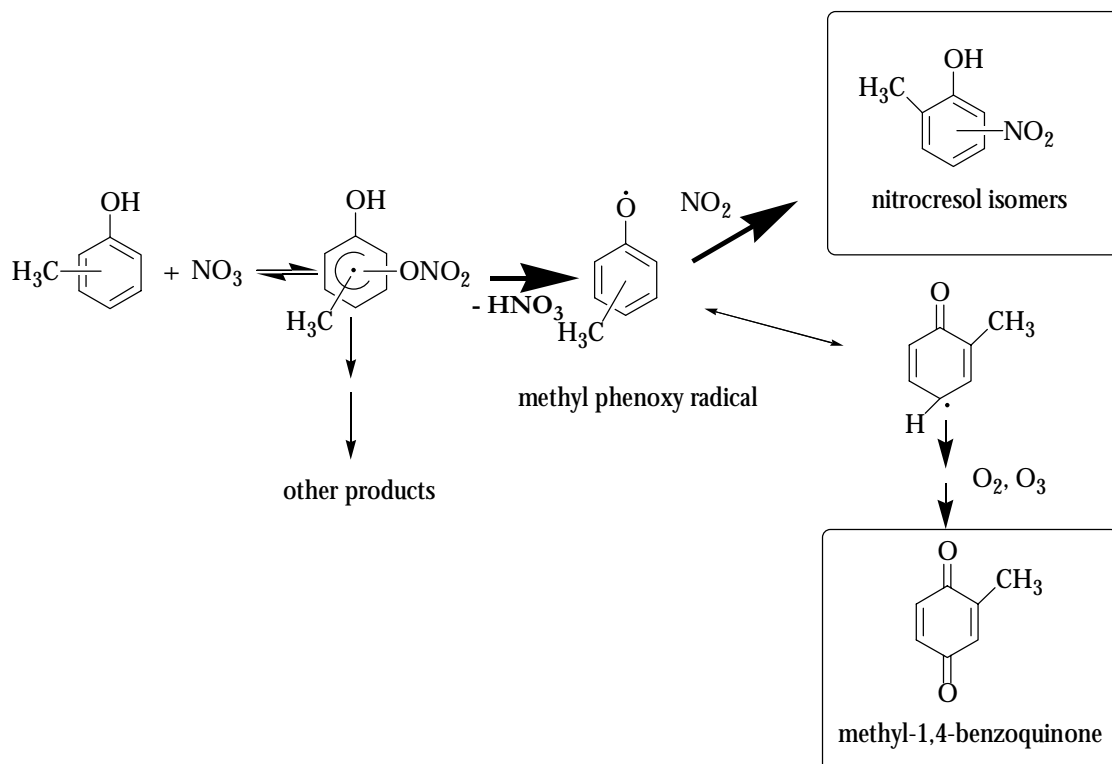


Figure 5.29 Simplified mechanism showing pathways to the observed products from the reaction of NO₃ radicals with cresol isomers. The bold arrows indicate suspected major reaction pathways.

Chapter 6

Summary

The objectives of this study were to measure the atmospheric reaction rates of dihydroxy(methyl)benzene and (methyl)benzoquinone compounds with the OH radical and to elucidate the atmospheric reaction mechanisms for phenol and the cresol isomers with both OH and NO₃ radicals. The study has yielded the following results:

Relative rate constants have been measured for the reactions of OH radicals with 1,2-dihydroxybenzene, 1,2-dihydroxy-3-methylbenzene, 1,2-dihydroxy-4-methylbenzene, 1,4-benzoquinone and methyl-1,4-benzoquinone. The rate constants (in units of cm³ molecule⁻¹ s⁻¹) were found to be $(10.4 \pm 2.1) \times 10^{-11}$ for 1,2-dihydroxybenzene; $(20.5 \pm 4.3) \times 10^{-11}$ and $(15.6 \pm 3.3) \times 10^{-11}$ for 1,2-dihydroxy-3-methylbenzene and 1,2-dihydroxy-4-methylbenzene, respectively; $(0.46 \pm 0.09) \times 10^{-11}$ and $(2.35 \pm 0.47) \times 10^{-11}$ for 1,4-benzoquinone and methyl-1,4-benzoquinone, respectively. The present kinetic data will improve the kinetic data base required to model the degradation mechanisms of aromatic compounds and to develop structure reactivity relationships for OH radicals with VOCs especially for oxygenated aromatic compounds. Using the kinetic data obtained in this study, in combination with an average tropospheric OH radical concentration of $[OH] = 1.6 \times 10^6 \text{ cm}^{-3}$ estimated atmospheric residence times of the compounds due to reaction with OH radicals have been determined. From the results it can be concluded that the 1,2-dihydroxybenzenes have very

short atmospheric lifetimes and probably will only influence the photochemical oxidant formation on a local scale, whereas the benzoquinones with significantly longer lifetimes will have a more regional influence.

Product analyses of the OH and NO₃ radical initiated oxidation of phenol and the cresol isomers under simulated atmospheric conditions were performed in a 1080 l quartz glass reactor at Wuppertal University and in the EUPHORE outdoor smog chamber facility in Valencia/Spain.

In the case of the OH initiated oxidation of phenol (or cresols), besides the already known nitrophenol products, new ring-retaining products were experimentally determined for the first time, namely, 1,2-dihydroxybenzene and 1,4-benzoquinone from phenol, 1,2-dihydroxy-3-methylbenzene and methyl-1,4-benzoquinone from *ortho*-cresol, 1,2-dihydroxy-3-methylbenzene, 1,2-dihydroxy-4-methylbenzene, methyl-1,4-benzoquinone and 3-methyl-4-nitrophenol from *meta*-cresol and 1,2-dihydroxy-4-methylbenzene from *para*-cresol.

From the results of the present study it can be concluded that 1,2-dihydroxy(methyl)benzenes isomers are the major gas-phase reaction products of the OH radical initiated oxidation of phenol and the cresol isomers. Interaction of the OH - phenol and OH - cresol adducts with O₂ will mainly lead to the formation of 1,2-dihydroxybenzenes and HO₂. In addition, the large yields of 1,2-dihydroxybenzenes support that addition at the position *ortho* to the OH substituent dominates. The results also support that formation of (methyl)benzoquinone compounds, mainly via the OH addition channel. The close similarity of the nitrophenol formation yields from phenol and cresol isomers with the fraction of overall OH radical reaction estimated to proceed by H-atom abstraction from the OH group implies that the nitrophenol formation from phenolic compounds arises from the abstraction channel.

Based on the results of the product studies, general degradation mechanisms have been constructed for the OH initiated oxidation of phenol and the cresol isomers.

Studies of the NO₃ radical initiated oxidation of phenol and the cresol isomers have been carried out in two chamber systems: 1080 l quartz glass reactor at Wuppertal University and in the EUPHORE outdoor smog chamber facility in Valencia/Spain. The observed oxidation products and their distribution can be used to improve the general degradation mechanism of phenol and cresol isomers towards NO₃ radicals.

The products detected during this study were as follows: 2-nitrophenol and 4-nitrophenol from phenol; 6-methyl-2-nitrophenol and 1,4-benzoquinone from *ortho*-cresol; 3-methyl-2-nitrophenol, 3-methyl-4-nitrophenol, 5-methyl-2-nitrophenol and methyl-1,4-benzoquinone from *meta*-cresol; 4-methyl-2-nitrophenol from *para*-cresol. HNO₃ has also been identified as important co-product. The experimental results support that the

degradation reactions initiated by NO_3 radicals of phenol and the cresol isomers form large yields of HNO_3 . Formation of methyl-1,4-benzoquinone in low yield has been identified for the first time as an oxidation product in the NO_3 radical initiated oxidation of *ortho*- and *meta*-cresol.

The results from this study show that major products from the NO_3 radical initiated reaction of phenol and cresol isomers are mixtures of nitrophenol isomers and with low yield of methyl-1,4-benzoquinone.

The gas-phase reactions of the NO_3 radical with phenolic compounds have been postulated to proceed via an overall H-atom abstraction mechanism which occurs through an NO_3 -aromatic adduct which can decompose back to reactants or to form methyl phenoxy radicals and HNO_3 . The methyl phenoxy radicals thus formed will react with NO_2 to form nitrophenols isomers. The results of the present study show that the abstraction reaction pathway leading to the phenoxy radical accounts for about 75 - 95% of the overall reaction of phenolic compounds with NO_3 radicals. Consequently reaction pathways leading to ring cleavage products, if indeed taking place, will be of minor importance.

The data obtained within the present work, concerning the products of the OH and NO_3 radical initiated oxidation of phenol and the cresol isomers, can be used to improve the knowledge on the atmospheric degradation mechanisms of aromatic hydrocarbons. The mechanisms constructed for the degradation of phenol and cresol isomers can be incorporated into atmospheric models to obtain more accurate estimates of production of O_3 , other photo-oxidants and HNO_3 through the photo-oxidation of aromatic compounds.

Appendix I

Syntheses

I.1 Synthesis of methyl nitrite (CH₃ONO)

Methyl nitrite was synthesised using the method previously described by Taylor *et al.* (1980). Methyl nitrite was generated by slow dropwise addition of 10 ml cold diluted sulphuric acid (50%) to a suspended solution of 7 g sodium nitrite (NaNO₂) in 20 ml methanol/water (1:1). The addition of the acid has to be very slow because the reaction is instantaneous. It is followed by an immediate development of the gaseous methyl nitrite. The gaseous methyl nitrite is first dried by passing it through a glass tube containing calcium chloride (CaCl₂) and is then collected in a glass cylinder cold trap. The cooling bath is a combination of dry ice and ethanol (- 68°C). The synthesised methyl nitrite was stored in the glass cylinder at - 78°C in dry ice.

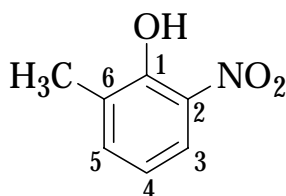
I.2 Synthesis of 6-methyl-2-nitrophenol

The method of Winzor (1935) was used for synthesis of 6-methyl 2-nitrophenol. The best formation yield was obtained from *o*-toluidine (23 g) dissolved in concentrated sulphuric acid (40 ml) and water (160 ml). The solution was cooled to 15°C. Sodium nitrite (60 g) in water (200 ml) was gradually added which caused the temperature to rise. The reaction mixture was purified in an excess of sulphuric acid (50%) contained in a large dish heated on a water-bath. After the vigorous evolution of gas had subsided, the mixture was steam distilled.

Yield 9.3 g (98%). The purity of the product was checked up GC-FID.

m.p. =67°C.

¹H-NMR (400 MHz, CDCl₃): δ(ppm)=7.94-7.92 (d, 1 H, CH-3), 7.43-7.41 (d, 1 H, CH-5) 7.24 (s, 1 H, Ar-OH), 6.87-6.85-6.83 (t, 1 H, CH-4), 2.31 (s, 3 H, Ar-CH₃).



Appendix II**Chamber wall loss rates for the compounds studied**

Table II.1 Wall loss rates of the compounds studied in the 1080 l quartz glass reactor.

compound	wall loss rate (s ⁻¹)
phenol	5.94 x 10 ⁻⁵
<i>ortho</i> -cresol	4.45 x 10 ⁻⁵
<i>meta</i> -cresol	4.57 x 10 ⁻⁵
<i>para</i> -cresol	4.45 x 10 ⁻⁵
1,2-dihydroxybenzene	2.08 x 10 ⁻⁴
1,2-dihydroxy-3-methylbenzene	3.04 x 10 ⁻⁴
1,2-dihydroxy-4-methylbenzene	2.12 x 10 ⁻⁴
1,4-benzoquinone	4.21 x 10 ⁻⁵
methyl-1,4-benzoquinone	9.40 x 10 ⁻⁵
2-nitrophenol	1.17 x 10 ⁻⁵
4-nitrophenol	1.70 x 10 ⁻⁴
6-methyl-2-nitrophenol	2.53 x 10 ⁻⁴
3-methyl-4-nitrophenol	2.05 x 10 ⁻⁴
3-methyl-2-nitrophenol	2.95 x 10 ⁻⁴
5-methyl-2-nitrophenol	2.86 x 10 ⁻⁴
4-methyl-2-nitrophenol	2.19 x 10 ⁻⁴
HNO ₃	5.10 x 10 ⁻⁵

Table II.2 Wall loss rates of the compounds studied in the EUPHORE chamber

compound	wall loss rate (s ⁻¹)
phenol	2.16 x 10 ⁻⁵
<i>ortho</i> -cresol	1.84 x 10 ⁻⁵
<i>meta</i> -cresol	3.07 x 10 ⁻⁵
<i>para</i> -cresol	4.45 x 10 ⁻⁵
2-nitrophenol	2.21 x 10 ⁻⁵
4-nitrophenol	1.05 x 10 ⁻⁴
3-methyl-2-nitrophenol	4.86 x 10 ⁻⁵
5-methyl-2-nitrophenol	2.05 x 10 ⁻⁵
3-methyl-4-nitrophenol	2.50 x 10 ⁻⁴
4-methyl-2-nitrophenol	2.12 x 10 ⁻⁴
HNO ₃	6.74 x 10 ⁻⁵

Appendix III**Gas-phase infrared absorption cross sections****III.1 Calibration method**

The 1080 l quartz glass reactor was used to determine absorption cross sections in the IR spectral region for all the identified ring-retaining products. The absolute and integral cross sections were determined using the procedure outlined by Etzkorn *et al.* (1999). A brief description of the method employed is given below.

Absorption cross sections are defined by Lambert-Beer's law:

$$\ln\left(\frac{I_0(\nu)}{I(\nu)}\right) = \sigma_{e(\nu)} \cdot c \cdot l = D_{(\nu)} \quad (\text{III.1})$$

were $I_{(\nu)}$ and $I_{0(\nu)}$ denote the measured light intensities at wave number ν with and without absorber present in the cell, $\sigma_{e(\nu)}$ is the absorption cross section at the wave number ν , c is the analyte concentration and L the optical path length through the cell. The term $\ln(I_{0(\nu)}/I_{(\nu)})$ is also known as the optical density $D_{(\nu)}$ at the wave number ν .

From equation III.1, an expression for the integrated band intensity (IBI) can be derived by integrating over the wave numbers covered by the absorption band of interest. This is a mathematical process which can be easily performed by the computer software. The IBI value is an often used parameter for the absorption intensity of a given molecule, because the IBI value normally is considered constant for a molecular absorption band if pressure, temperature and instrumental resolution are constant. Therefore, if the IBI value for a compound is known, the concentration can be found by equation III.2:

$$\text{IBI} = \frac{\int \ln \frac{I_0(\nu)}{I(\nu)} d\nu}{c \cdot l} \Leftrightarrow c = \frac{\int \ln \frac{I_0(\nu)}{I(\nu)} d\nu}{(\text{IBI}) \cdot l} \quad (\text{III.2})$$

If the IBI values is not known for a compound, a calibration of the compound has to be made. A calibration is normally made by adding known amounts of the compound into the reactor and by calculating the integral area. This is performed for several different concentrations of the compound. The method is valid only for reasonably volatile compounds.

Most of compounds used in the present work are solid (see Appendix VI), and their vapour pressures are very low. As was indicated in the experimental section (see Chapter 2), in

order to transfer these compounds to the gas-phase, a special inlet system was used. Condensation of these compounds onto the inlet system could not be completely avoided, even if this was heated by covering it with a electrical heating band. In order to obtain a reproducible and quantitative transfer of the compounds into the gas phase, weighed amounts of the organics were dissolved in HPLC grade dichlormethane. The concentrations of solutions were chosen to result in total injected volumes between 100 and 1000 μl for the calibration. For injection of the dissolved samples, a lockable syringe Hamilton 1001 SLK equipped with an extra long needle was used.

The transfer of the sample solution into the gas phase was accomplished by injecting the needle of the syringe into the evacuated cell through the septum. The valve controlling the nitrogen (or synthetic air) was then opened to produce a strong nitrogen (or air) flow across the needle tip. The lock of the syringe was opened and the solution allowed to vaporise into the cell. The syringe was then removed and the cell was filled with nitrogen (or synthetic air) to a final pressure of 1000 mbar. Approximately 1 min was allowed for fan assisted mixing and the adjustment of thermal equilibrium before a FT-IR spectrum was recorded.

For the calculation of the concentration in the cell the uncertainty of the injected volume has to be taken into account. Because the volume of the needle is unknown and the syringe calibration ticks possess a certain width, the “true” concentration, $c_{i,t}$ in the cell will be different from the concentration calculated from the injected volumes c_i by an offset a . By injecting different volumes (i) for one compound, this offset can be corrected:

$$c_i = (\alpha_i \cdot c_{\text{ref},i}) - a \quad (\text{III.3})$$

In this work, at least, five different volumes were injected into the cell for each compound. In the evaluation, the optical density D_i (see Eq. III.1) was separately calculated for each injected concentration. The ratios $\alpha_i (D_i/D_{\text{ref}})$ were obtained by made the subtraction of the non-calibrated reference spectra of the pure compounds recorded in absence of a solvent from the spectra recorded for different injected volumes in the chamber. The subtraction factors obtained were plotted as a function of the calculated concentrations of the analyte in the quartz glass reactor. A linear least square fit through these data point was performed, with the slope of the fit giving the concentration corresponding to reference spectrum. Absorption cross sections and integrated band intensities were determined using Lambert-Beer’s law: the optical densities and integrated optical densities of the reference spectra were divided by the concentrations determined (Eq. III.3) and the optical path length of the White mirror system (see Eq. III.2).

Tables III.1-III.3 gives the absorption cross sections and integrated band intensities for the identified oxidation products from the OH and NO_3 radical initiated reaction of phenol and the cresol isomers.

Table III.1 FT-IR absorption cross sections of the dihydroxybenzene compounds.

compound	absolute cross section		integrated cross section	
	wavenumber (cm ⁻¹)	(cm ² molecule ⁻¹)	region (cm ⁻¹)	(cm molecule ⁻¹)
1,2-dihydroxybenzene	1619	$(13.5 \pm 0.24) \times 10^{-20}$	1653-1590	$(3.56 \pm 0.60) \times 10^{-18}$
	1517	$(35.8 \pm 0.90) \times 10^{-20}$	1537-1495	$(8.50 \pm 0.21) \times 10^{-18}$
	1325	$(13.6 \pm 0.31) \times 10^{-20}$	1340-1306	$(2.02 \pm 0.40) \times 10^{-18}$
	1092	$(20.8 \pm 0.70) \times 10^{-20}$	1112-1072	$(3.45 \pm 0.11) \times 10^{-18}$
1,2-dihydroxy-3-methylbenzene	3671	$(20.2 \pm 0.80) \times 10^{-20}$	3689-3648	$(3.90 \pm 0.15) \times 10^{-18}$
	3608	$(25.9 \pm 1.52) \times 10^{-20}$	3629-3583	$(6.04 \pm 0.35) \times 10^{-18}$
	1488	$(20.6 \pm 0.95) \times 10^{-20}$	1545-1467	$(8.66 \pm 0.40) \times 10^{-18}$
	1359	$(7.83 \pm 0.40) \times 10^{-20}$	1377-1343	$(1.56 \pm 0.10) \times 10^{-18}$
	1188	$(20.6 \pm 1.14) \times 10^{-20}$	1207-1136	$(9.35 \pm 0.52) \times 10^{-18}$
	759	$(20.2 \pm 0.80) \times 10^{-20}$	785-742	$(2.93 \pm 0.12) \times 10^{-18}$
1,2-dihydroxy-4-methylbenzene	3666	$(11.3 \pm 0.67) \times 10^{-20}$	3689-3648	$(2.51 \pm 0.15) \times 10^{-18}$
	3608	$(18.9 \pm 0.13) \times 10^{-20}$	3629-3583	$(3.87 \pm 0.27) \times 10^{-18}$
	1527	$(22.2 \pm 1.32) \times 10^{-20}$	1545-1467	$(5.31 \pm 0.22) \times 10^{-18}$
	1315	$(5.41 \pm 0.42) \times 10^{-20}$	1343-1377	$(9.55 \pm 0.75) \times 10^{-19}$
	1200	$(4.85 \pm 0.21) \times 10^{-20}$	1207-1185	$(6.54 \pm 0.52) \times 10^{-19}$
	1168	$(12.3 \pm 1.01) \times 10^{-20}$	1182-1153	$(2.17 \pm 0.18) \times 10^{-18}$
	1110	$(14.5 \pm 0.93) \times 10^{-20}$	1123-1090	$(2.57 \pm 0.10) \times 10^{-18}$
	790	$(8.52 \pm 0.52) \times 10^{-20}$	828-764	$(2.80 \pm 0.17) \times 10^{-18}$

Table III.2 FT-IR absorption cross sections of the benzoquinone compounds.

compound	absolute cross section		integrated cross section	
	wavenumber (cm ⁻¹)	(cm ² molecule ⁻¹)	region (cm ⁻¹)	(cm molecule ⁻¹)
1,4-benzoquinone	1683	$(18.7 \pm 0.92) \times 10^{-19}$	1696-1662	$(39.5 \pm 1.95) \times 10^{-18}$
			1090-1040	$(6.54 \pm 0.33) \times 10^{-18}$
	885	$(7.50 \pm 0.33) \times 10^{-19}$	908-861	$(11.9 \pm 0.53) \times 10^{-18}$
methyl-1,4-benzoquinone	1679	$(19.2 \pm 0.59) \times 10^{-19}$	1696-1656	$(35.2 \pm 1.09) \times 10^{-18}$
	1094	$(17.8 \pm 0.05) \times 10^{-19}$	1105-1072	$(3.34 \pm 0.10) \times 10^{-18}$
	906	$(5.25 \pm 0.17) \times 10^{-19}$	924-885	$(5.73 \pm 0.18) \times 10^{-18}$

Table III.3 FT-IR absorption cross sections of the nitrophenol compounds.

compound	absolute cross section		integrated cross section	
	wavenumber (cm ⁻¹)	(cm ² molecule ⁻¹)	region (cm ⁻¹)	(cm molecule ⁻¹)
2-nitrophenol	1627	$(3.80 \pm 0.61) \times 10^{-19}$	1654-1610	$(8.32 \pm 1.55) \times 10^{-18}$
	1343	$(9.40 \pm 0.45) \times 10^{-19}$	1367-1305	$(26.8 \pm 1.30) \times 10^{-18}$
	1199	$(4.59 \pm 0.24) \times 10^{-19}$	1221-1177	$(11.2 \pm 0.58) \times 10^{-18}$
			1047-1011	$(18.2 \pm 0.87) \times 10^{-19}$
	872	$(2.07 \pm 0.10) \times 10^{-19}$	866-859	$(2.73 \pm 0.13) \times 10^{-18}$
	748	$(10.4 \pm 0.48) \times 10^{-19}$	765-730	$(7.90 \pm 0.36) \times 10^{-18}$
4-nitrophenol	1610	$(10.4 \pm 0.47) \times 10^{-20}$	1629-1587	$(2.33 \pm 0.10) \times 10^{-18}$
	1356	$(17.8 \pm 1.26) \times 10^{-20}$	1379-1323	$(3.94 \pm 0.28) \times 10^{-18}$
6-methyl-2-nitrophenol	1614	$(65.3 \pm 1.69) \times 10^{-20}$	1637-1597	$(12.2 \pm 0.31) \times 10^{-18}$
	1356	$(60.9 \pm 1.65) \times 10^{-20}$	1372-1336	$(10.5 \pm 0.28) \times 10^{-18}$
	1162	$(22.7 \pm 0.35) \times 10^{-20}$	1181-1137	$(4.85 \pm 0.07) \times 10^{-18}$
	745	$(92.9 \pm 3.93) \times 10^{-20}$	761-733	$(7.62 \pm 0.32) \times 10^{-18}$
3-methyl-4-nitrophenol	3656	$(62.9 \pm 0.10) \times 10^{-20}$	3674-3636	$(12.4 \pm 0.02) \times 10^{-18}$
	1546	$(10.7 \pm 0.47) \times 10^{-19}$	1561-1519	$(23.5 \pm 0.04) \times 10^{-18}$
	1356	$(10.7 \pm 0.02) \times 10^{-19}$	1373-1337	$(20.6 \pm 0.04) \times 10^{-18}$
3-methyl-2-nitrophenol	1609	$(41.8 \pm 6.34) \times 10^{-20}$	1643-1580	$(23.7 \pm 0.89) \times 10^{-18}$
	1351	$(48.7 \pm 2.02) \times 10^{-20}$	1373-1308	$(17.4 \pm 0.72) \times 10^{-18}$
	1206	$(36.2 \pm 1.61) \times 10^{-20}$	1234-1157	$(15.1 \pm 0.66) \times 10^{-18}$
	1073	$(12.5 \pm 0.50) \times 10^{-20}$	1088-1054	$(2.14 \pm 0.10) \times 10^{-18}$
	787	$(45.2 \pm 1.72) \times 10^{-20}$	802-771	$(4.20 \pm 0.16) \times 10^{-18}$
5-methyl-2-nitrophenol	1634	$(82.0 \pm 1.58) \times 10^{-20}$	1660-1618	$(17.1 \pm 0.33) \times 10^{-18}$
	1550	$(48.4 \pm 1.14) \times 10^{-20}$	1570-1527	$(11.6 \pm 0.27) \times 10^{-18}$
	1335	$(97.5 \pm 1.25) \times 10^{-20}$	1362-1315	$(26.0 \pm 0.33) \times 10^{-18}$
	1086	$(13.1 \pm 0.26) \times 10^{-20}$	1102-1068	$(2.09 \pm 0.03) \times 10^{-18}$
	758	$(41.0 \pm 1.01) \times 10^{-20}$	774-744	$(2.65 \pm 0.08) \times 10^{-18}$
4-methyl-2-nitrophenol	1331	$(86.4 \pm 0.82) \times 10^{-20}$	1364-1307	$(30.4 \pm 0.29) \times 10^{-18}$
	1192	$(63.0 \pm 0.61) \times 10^{-20}$	1207-1171	$(12.2 \pm 0.11) \times 10^{-18}$
	1080	$(10.2 \pm 0.18) \times 10^{-20}$	1097-1062	$(1.68 \pm 0.03) \times 10^{-18}$
	827	$(55.9 \pm 1.02) \times 10^{-20}$	843-811	$(6.14 \pm 0.11) \times 10^{-18}$

III.2 FT-IR absorption cross sections and intergated cross sections of phenol and the cresol isomers

Table III.4 FT-IR absorption cross sections of phenol and the cresol isomers (Etzkorn *et al.*, 1999).

compound	absolute cross section		integrated cross section	
	wavenumber (cm ⁻¹)	(cm ² molecule ⁻¹)	region (cm ⁻¹)	(cm molecule ⁻¹)
phenol	365	$(29.2 \pm 1.0) \times 10^{-20}$	3708-3625	$(6.36 \pm 0.22) \times 10^{-18}$
	1610	$(42.0 \pm 1.5) \times 10^{-20}$	1638-1577	$(8.26 \pm 0.29) \times 10^{-18}$
	1261	$(39.5 \pm 1.4) \times 10^{-20}$	1286-1231	$(8.26 \pm 0.29) \times 10^{-18}$
	1184	$(58.0 \pm 2.0) \times 10^{-20}$	1228-1121	$(18.5 \pm 0.70) \times 10^{-18}$
	752	$(45.0 \pm 1.6) \times 10^{-20}$	787-717	$(6.45 \pm 0.23) \times 10^{-18}$
<i>ortho</i> -cresol	3661	$(27.9 \pm 1.3) \times 10^{-20}$	3692-3614	$(6.22 \pm 0.29) \times 10^{-18}$
	1600	$(14.0 \pm 0.6) \times 10^{-20}$	1650-1558	$(4.61 \pm 0.21) \times 10^{-18}$
	849	$(8.6 \pm 0.39) \times 10^{-20}$	898-785	$(2.26 \pm 0.10) \times 10^{-18}$
<i>meta</i> -cresol	3656	$(29.4 \pm 1.4) \times 10^{-20}$	3688-3619	$(5.82 \pm 0.27) \times 10^{-18}$
	3046	$(11.1 \pm 0.5) \times 10^{-20}$	3178-2706	$(12.6 \pm 0.60) \times 10^{-18}$
	936	$(11.0 \pm 0.5) \times 10^{-20}$	1352-1239	$(10.3 \pm 0.50) \times 10^{-18}$
	930	$(12.6 \pm 0.6) \times 10^{-20}$	953-898	$(2.25 \pm 0.11) \times 10^{-18}$
	777	$(28.1 \pm 1.3) \times 10^{-20}$	804-715	$(4.81 \pm 0.23) \times 10^{-18}$
<i>para</i> -cresol	3662	$(34.0 \pm 2.6) \times 10^{-20}$	3687-3629	$(7.61 \pm 0.58) \times 10^{-18}$
	1617	$(13.8 \pm 1.0) \times 10^{-20}$	3180-2804	$(16.5 \pm 1.20) \times 10^{-18}$
	1331	$(15.5 \pm 1.2) \times 10^{-20}$	1662-1572	$(5.14 \pm 0.39) \times 10^{-18}$
	820	$(35.5 \pm 0.7) \times 10^{-20}$	864-773	$(9.15 \pm 0.69) \times 10^{-18}$

Table III.5 FT-IR absorption range and concentration of reference spectra used in the quantitative analyses.

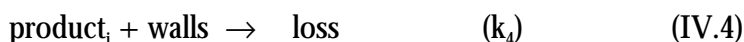
compound	region(cm ⁻¹)	ν (cm ⁻¹)	c (ppm m)	condition
CH ₃ ONO	887-751	812	872±97 ^a	1000 mbar N ₂ , 24 ^o C
CH ₃ ONO ₃	900-813	855	qualitativ ^a	1000 mbar air, 26 ^o C
NO	1970-1751	1904	2292±114 ^b	1000 mbar N ₂ , 24 ^o C
NO ₂	1673-1527	1629	650±32 ^b	1000 mbar N ₂ , 26 ^o C
N ₂ O	2277-2142	2238	931 ^a	1000 mbar air, 26 ^o C
HNO ₃	940-830	896	423±21 ^c	1000 mbar air, 24 ^o C
HONO	895-751	852	499±25 ^d	1000 mbar air, 25 ^o C
HCOH	3100-2580	2802	1550±240 ^e	1000 mbar air, 25 ^o C
HCOOH	1841-1710	1776	533 ^e	1000 mbar air, 25 ^o C
H ₂ O	2098-1249	-	qualitativ ^a	1000 mbar air, 25 ^o C
CO	2246-1999	-	qualitativ ^e	1000 mbar N ₂ , 25 ^o C
CO ₂	2390-2236	-	qualitativ ^a	1000 mbar air, 25 ^o C
O ₃	1080-950	1054	1875±94 ^a	1000 mbar air, 25 ^o C
isoprene	949-845	893	7µl injected	1000 mbar air, 26 ^o C
1,3-butadiene	963-817	908	3 ml injected	1000 mbar air, 26 ^o C
E-2-butene	1027-885	963	3 ml injected	1000 mbar air, 26 ^o C

^a Klotz (1998); ^b Wirtz (1998); ^c Mendel *et al.* (1996); ^d Brust (1997); ^e Ruppert (1998).

Appendix IV**Correction of the formation yields of dihydroxy(methyl)benzene and (methyl)benzoquinone in the OH-initiated oxidation of phenol and cresol isomers**

The measured formation yields of dihydroxy(methyl)benzene and (methyl)benzoquinone compounds in the oxidation of phenols are affected by losses due to their reaction with OH radicals and wall losses. Their yields were corrected using the mathematical formalism outlined by Tuazon *et al.* (1986). The mathematical formalism is explained using 1,2-dihydroxybenzene which was identified as a model.

The following reaction sequence has to be considered:



where in the reaction (IV.1), Y, is the formation yield of the individual product from the precursor substance.

By making the assumption that the OH radical concentrations were essentially constant over the irradiation period, then:

$$[\text{phenol}]_{t_2} = [\text{phenol}]_{t_1} e^{-(k_1[\text{OH}] + k_2)(t_2 - t_1)} \quad (\text{IV.5})$$

From IV.5 it is possible to calculate the concentration of OH radicals in the system. The value of the rate constant k_1 , was taken from the literature (Calvert *et al.*, 2001) (see Table IV.1). The value, k_2 , was obtained in dark experiments. The values k_3 and k_4 for the 1,2-dihydroxybenzenes were taken from a recent relative kinetic study from this laboratory (Olariu *et al.*, 2000a) (see Table IV.1).

Using the relation obtained by Tuazon *et al.* (1986) for the corrected concentration of α -dicarbonyls a similar equation can be written for the corrected concentration of the 1,2-dihydroxybenzene:

$$\begin{aligned}
 [\text{product}_i]_{t_2} &= [\text{product}_i]_{t_1} \cdot e^{-(k_3[\text{OH}]+k_4)(t_2-t_1)} + \\
 &+ \frac{Y_{t_1-t_2} \cdot [\text{phenol}]_{t_1} \cdot k_1 [\text{OH}]}{\{(k_3 - k_1) \cdot [\text{OH}] + k_4\}} \cdot [e^{-(k_1[\text{OH}]+k_2)(t_2-t_1)} e^{-(k_3[\text{OH}]+k_4)(t_2-t_1)}]
 \end{aligned}
 \tag{IV.6}$$

where $[\text{phenol}]_{t_1}$, $[\text{product}_i]_{t_1}$ and $[\text{phenol}]_{t_2}$, $[\text{product}_i]_{t_2}$ are the phenol and the 1,2-dihydroxybenzene concentrations observed at times t_1 and t_2 , respectively, and $Y_{t_1-t_2}$ is the formation yield of the individual product over the time period t_1-t_2 .

Using eq.IV.5 and IV.6 allows $Y_{t_1-t_2}$ to be calculated. The 1,2-dihydroxybenzene concentration, corrected for reaction with OH radicals and other loss process, is the given by:

$$[\text{product}_i]_{t_2}^{\text{corr}} = [\text{product}_i]_{t_1}^{\text{corr}} + Y_{t_1-t_2} \cdot ([\text{phenol}]_{t_1} - [\text{phenol}]_{t_2}) \tag{IV.7}$$

where: $[\text{product}_i]_{t_1}^{\text{corr}}$ and $[\text{product}_i]_{t_2}^{\text{corr}}$, are the corrected ring-retaining product concentrations at time t_1 and t_2 , respectively.

Table IV.1 Rate constants used to correct the formation yields of ring-retaining products.

compound	$k \times 10^{11}$ ($\text{cm}^3 \text{ molecule}^{-1} \text{ s}^{-1}$)	reference
phenol	2.70	Calvert <i>et al.</i> , (2001)
<i>ortho</i> -cresol	4.10	Calvert <i>et al.</i> , (2001)
<i>meta</i> -cresol	6.80	Calvert <i>et al.</i> , (2001)
<i>para</i> -cresol	5.00	Calvert <i>et al.</i> , (2001)
1,2-dihydroxybenzene	10.4	Olariu <i>et al.</i> , (2000a)
1,2-dihydroxy-3-methylbenzene	20.5	Olariu <i>et al.</i> , (2000a)
1,2-dihydroxy-4-methylbenzene	15.6	Olariu <i>et al.</i> , (2000a)
1,4-benzoquinone	0.46	Olariu <i>et al.</i> , (2000a)
methyl-1,4-benzoquinone	2.40	Olariu <i>et al.</i> , (2000a)
2-nitrophenol	0.09	Atkinson <i>et al.</i> , (1992a)

Appendix V

Origin and purity of the chemicals and gases used

V.1 Gases

compound	origin	purity
synthetic air 20.5:79.5 = O ₂ :N ₂ (%)	Messer-Griesheim	hydrocarbons free 99.999%
O ₂	Messer-Griesheim	99.995%
N ₂	Messer-Griesheim	99.999%
NO	Messer-Griesheim	99.5%
NO ₂	Messer-Griesheim	98%
SF ₆	Messer-Griesheim	99.99%
1,3-butadiene	Aldrich	99%
<i>E</i> -2-butene	Messer-Griesheim	99%

V.2 Chemicals

compound	state	origin	purity
phenol	solid	Aldrich	99.99%
<i>ortho</i> -cresol	liquid	Aldrich	99.99%
<i>meta</i> -cresol	liquid	Aldrich	97%
<i>para</i> -cresol	liquid	Aldrich	99.99%
2-nitrophenol	solid	Aldrich	98%
4-nitrophenol	solid	Sigma	99.99%
1,2-dihydroxybenzene	solid	Aldrich	99%
1,2-dihydroxy-3-methylbenzene	solid	Aldrich	99%
1,2-dihydroxy-4-methylbenzene	solid	Aldrich	98%
1,4-benzoquinone	solid	Aldrich	98%
methyl-1,4-benzoquinone	solid	Aldrich	98%
6-methyl-2-nitrophenol	solid	synthesis (see Appendix I.2)	98%
3-methyl-2-nitrophenol	solid	Fluka	98%
3-methyl-4-nitrophenol	solid	Fluka	98%
5-methyl-2-nitrophenol	solid	Aldrich	97%
4-methyl-2-nitrophenol	solid	Aldrich	99%
isoprene	liquid	Aldrich	99%
CH ₃ CN	liquid	Fluka	99.5%
CH ₂ Cl ₂	liquid	Aldrich	99.9%

References

- Ackermann, R., Proceeding of the "Workshop on the Chemical Behaviour of Aromatic Hydrocarbons in the Troposphere", Valencia, Spain, February 27-29, 2000.
- Atkinson, R., Kinetics and mechanisms of the gas-phase reactions of the hydroxyl radical with organic compounds under atmospheric conditions, *Chem. Rev.*, **86**, 69-201, 1986.
- Atkinson, R., A structure-activity relationship for the estimation of the rate constants of OH radicals with organic compounds, *Int. J. Chem. Kinet.*, **19**, 799-828, 1987.
- Atkinson, R., Kinetics and mechanisms of the gas-phase reactions of the hydroxyl radical with organic compounds, *J. Phys. Chem. Ref. Data*, Monograph No. 1, 1-246, 1989.
- Atkinson, R., Kinetics and mechanisms of the gas-phase reactions of the NO₃ radical with organic compounds, *J. Phys. Chem. Ref. Data*, **20**, 459-507, 1991.
- Atkinson, R., Gas-phase tropospheric chemistry of organic compounds, *J. Phys. Chem. Ref. Data*, Monograph No. 2, 1-216, 1994.
- Atkinson, R., Product studies of gas-phase reaction of organic compounds, *Pure & Appl. Chem.*, **70** (7), 1335-1343, 1998.
- Atkinson, R., Atmospheric chemistry of VOCs and NO_x, *Atmos. Environ.*, **34**, 2063-2101, 2000.
- Atkinson, R., and S.M. Aschmann, Products of the gas-phase reactions of aromatic hydrocarbons: Effect of NO₂ concentration, *Int. J. Chem. Kinet.*, **26**, 929-944, 1994.
- Atkinson, R., and S.M. Aschmann, and J. Arey, Formation of ring-retaining products from the OH radical-initiated reactions of o-, m-, and p-xylene, *Int. J. Chem. Kinet.*, **23**, 77-97, 1991.

References

- Atkinson, R., S.M. Aschmann, and J. Arey, Reactions of OH and NO₃ radicals with phenol, cresols, and 2-nitrophenol at 296 ± 2 K, *Environ. Sci. Technol.*, **26**, 1397-1403, 1992a
- Atkinson, R., S.M. Aschmann, J. Arey, and W.P.L. Carter, Formation of ring-retaining products from the OH radical-initiated reactions of benzene and toluene, *Int. J. Chem. Kinet.*, **21**, 801-827, 1989.
- Atkinson, R., S.M. Aschmann, J.N. Pitts, Jr., Rate Constants for Gas-Phase Reaction of the NO₃ Radical with a Series of Organic Compounds at 298 ± 2 K, *J. Phys. Chem.*, **92**, 3454-3457, 1988.
- Atkinson, R., D.L. Baulch, R.A. Cox, R.F. Hampson, Jr., J.A. Kerr, and J. Troe, Evaluated kinetic and photochemical data for atmospheric chemistry: Supplement IV., *J. Phys. Chem. Ref. Data*, **21**, 1125-1568, 1992b.
- Atkinson, R., D.L. Baulch, R.A. Cox, R.F. Hampson, Jr., J.A. Kerr, M.J. Rossi, and J. Troe, Evaluated kinetic and photochemical data for atmospheric chemistry: Supplement VI. IUPAC subcommittee on gas kinetic data evaluation for atmospheric chemistry, *J. Phys. Chem. Ref. Data*, **26**, 1329-1499, 1997.
- Atkinson, R., W.P.L. Carter, K.R. Darnall, A.M. Winer, and J.N. Pitts, Jr., A smog chamber and modeling study of the gas phase NO_x-air photooxidation of toluene and the cresols, *Int. J. Chem. Kinet.*, **12**, 779-836, 1980.
- Atkinson, R., W.P.L. Carter, C.N. Plum, A.M. Winer, and J.N. Pitts, Jr., Kinetics of the gas-phase reactions of NO₃ radicals with a series of aromatics at 296 ± 2 K, *Int. J. Chem. Kinet.*, **16**, 887-898, 1984.
- Atkinson, R., E.C. Tuazon, and J. Arey, Reactions of naphthalene in N₂O₅-NO₃-NO₂-air mixtures, *Int. J. Chem. Kinet.*, **22**, 1071-1082, 1990.
- Atkinson, R., E.C. Tuazon, T.J. Wallington, S.M. Aschmann, J. Arey, A.M. Winer, and J.N. Pitts, Jr., Atmospheric chemistry of aniline, N,N-dimethylaniline, pyridine, 1,3,5-triazine, and nitrobenzene, *Environ. Sci. Technol.*, **21**, 64-72, 1987.

- Barletta, B., E. Bolzacchini, S. Meinardi, M. Orlandi, and B. Rindone, The NO₃ Radical-Mediated Liquid Phase Nitration of Phenols with Nitrogen Dioxide, *Environ. Sci. Technol.*, **34**, 2224-2230, 2000.
- Barnes, I., K.H. Becker, N. Mihalopoulos, An FT-IR Product Study of the Photo-oxidation of Dimethyl Disulfide, *J Atmos Chem.*, **18**, 267-289, 1994
- Barnes, I., and K. Brokmann, (ed.); 2-ed EUPHORE Report 1998-1999, Bergische Universität Wuppertal, Physikalische Chemie , FB9, Germany, 2001.
- Becker, K. H., (ed.); EUPHORE final report, EV5V-CT92-0059, 1996.
- Belloli, R., B. Barletta, E. Bolzacchini, S. Meinardi, M. Orlandi, B. Rindone, Determination of toxic nitrophenols in the atmosphere by high-performance liquid chromatography, *J.Cromatogr. A*, **846**, 277-281, 1999.
- Benson, S.W., Thermochemical Kinetics, Wiley, New York, 1976.
- Berho, F., F. Caralp, M.T. Rayez, R. Lesclaux, and E. Ratajczak, Kinetics and thermochemistry of the reversible combination reaction of the phenoxy radical with NO, *J. Phys. Chem. A*, **102**, 1-8, 1998.
- Berndt, T., O. Böge, H. Herrmann, On the formation of benzene oxide/oxepin in the gas-phase reaction of OH radicals with benzene, *Chem. Phys. Lett.*, **314**, 435-442, 1999.
- Bjergbakke, E., A. Sillesen, P. Pagsberg, UV spectrum and kinetics of hydroxycyclohexadienyl radicals, *J. Phys. Chem.*, **100**, 5729-5736, 1996.
- Bidleman, T.F., Atmospheric processes, *Environ. Sci. Technol.*, **22**, 361-367, 1988.
- Bierbach, A., I. Barnes, K.H. Becker, and E. Wiesen, Atmospheric chemistry of unsaturated carbonyls: Butenedial, 4-oxy-2-pentenal, 3-hexene-2,5-dione, maleic anhydride, 3H-furan-2-one, and 5-methyl-3H-furan-2-one, *Environ. Sci. Technol.*, **28**, 715-729, 1994.

References

- Bohn, B., Formation of peroxy radicals from OH-toluene adducts and O₂, *J. Phys. Chem. A*, **105**, 6092-6101, 2001.
- Bohn, B., and C. Zetzsch, Gas-phase reaction of the OH-benzene adduct with O₂: reversibility and secondary formation of HO₂, *Phys. Chem. Chem. Phys.*, **1**, 5097-5107, 1999.
- Bolzacchini, E., M. Bruschi, J. Hjorth, S. Meinardi, M. Orlandi, B. Rindone, and E. Rosenbohm, Gas-Phase Reaction of Phenol with NO₃, *Environ. Sci. Technol.*, **35**, 1791-1797, 2001.
- Bowman, F.M., and J.H. Sienfeld, Ozone productivity of atmospheric organics, *J. Geophys. Res.*, **99**, 5390-5324, 1994.
- Brust, A. S., Untersuchungen der IR- und UV- Absorption instabiler, atmosphärischer Spurengase, Ph.D. Thesis, University of Wuppertal, 1997.
- Calvert, J., R. Atkinson, K.H. Becker, R. Kamens, J. Seinfeld, T. Wallington, and G. Yarwood, *Mechanisms of Atmospheric Oxidation of Aromatic Hydrocarbons*, Oxford University Press, 2001.
- Carter, W.P.L., A detailed mechanism for the gas-phase atmospheric reactions of organic compounds, *Atmos. Environ.*, **24A**, 481-518, 1990.
- Carter, W.P.L., Development of reactivity scales for volatile organic compounds, *J. Air Waste Management Assoc.*, **44**, 881-899, 1994.
- Carter, W.P.L., and R. Atkinson, An experimental study of incremental hydrocarbon reactivity, *Environ. Sci. Technol.*, **21**, 670-679, 1987.
- Carter, W.P.L., A.M. Winer, and J.N. Pitts, Jr., Major atmospheric sink for phenol and cresols. Reaction with the nitrate radical, *Environ. Sci. Technol.*, **15**, 829-831, 1981.

- Choure, S.C., M.M.M. Bamatraf, B.S.M. Rao, R. Das, H. Mohan, and J.P. Mittal, Hydroxylation of chlorotoluenes and cresols: A pulse radiolysis, laser flash photolysis, and product study, *J. Phys. Chem.*, **101**, 9837-9845, 1997.
- Ciccioli, P., E. Brancaleoni, and M. Frattoni, Reactive hydrocarbons in the atmosphere at urban and regional scales, pp. 159-207 in *Reactive Hydrocarbons in the Atmosphere*, C.N. Hewitt (ed.), Academic Press, San Diego, 1999.
- Crutzen, P. J., and P.H Zimmermann, The changing photochemistry in the troposphere, *Tellus*, **43AB**, 136-151, 1991.
- DeMore, W.B., S.P. Sander, D.M. Golden, R.F. Hampson, M.J. Kurylo, C.J. Howard, A.R. Ravishankara, C.E. Kolb, and M.J. Molina, Chemical kinetics and photochemical data for use in stratospheric modeling, Jet Propulsion Laboratory, Pasadena, CA, NASA Evaluation No. 13, JPL Publication 97-4, 1997.
- Derwent, R.G., M.E. Jenkin, and S.M. Saunders Photochemical ozone creation potentials for a large number of reactive hydrocarbons under European conditions, *Atmos. Environ.*, **30**, 181-199, 1996.
- Derwent, R.G., M.E. Jenkin, S.M. Saunders, and M.J. Pillings, Photochemical ozone creation potentials for organic compounds in Northwest Europe calculated with a master chemical mechanism, *Atmos. Environ.*, **32**, 2429-2441, 1998.
- Dumdei, B.E., D.V. Kenny, P.B. Shepson, T.E. Kleindienst, C.M. Nero, L.T. Cupitt, and L.D. Claxton, MS/MS analysis of the products of toluene photooxidation and measurement of their mutagenic activity, *Environ. Sci. Technol.*, **22**, 1493-1498, 1988.
- Dumdei, B.E., and R.J. O'Brien, Toluene degradation products in simulated atmospheric conditions, *Nature*, **311**, 248-250, 1984.
- Etzkorn, T., B. Klotz, S. Sørensen, I. Patroescu, I. Barnes, K.H. Becker, and U. Platt, Gas-phase absorption cross sections of 24 monocyclic aromatic hydrocarbon in the UV and IR spectral ranges, *Atmos. Environ.*, **33**, 525-540, 1999.

References

- Fateley, W., R. Hammaker, M. Tucker, M. Witkowski, C. Chaffin, T. Marschall, M. Davis, M. J. Thomas, J. Arellano, J. Hudson, and B. Fairless, Observing industrial atmospheric environments by FT-IR, *J. Molec. Struct.*, **347**, 153-168, 1995.
- Finizio, A., D. Mackay, T.F. Bidleman, and T. Harner, Octanol-air partitioning coefficient as a predictor of partitioning of semi-volatile organic chemicals to aerosols, *Atmos. Environ.*, **31**, 2289-2296, 1997.
- Finlayson-Pitts, B.J., S.K. Hernandez, and H.N. Berko, A new dark source of the gaseous hydroxyl radical for relative rate measurements, *J. Phys. Chem.*, **97**, 1172-1177, 1993.
- Finlayson-Pitts, B.J., and J.N. Pitts, Jr., *Atmospheric Chemistry*, pp.1-1098, John Wiley & Sons, New York, 1986.
- Finlayson-Pitts, B.J., and J.N. Pitts, Jr., *Upper and Lower Atmosphere*, pp.1-969, Academic Press, New York, 1999.
- Forstner, H.J.L., R.C. Flagan, and J.H. Seinfeld, Secondary organic aerosol from the photooxidation of aromatic hydrocarbons: Molecular composition, *Environ. Sci. Technol.*, **31**, 1346-1358, 1997.
- Fujita, E.M., Z. Lu, L. Sheetz, G. Harshfeld, and B. Zielinska, Determination of mobile source emission fraction using ambient field measurements, Report available from the Coordinating Research Council, 3650 Mansell Road, Suite 140, Alpharetta, Georgia, 1997.
- Grosjean, D., Atmospheric reactions of o-cresol: Gas phase and aerosol products, *Atmos. Environ.*, **18**, 1641-1652, 1984.
- Grosjean, D., Reactions of o-cresol and nitrocresol with NO_x in sunlight and with ozone-nitrogen dioxide mixtures in the dark, *Environ. Sci. Technol.*, **19**, 968-974, 1985.
- Grosjean, D., *Atmospheric Chemistry of Toxic Contaminants*, 1. Reaction Rates and Atmospheric Persistence, *J. Air Waste Manage. Assoc.*, **40**, 1397-1402, 1990.

- Grosjean, D., Atmospheric fate of toxic aromatic compounds, *Sci. Total Environ.*, **100**, 367-414, 1991.
- Hawthorne, S.B, D.J., Miller, R.M., Barkley, and M.S., Krieger, Identification of Methoxylated Phenols as Candidate Traces for Atmospheric Wood Smoke Pollution, *Environ. Sci. Technol.*, **22**, 1191-1196, 1988.
- Hawthorne, S.B, M.S., Krieger, D.J., Miller, and M.B. Mathlason, Collection and Quantitation of Methoxylated Phenol Tracers for Atmospheric Pollution from Residential Wood Stoves, *Environ. Sci. Technol.*, **23**, 470-475, 1989.
- Hawthorne, S.B, D.J., Miller, J.J. Langenfeld, and M.S., Krieger, PM-10 High Volume Collection and Quantitation of Semi- and Nonvolatile Phenols, Methoxylated Phenols, Alkanes, and Polycyclic Aromatic Hydrocarbons from Winter Urban Air and Their Relationship to Wood Smoke Emissions , *Environ. Sci. Technol.*, **26**, 2251-2262, 1992.
- Hoshika, Y., and G. Muto, Gas-liquid-solid chromatographic determination of phenols in air using Tenax GC and alkaline precolumns, *J. Chromatogr.*, **157**, 277-284, 1978.
- Hurley, M.D., O. Sokolov, T.J. Wallington, H. Takekawa, M. Karasawa, B. Klotz, I. Barnes, and K.H. Becker, Organic Aerosol Formation During the Atmospheric Degradation of Toluene, *Environ. Sci. Technol.*, **35**, 1358-1366, 2001.
- Jeffries, H.E., "Photochemical Air Pollution" in "Composition, Chemistry, and Climate of the Atmosphere", ed. Singh, H. B., Van Nostrand Reinhold, New York, 1995.
- Jobson, B.T., H. Niki, Y. Yokouchi, J. Bottenheim, F. Hopper, and R. Leitch. Measurements of C2-C6 hydrocarbons during the Polar Sunrise 1992 Experiment: Evidence for Cl atom and Br atom chemistry, *J. Geophys. Res.*, **99**, 25355-25368, 1994.
- Kawamura, K., and I.R. Kaplan, Organic compounds in the rainwater of Los Angeles, *Environ. Sci. Technol.*, **17**, 497-501, 1983.

References

- Kawamura, K., and I.R. Kaplan, Compositional change of organic matter in rainwater during precipitation events, *Atmos. Environ.*, **20**, 527-535, 1986.
- Kleindienst, T.E., D.F. Smith, W. Li, E.O. Edney, D.J. Driscoll, R.E. Speer, and W.S. Weathers, Secondary organic aerosol formation from the oxidation of aromatic hydrocarbons in the presence of dry submicron ammonium sulfate aerosol, *Atmos. Environ.*, **33**, 3669-3681, 1999.
- Klotz, B.G., personal communication, 1998.
- Klotz, B., S. Sørensen, I. Barnes, K.H. Becker, T. Eitzkorn, R. Volkamer, U. Platt, K. Wirtz, and M. Martin-Reviejo, Atmospheric Oxidation of Toluene in a Large-volume Outdoor Photoreactor: In Situ Determination of Ring-Retaining Products Yields, *J. Phys. Chem. A*, **102**, (50), 10289-10299, 1998.
- Knispel, R., R. Koch, M. Siese, C. Zetzsch, Adduct formation of OH radicals with benzene, toluene, and phenol and consecutive reactions of the adduct with NO_x and O₂, *Ber. Bunsenges. Phys. Chem.*, **94**, 1375-1379, 1990.
- Kurtenbach, R., R. Ackermann, K.J. Brockmann, A. Geyer, J.A.G. Gomes, J.C. Lörzer, A. Niedojadlo, U. Platt, and K.H. Becker, VOC-Measurements in a road traffic tunnel and in urban air of the city of Wuppertal, in TFS-LT3 Annual Report 1998 (German), edited by K.H. Becker, University of Wuppertal, Germany, 1999a.
- Kurtenbach, R., K.J. Brockmann, A. Brust, J.A.G. Gomes, J. Lörzer, W. Thomas, and K.H. Becker, VOC-Measurements in rural air within the BERLIOZ campaign, in The BERLIOZ Campaign/TFS-LT3 Annual Report 1998 (German), edited by K.H. Becker, University of Wuppertal, Germany, 1999b.
- Kurtenbach, R., R. Ackermann, K.J. Brockmann, A. Geyer, J.A.G. Gomes, J.C. Lörzer, A. Niedojadlo, U. Platt, and K.H. Becker, VOC-Measurements in a road traffic tunnel and in urban air of the city of Wuppertal, in TFS-LT3 Annual Report 1998 (German), edited by K.H. Becker, University of Wuppertal, Germany, 2000.

- Kuwata, K., M. Uerobi, and Y. Yamazaki, Determination of phenol in polluted air as p-nitrobenzeneazophenol derivative by reversed phase high performance liquid chromatography, *Anal. Chem.*, **52**, 857-860, 1980.
- Kwok, E.S.C., and R. Atkinson, Estimation of hydroxyl radical reaction rate constants for gas-phase organic compounds using a structure-reactivity relationship: an update, *Atmos. Environ.*, **29**, 1685-1695, 1995.
- Leone, J.A., and J.H. Seinfeld, An updated mechanism for the atmospheric photooxidation of toluene, *Int. J. Chem. Kinet.*, **16**, 159-193, 1984.
- Lesh, S.A, and R.C. Mead, Sources screening for phenol. Prepared by Radian Corporation for U.S. Environmental Protection Agency, Research Triangle Park, N.C, Contract No. 68-02-3889, 1985.
- Leuenberger, C., M.P. Ligocki, and J.F. Pankow, Trace organic compounds in rain, IV Identities, concentrations and scavenging mechanisms for phenols in urban air and rain, *Environ. Sci. Technol.*, **19**, 1053-1058, 1985.
- Logan, J.A., Tropospheric ozone: Seasonal behaviour, trends, and anthropogenic influence, *Geophys. Res.*, **90**, 10463-10482, 1985.
- Lüttke, J., and K. Levsen, Phase partitioning of phenol and nitrophenols in clouds, *Atmos. Environ.*, **31**, 2649-2655, 1997.
- Lüttke, J., V. Scheer, K. Levsen, G. Wunsch, J.N. Cape, K.J. Hargreaves, R.L. Storeton-West, K. Acker, W. Wieprecht, and B. Jones, Occurrence and formation of nitrated phenols in and out of cloud, *Atmos. Environ.*, **31**, 2637-2648, 1997.
- Mentel, Th.F., D. Bleilebens, and A. A. Wahner, Study of Night-Time Nitrogen Oxide Oxidation in a Large Reaction Chamber-The Fate of the NO₂, N₂O₅, HNO₃, and O₃ at Different Humidities, *Atmos. Environ.*, **30**, 4007-4020, 1996.

References

- Odum, J.R., T. Hoffmann, F. Bowman, D. Collins, R.C. Flagan, and J.H. Seinfeld, Gas/particle partitioning and secondary organic aerosol yields, *Environ. Sci. Technol.*, **30**, 2580-2585, 1996.
- Odum, J.R., P.W. Jungkamp, R.J. Griffin, H.J.L. Forstner, R.C. Flagan, and J.H. Seinfeld, The atmospheric aerosol-forming potential of whole gasoline vapor. *Sciences*, **276**, 96-99, 1997a.
- Odum, J.R., P.W. Jungkamp, R.J. Griffin, H.J.L. Forstner, R.C. Flagan, and J.H. Seinfeld, Aromatics, reformulated gasoline, and atmospheric organic aerosol formation, *Environ. Sci. Technol.*, **31**, 1890-1897, 1997b.
- Olariu, R.I., I. Barnes, K.H. Becker, and B. Klotz, Rate coefficients for the gas-phase reaction of OH with selected dihydroxybenzenes and benzoquinones, *Int. J. Chem. Kinet.*, **32**, 696-702, 2000a.
- Olariu, R.I., I. Barnes, K.H. Becker, B. Klotz, and R. Mocanu, FT-IR primary product distribution study of the OH radicals initiated oxidation of Phenol, o-, m-, p-Cresol, Poster presented at the EC/EUROTRAC-2 joint workshop: Atmospheric gas phase processes, Lausanne-Ecublens, Switzerland, September 11-13, edited by M. J. Rossi and E. M. Rossi in Proceedings of the EC/EUROTRAC-2 joint workshop, pp 60-63, 2000b.
- Olariu, R.I., I. Barnes, K.H. Becker, and B. Klotz, FT-IR Product Study on the Gas-Phase Reaction of NO₃ Radical with Phenolic Compounds, Poster presented at A Changing Atmosphere, 8th European Symposium on the Physico-Chemical Behaviour of Atmospheric Pollutants, Torino, September 17-20, 2001.
- Pankow, J.F., Review and comparative analysis of the theories on partitioning between the gas and aerosol particulate phases in the atmosphere, *Atmos. Environ.*, **21**, 2275-2283, 1987.
- Patai, S., The chemistry of the quinonoid compounds (Part 1), John Wright & Sons Ltd. Bristol, 1974.

- Pellizzari, E.D., Information on the characteristic of ambient organic vapours in areas of high chemical production. Prepared for U.S. EPA by Research Triangle Institute, Research Triangle Park, NC, 1979.
- Platt, U., and F. Heintz, Nitrate Radicals in Tropospheric Chemistry, *I. J. of Chem.*, **34**, 289-300, 1994
- Platz, J., O.J. Nielsen, T.J. Wallington, J.C. Ball, M.D. Hurley, A.M. Straccia, W.F. Schneider, and J. Sehested, Atmospheric chemistry of the phenoxy radical, C₆H₅O•: UV spectrum and kinetics of reactions with NO, NO₂ and O₂, *J. Phys. Chem. A*, **102**, 7964-7974, 1998.
- Prinn, R., D. Cunnold, P. Simmonds, F. Alyea, R. Boldi, A. Crawford, P. Fraser, D. Guterl, D. Hartley, R. Rosen, and R. Rasmussen, Global average concentration and trend for hydroxy radicals deduced from ALE/GAGE trichloroethane (methylchloroform) data from 1978-1990, *J. Geophys. Res.*, **97**, 2445-2461, 1992.
- Richartz, H., A. Reischl, F. Trautner, and O. Hutzinger, Nitrated phenols in fog, *Atmos. Environ.*, **24A**, 3067-3071, 1990.
- Roberts, J.M., The Atmospheric Chemistry of the Organic Nitrates, *Atmos. Environ.*, **24A**, 243-287, 1990.
- Rogozen, M.B., H.E., Rich, M.A. Gutman and D. Grosjean, Evaluation of potential toxic air contaminants, Phase 1. Final report Dec. 23, Contract A4-131-132, State of California Air Resources Board, Sacramento, CA, 1987.
- Ruppert, L., personal communication, 1998.
- Shepson, P.B., T.E. Kleindienst, E.O. Edney, G.R. Namie, and J.H. Pittman, The mutagenic activity of irradiated toluene/NO_x/H₂O/air mixtures, *Environ. Sci. Technol.*, **19**, 249-255, 1985.
- Schmitz, T., D. Hassel, F.J. Weber, Determination of VOC-components in the exhaust of gasoline and diesel passenger cars, *Atmos. Environ.*, **34**, 4639-4647, 2000.

References

- Schwartz, S.E., Acid deposition: Unraveling a regional phenomenon, *Science*, **243**, 753-763, 1989.
- Scharzenbach, R., R. Stierli, B. Folsom, and J. Zeyer, Compound properties relevant for assessing the environmental partitioning of nitrophenols, *Environ. Sci. Technol.*, **22**, 83-92, 1988.
- Smith, D.F., C.D. McIver, and T.E. Kleindienst, Primary product distribution from the reaction of hydroxyl radicals with toluene at ppb NO_x mixing ratios, *J. Atmos. Chem.*, **30**, 209-228, 1998.
- Stockwell, W.R., F. Kirchner, M. Kuhn, and S. Seefeld, A new mechanism for regional atmospheric chemistry modeling, *J. Geophys. Res.*, **102**, 25847-25879, 1997.
- Taylor, W.D., T.D. Allston, M.J. Moscato, G.B. Fazekas, R. Kozlowski, and G.A. Takacs, Atmospheric photodissociation lifetime for nitromethane, methyl nitrite and methyl nitrate, *Int. J. Chem. Kinet.*, **12**, 231-240, 1980.
- Thomson, R.H., Natural Occuring Quinones, Academic Press, London, 1971.
- Thüner, L.P., T. Maurer, B. Donner, I. Barnes, K.H. Becker, J. Bea, M. Ponns, and K. Wirtz, Exhaust gas experiment in the EUPHORE simulation chamber, Chapter B1.3 in K.H. Becker (ed.) Influence of Fuel Formulation on Reactivity of Exhaust Gases (INFORMATEX), EC-Project ENV4-CT95-0015, Final Report, University Wuppertal, 1998.
- Tuazon, E.C., H. Mac Leod, R. Atkinson, and W.P.L. Carter, α -Dicarbonyl yields from the NO_x-air photooxidations of a series of aromatic hydrocarbons in air, *Environ. Sci. Technol.*, **20**, 383-387, 1986.
- Volkamer, R., K. Wirtz, K.H. Becker, B. Klotz, U. Platt, J. Uecker, The Phenol Yield from the OH-Radical Initiated Oxidations of Benzene, in: Barnes, I., and K. Brokmann, (ed.), EUPHORE Report 1998-1999, Bergische Universität Wuppertal, Physikalische Chemie, FB9, Germany, pp. 278-285, 2001.

Winzor, F.L., The Colouring Matters of *Drosera Whittakeri*. Part III. The Synthesis of Hydroxydroserone, *J. Chem. Soc. Lond.*, pp. 336-338, 1935.

Wirtz, K., personal communication, 1998.

Yu, J., H.E. Jeffries, and K.G. Sexton, Atmospheric photooxidation of alkylbenzenes-1. Carbonyl product analyses, *Atmos. Environ.*, **31**, 2261-2280, 1997.

Zetzsch, C., R. Koch, B. Bohn, R. Knispel, M. Siese, and F. Witte, Adduct formation of OH with aromatics and unsaturated hydrocarbons and consecutive reactions with O₂ and NO_x to regenerate OH, in *Chemical Processes in Atmospheric Oxidation*, G. LeBras (ed.), pp. 247-256, Springer-Verlag, Berlin, Germany, 1997.